UNCLASSIFIED

AD NUMBER

ADB086681

NEW LIMITATION CHANGE

TO

Approved for public release, distribution unlimited

FROM

Distribution authorized to U.S. Gov't. agencies only; Test and Evaluation; SEP 1983. Other requests shall be referred to Air Force Wright Aeronautical Labs., Attn: MLPO, Wright-Patterson AFB, OH 45433.

AUTHORITY

WRDC/IST ltr dtd 16 Oct 1990

THIS PAGE IS UNCLASSIFIED

THIS REPORT HAS BEEN DELIMITED
AND CLEARED FOR PUBLIC RELEASE
UNDER DOD DIRECTIVE 5200.20 AND
NO RESTRICTIONS ARE IMPOSED UPON
ITS USE AND DISCLOSURE.

DISTRIBUTION STATEMENT A

APPROVED FOR PUBLIC RELEASE;
DISTRIBUTION UNLIMITED.

AFWAL-TR-84-4034

EROSION RESISTANT FLIR WINDOWS: COLORLESS ZnS

CVD Incorporated
35 Industrial Parkway
Woburn, MA 01801

April 1984

Final Report for Period September 1981 - September 1983

SUBJECT TO EXPORT CONTROL LAWS

This document contains information for manufacturing or using munitions of war. Export of the information contained herein, or release to foreign nationals within the United States, without first obtaining an export license, is a violation of the International Traffic-in-Arms Regulations. Such violation is subject to a penalty of up to 2 years imprisonment and a fine of $100,000 under 22 USC 2778.

Include this notice with any reproduced portion of this document.

DTIC ELECTE OCT 1 8 1984 S D A

AD-B086 681

DTIC FILE COPY

Distribution limited to U. S. Government agencies only; test and evaluation; September, 1983. Other requests for this document must be referred to the AFWAL/MLPO, WPAFB, Ohio 45433.

MATERIALS LABORATORY
AF WRIGHT AERONAUTICAL LABORATORIES
AIR FORCE SYSTEMS COMMAND
WRIGHT-PATTERSON AFB, OHIO 45433

Best Available Copy

84 10 16 111

NOTICE

When Government drawings, specifications, or other data are used for any purpose other than in connection with a definitely related Government procurement operation, the United States Government thereby incurs no responsibility nor any obligation whatsoever; and the fact that the government may have formulated, furnished, or in any way supplied the said drawings, specifications, or other data, is not to be regarded by implication or otherwise as in any manner licensing the holder or any other person or corporation, or conveying any rights or permission to manufacture, use, or sell any patented invention that may in any way be related thereto.

This technical report has been reviewed and is approved for publication.

DONALD J. EVANS
Project Monitor
Laser & Optical Materials Branch

G. EDWARD KUHL, Chief
Laser & Optical Materials Branch
Electromagnetic Materials Division

FOR THE COMMANDER:

MERRILL L. MINGES, Chief
Electromagnetic Materials Division
Materials Laboratory
Air Force Wright Aeronautical Laboratories

If your address has changed, if you wish to be removed from our mailing list, or if the addressee is no longer employed by your organization please notify AFWAL/MLPO, W-PAFB, OH 45433 to help maintain a current mailing list.

Copies of this report should not be returned unless return is required by security considerations, contractual obligations, or notice on a specific document.

UNCLASSIFIED

SECURITY CLASSIFICATION OF THIS PAGE

REPORT DOCUMENTATION PAGE

1a. REPORT SECURITY CLASSIFICATION UNCLASSIFIED	1b. RESTRICTIVE MARKINGS
2a. SECURITY CLASSIFICATION AUTHORITY	3. DISTRIBUTION/AVAILABILITY OF REPORT Distribution limited to U. S. Government agencies only (Continued in Item 9, reverse side.)
2b. DECLASSIFICATION/DOWNGRADING SCHEDULE	
4. PERFORMING ORGANIZATION REPORT NUMBER(S) AFWAL-TR-84-4034	5. MONITORING ORGANIZATION REPORT NUMBER(S)
6a. NAME OF PERFORMING ORGANIZATION CVD Incorporated 6b. OFFICE SYMBOL (If applicable)	7a. NAME OF MONITORING ORGANIZATION AFWAL/MLPO
6c. ADDRESS (City, State and ZIP Code) 35 Industrial Parkway Woburn, MA 01801	7b. ADDRESS (City, State and ZIP Code) Wright-Patterson AFB, OH 45433
8a. NAME OF FUNDING/SPONSORING ORGANIZATION AFWAL 8b. OFFICE SYMBOL (If applicable) MLPO	9. PROCUREMENT INSTRUMENT IDENTIFICATION NUMBER F33615-81-C-5076
8c. ADDRESS (City, State and ZIP Code) Wright-Patterson AFB, OH 45433	10. SOURCE OF FUNDING NOS. PROGRAM ELEMENT NO.: 62102F; PROJECT NO.: 2423; TASK NO.: 01; WORK UNIT NO.: 48
11. TITLE (Include Security Classification) EROSION RESISTANT FLIR WINDOWS: COLORLESS ZnS	
12. PERSONAL AUTHOR(S) R. L. Taylor, M. J. Lefebvre, P. E. Price and M. M. Maderazzo	
13a. TYPE OF REPORT Final 13b. TIME COVERED FROM 15 Sep 81 TO 15 Sep 83	14. DATE OF REPORT (Yr., Mo., Day) April 1984 15. PAGE COUNT 158
16. SUPPLEMENTARY NOTATION	

17. COSATI CODES		
FIELD	GROUP	SUB. GR.
11	02	
16	04	

18. SUBJECT TERMS (Continue on reverse if necessary and identify by block number)
Water-clear ZnS, Optical material, Rain erosion, Optical data, Mechanical data

19. ABSTRACT (Continue on reverse if necessary and identify by block number)

A water-clear zinc sulfide (ZnS) has been developed and characterized. This material possesses good optical transmission over the wavelength range of 0.34 to 12 μm and is useful in many multispectral applications. This water-clear ZnS is produced by initially making ZnS by chemical vapor deposition (CVD) and then processing the material by hot isostatic pressing (HIP). The optimum CVD and HIP parameters for producing water-clear ZnS ~~have been~~ established in this program. Because of the high temperatures required in the production processes, water-clear ZnS exhibits larger crystallites and decreased rain-erosion resistance than standard CVD ZnS. A number of →

20. DISTRIBUTION/AVAILABILITY OF ABSTRACT UNCLASSIFIED/UNLIMITED ☐ SAME AS RPT ☒ DTIC USERS ☐	21. ABSTRACT SECURITY CLASSIFICATION UNCLASSIFIED
22a. NAME OF RESPONSIBLE INDIVIDUAL Donald J. Evans	22b. TELEPHONE NUMBER (Include Area Code) 513-255-4474 22c. OFFICE SYMBOL AFWAL/MLPO

SECURITY CLASSIFICATION OF THIS PAGE

surface and bulk treatments were investigated in an attempt to increase the hardness and improve ~~the~~ its rain-erosion resistance ~~of the water-clear ZnS~~. Two approaches appear promising. The first ~~of these~~ involves the incorporation, either by thermal diffusion or during the CVD process, of cadmium (Cd) atoms into the ZnS lattice to produce strain. The second approach would involve the deposition of a thin layer of CVD ZnS onto the water clear material analogous to the previously developed ZnS/ZnSe sandwich material. Other treatment processes investigated ~~in this program~~ involved grain refinement, thermal tempering, ion implantation, pulsed electron beam annealing (PEBA), and surface coatings. None of these treatments appeared to either provide increase hardness or to be practical techniques for optical materials. A large number of optical, physical and mechanical parameters of water-clear ZnS were measured ~~in~~ the course of this program. These data should allow optical engineers and designers to ~~utilize~~ use this material in various electro-optical systems.

Item 3 Continued: test and evaluation; September 1983. Other requests for this document must be referred to the AFWAL/MLPO, WPAFB, Ohio 45433.

AFIT COPY INSPECTED

Accession For
NTIS GRA&I
DTIC TAB
Unannounced
Justification
Distribution/
Availability Codes
Dist | Avail and/or Special
A-1

PREFACE

This report was prepared by the Research and Engineering Center of CVD Incorporated, Woburn, MA, under Contract No. F33615-81-C-5076 entitled, "Erosion Resistant FLIR Windows: Colorless ZnS." This work was administered by Air Force Wright Aeronautical Laboratories (AFSC), Wright-Patterson Air Force Base, Ohio. Mr. Donald J. Evans was the Project Monitor.

At CVD Incorporated the bulk of the work was performed by Mr. Mark J. Lefebvre supervised by Dr. Raymond L. Taylor. A significant portion of the effort was performed under subcontract to Industrial Materials Technology, Inc. (IMT). Dr. Peter E. Price and Mr. Marc Maderazzo of IMT contributed substantially to the program.

The authors benefited from technical discussions with Mr. Robert N. Donadio, President and Mr. Joseph F. Connolly, Vice President of Manufacturing of CVD Inc. The authors would also like to express their thanks to Richard J. Harris at the University of Dayton Research Institute for his extensive work in establishing several physical constants and numerous discussions and suggestions concerning the measurement of properties of CVD water-clear ZnS.

This Final Technical Report covers the period of performance of 15 September 1981 to 15 September 1983. The report has been given CVD Inc. internal number TR-028.

TABLE OF CONTENTS

		Page No.
1.0	Introduction	1
2.0	Task I - Optimization of Growth and Treatment Process	10
	2.1 Introduction	10
	2.2 Phase I - CVD Deposits	12
	2.3 Phase II - Hot Isostatic Pressing	15
	2.4 Summary and Conclusion - Task I	55
3.0	Task II - Material Toughening Techniques	56
	3.1 Introduction	56
	3.2 Grain Size Refinement	56
	3.3 Thermal Tempering	61
	3.4 Surface Diffusion	62
	3.5 Coatings	77
	3.6 Pulsed Electron Beam Annealing	82
	3.7 Ion Implantation	86
	3.8 CVD Overcoat	106
	3.9 Summary and Conclusion - Task II	113
4.0	Task III - Validating Measurements and Tests	115
	4.1 Introduction	115
	4.2 Test Results	115
	References	143

LIST OF ILLUSTRATIONS

Figure		Page No.
1-1.	Schematic of Chemical Vapor Deposition Process	2
1-2.	Cross Sectional View of a Typical CVD Furnace	3
1-3.	Visible-Near Infrared (top) and Infrared (bottom) Transmittance of As Deposited CVD ZnS	5
1-4.	Visible-Near Infrared (top) and Infrared (bottom) Transmittance of Water-Clear ZnS	6
1-5.	Photograph of ZnS Dome Before and After HIP Treatment	7
1-6.	Process Optimization Matrix Ladder	9
2-1.	HIP Unit Schematic (Courtesy of Dr. Peter Price of IMT Inc.)	11
2-2.	Infrared Transmittance of CVD ZnS AF-1, As Deposited	16
2-3.	Infrared Transmittance of CVD ZnS AF-2, As Deposited	16
2-4.	Infrared Transmittance of CVD ZnS AF-3, As Deposited	17
2-5.	Infrared Transmittance of CVD ZnS AF-4, As Deposited	17
2-6.	Infrared Transmittance of CVD ZnS AF-5, As Deposited	18
2-7.	Infrared Transmittance of CVD ZnS AF-6, As Deposited	18
2-8.	Photomicrographs of Etched Surface of CVD ZnS AF-3 (a) and AF-4 (b) 250x	20
2-9.	Infrared Transmittance of CVD ZnS AF-1 HIP Processed at 990 C, 15 ksi for 25 h, Pt Wrapped	23
2-10.	Infrared Transmittance of CVD ZnS AF-2 HIP Processed at 990 C, 15 ksi for 25 h, Pt Wrapped	23
2-11.	Infrared Transmittance of CVD ZnS AF-3 HIP Processed at 990 C, 15 ksi for 25 h, Pt Wrapped	24
2-12.	Infrared Transmittance of CVD ZnS AF-4 HIP Processed at 990 C, 15 ksi for 25 h, Pt Wrapped	24
2-13.	Infrared Transmittance of CVD ZnS AF-5 HIP Processed at 990 C, 15 ksi for 25 h, Pt Wrapped	25
2-14.	Infrared Transmittance of CVD ZnS AF-6 HIP Processed at 990 C, 15 ksi for 25 h, Pt Wrapped	25
2-15.	Photomicrographs of Etched Surface of CVD ZnS AF-4 As Deposited (a) and HIP Processed (b), 250x	26
2-16.	Visible-Near Infrared Transmittance of ZnS AF-1 HIP Processed at 990 C, 15 ksi for 25 h, Pt Wrapped	27
2-17.	Visible-Near Infrared Transmittance of ZnS AF-1 HIP Processed at 990 C, 30 ksi for 25 h, Pt Wrapped	28

LIST OF ILLUSTRATIONS (cont.)

Figure		Page No.
2-18.	Visible-Near Infrared Transmittance of ZnS AF-2 HIP Processed at 990 C, 15 ksi for 25 h, Pt Wrapped	29
2-19.	Visible-Near Infrared Transmittance of ZnS AF-2 HIP Processed at 990 C, 30 ksi for 25 h, Pt Wrapped	30
2-20	Visible-Near Infrared Transmittance of ZnS AF-3 HIP Processed at 990 C, 15 ksi for 25 h, Pt Wrapped	31
2-21.	Visible-Near Infrared Transmittance of ZnS AF-3 HIP Processed at 990 C, 30 ksi for 25 h, Pt Wrapped	32
2-22.	Visible-Near Infrared Transmittance of ZnS AF-4 HIP Processed at 990 C, 15 ksi for 25 h, Pt Wrapped	33
2-23.	Visible-Near Infrared Transmittance of ZnS AF-4 HIP Processed at 990 C, 30 ksi for 25 h, Pt Wrapped	34
2-24.	Visible-Near Infrared Transmittance of ZnS AF-5 HIP Processed at 990 C, 15 ksi for 25 h, Pt Wrapped	35
2-25.	Visible-Near Infrared Transmittance of ZnS AF-5 HIP Processed at 990 C, 30 ksi for 25 h, Pt Wrapped	36
2-26.	Visible-Near Infrared Transmittance of ZnS AF-6 HIP Processed at 990 C, 15 ksi for 25 h, Pt Wrapped	37
2-27.	Visible-Near Infrared Transmittance of ZnS AF-6 HIP Processed at 990 C, 30 ksi for 25 h, Pt Wrapped	38
2-28.	Infrared Transmittance of CVD ZnS AF-4, HIP Processed at 1047 C, 15 ksi for 12.5 h, Pt Wrapped	40
2-29.	Infrared Transmittance of CVD ZnS AF-4, HIP Processed at 1047 C, 15 ksi for 12.5 h, Graphite Enclosed	40
2-30.	Photomicrograph of CVD ZnS After HIP Processing at 1067 C (a) and 1110 C (b), 30 ksi for 12.5 h, Pt Wrapped, 100x	42
2-31.	Visible Transmittance AF-1, 4 and 6 Water-Clear ZnS	46
2-32.	Infrared Transmittance of CVD ZnS AF-4, Heat Treated at 990 C, 1 atm for 25 h, Pt Wrapped	51
2-33.	Infrared Transmittance of CVD ZnS AF-4, Heat Treated at 1047 C, 1 atm for 12.5 h, Pt Wrapped	51
2-34.	Infrared Transmittance of CVD ZnS AF-4, Heat Treated at 990 C, 1 atm, for 25 h, Pt Wrapped, then HIP Processed at 990 C, 15 ksi, for 25 h, Pt Wrapped	52
2-35.	Infrared Transmittance of CVD ZnS AF-4, Heat Treated at 1047 C, 1 atm, for 12.5 h, Pt Wrapped, then HIP Processed at 990 C, 15 ksi, for 25 h, Pt Wrapped	52

LIST OF ILLUSTRATIONS (cont.)

Figure		Page No.
3-1.	Infrared Transmittance of CVD ZnS (top) and Water-Clear ZnS (bottom), Before (top trace) and After (bottom trace) Rain Erosion Testing at 475 mph, 90° Impact Angle, 1 inch/h Rainfall, 30 min Exposure	59
3-2.	Infrared Transmittance of AF-4 Water-Clear ZnS Exposed to 1110 C, Cd Vapor, 3 h, 1 atm	65
3-3.	Infrared Transmittance of AF-4 Water-Clear ZnS Exposed to 1110 C, Cd Vapor, 3 h, 1 atm, Repolished	65
3-4.	Infrared Transmittance of CVD ZnS AF-4, Before Cd Diffusion Experiment	71
3-5.	Infrared Transmittance of CVD ZnS AF-4, After Cd Coating and HIP Processing at 750 C, 15 ksi for 12 h	71
3-6.	Infrared Transmittance of Water-Clear AF-4 ZnS, Before Cd Diffusion Experiment	72
3-7.	Infrared Transmittance of Water-Clear AF-4 ZnS, After Cd Coating and HIP Processing at 750 C, 15 ksi for 12 h	72
3-8	Photograph of Titanium Can Which Encloses ZnS and CdS Diameters	74
3-9.	Photograph of Polished Surface of ZnS/CdS Diffusion Billet	74
3-10.	Photomicrograph of ZnS/CdS Surface Showing Vickers Indentation, 400x	75
3-11.	Photomicrograph of Etched ZnS/CdS Interface Showing Diffusion Zone, 1000x	75
3-12.	Infrared Transmittance of AF-4 Water-Clear ZnS Before SiO_2 Coating	79
3-13.	Infrared Transmittance of AF-4 Water-Clear ZnS with 1000 Å SiO_2 Coating.	79
3-14.	Infrared Transmittance of BN from Sadtler Grating Infrared Spectra	80
3-15.	Infrared Transmittance of AF-4 Water-Clear ZnS Coated with Approximately 1000 A Cubic BN	80
3-16.	Photograph of Water-Clear ZnS with ~1 μm Coating of Cubic BN, Showing the Powdery Film	83
3-17.	Infrared Transmittance of Water-Clear ZnS Coated with ~1 μm Cubic BN. Film is White and Powdery	83

LIST OF ILLUSTRATIONS (cont.)

Figure		Page No.
3-18.	Schematic of Pulsed Electron Beam Annealing Process Showing Recrystallization Front (Courtesy of Spire Corp.)	85
3-19.	Schematic of Ion Implantation Process (Courtesy of Spire Corp.)	87
3-20.	Infrared Transmittance of Water-Clear ZnS Before [S^{2-}] Ion Implantation	90
3-21.	Infrared Transmittance of Water-Clear ZnS Which Has Been Implanted with [S^{2-}] Ions at 85 keV and $2x10^{17}$ ions/cm^2	90
3-22.	Infrared Transmittance of AF-4 Water-Clear ZnS Subjected to [I^-] Ion Implantation, 85 keV, $5x10^{14}$ ions/cm^2	91
3-23.	Infrared Transmittance of AF-4 Water-Clear ZnS Subjected to [I^-] Ion Implantation, 85 keV, $2x10^{17}$ ions/cm^2.	91
3-24.	Infrared Transmittance of AF-4 Water-Clear ZnS Before [Al^{3+}] Ion Implantation	94
3-25.	Infrared Transmittance of AF-4 Water-Clear ZnS After [Al^{3+}] Ion Implanted at 85 keV, $2x10^{17}$ ions/cm^2.	94
3-26.	Infrared Transmittance of AF-4 Water-Clear ZnS Before Cd Ion Implantation	97
3-27	Infrared Transmittance of AF-4 Water-Clear ZnS After [Cd^{2+}] Ion Implanted, 85 keV, $2x10^{17}$ ions/cm^2	97
3-28.	Visible-Near Infrared Transmittance of Water-Clear ZnS Before [Li^+] Ion Implantation	98
3-29.	Visible-Near Infrared Transmittance of Water-Clear ZnS Which Has Been [Li^+] Ion Implanted at 75 keV, $2x10^{17}$ ions/cm^2	99
3-30.	Infrared Transmittance of Water-Clear ZnS Which Has Been Ion Implanted with [Li^+] Ions at 75 keV, $2x10^{17}$ ions/cm^2 Before PEBA Processing	100
3-31.	Infrared Transmittance of Water-Clear ZnS Which Has Been Ion Implanted with [Li^+] Ions at 75 keV, $2x10^{17}$ ions/cm^2 After PEBA Processing at 0.20 cal/cm^2	100
3-32.	Infrared Transmittance of AF-4 Water-Clear ZnS Subjected to [Li^+] Ion Implantation, 150 keV, $2x10^{17}$	105

LIST OF ILLUSTRATIONS (cont.)

Figure		Page No.
3-33.	Infrared Transmittance of AF-4 Water-Clear ZnS Subjected to [Li^+] Ion Implantation, 150 keV, $4x10^{17}$ ions/cm^2.	105
3-34.	Visible-Near Infrared Transmittance of CVD ZnS/ Water-Clear ZnS Sandwich Composite. CVD ZnS Layer=.035 in, Total Thickness=.275 in.	110
3-35	Visible-Near Infrared Transmittance of CVD ZnS/ Water-Clear ZnS Sandwich Composite. CVD ZnS Layer=.035 in, Total Thickness=.240 in.	111
3-36.	Infrared Transmittance of CVD ZnS/Water-Clear ZnS Sandwich Composite. ZnS Layer=.085 in, Total Thickness=.275 in.	112
3-37.	Infrared Transmittance of CVD ZnS/Water-Clear ZnS Sandwich Composite. ZnS Layer=.035 in, Total Thickness=0.240 in.	112
4-1.	Visible Transmittance of Water-Clear ZnS at 23 C (top) and 200 C (bottom).	117
4-2.	Near-Infrared (0.7-2.5 μm) Transmittance Curve of Water-Clear ZnS at 23 C (left) and 200 C (right).	118
4-3.	Infrared Transmittance Curve of Water-Clear ZnS at 23 C (bottom) and 200 C (top).	119
4-4.	Percent of Light Scattered Out of a 4-degree Half Angle Cone by Water-Clear ZnS, Runs AF-1, 4 and 6.	121
4-5.	Twyman-Green (top and middle) and Fizeau (bottom) Interferograms of AF-4 Water-Clear ZnS.	122
4-6.	MTF Curve of Water-Clear ZnS, 8-12 μm.	124
4-7.	MTF Curve of Water-Clear ZnS, 8-12 μm.	125
4-8.	MTF Curve of Water-Clear ZnS, 8-12 μm.	126
4-9.	Visible-Near Infrared Transmittance of Water-Clear ZnS Before Exposure to UV Radiation.	129
4-10.	Visible-Near Infrared Transmittance of Water-Clear ZnS After Exposure to UV Radiation.	130
4-11.	Infrared Transmittance of Water-Clear ZnS Before Exposure to UV Radiation.	131
4-12.	Infrared Transmittance of Water-Clear ZnS After Exposure to UV Radiation.	131
4-13.	Photomicrographs of Etched Surface of Two Samples of CVD Water-Clear ZnS, 500x.	133

LIST OF ILLUSTRATIONS (concluded)

Figure		Page No.
4-14	Infrared Transmittance of As Deposited AF-1 (top) and AF-4 (bottom) ZnS Before and After Rain Erosion Testing at 475 miles/hour, 90° Impact Angle, 1 inch/hour Simulated Rainfall for 30.0 min.	139
4-15	Infrared Transmittance of As Deposited AF-6 (top) and AF-4 Water-Clear (bottom) ZnS Before and After Rain Erosion Testing at 475 Miles/hour, 90° Impact Angle, 1 inch/hour Simulated Rainfall for 30.0 min.	140
4-16	Infrared Transmittance of AF-4 Water-Clear ZnS Coated with 1000 Å Cubic BN Before and After Rain Erosion Testing at 475 Miles/hour, 90° Impact Angle, 1 inch/hour Simulated Rainfall for 30.0 min.	141

LIST OF TABLES

Table		Page No.
2-1.	CVD ZnS Deposition Parameter Matrix	13
2-2.	CVD ZnS Deposition Conditions	14
2-3.	Knoop Hardness (HK_{50}) CVD ZnS	19
2-4.	Hot Isostatic Pressing Parameters	21
2-5.	Knoop Hardness (HK_{50}) Water-Clear ZnS	41
2-6.	Knoop Hardness (HK_{50}) Water-Clear ZnS	43
2-7.	Attenuations Coefficients for HIP Processed Samples	45
2-8.	Effective Absorption Coefficient, Water-Clear ZnS	47
2-9.	Flexural Strength Water-Clear ZnS	49
2-10.	Heat Treatment Conditions, 1 Atmosphere Argon	50
2-11.	Heat Treatment - HIP Experiment, Knoop Hardness (HK_{50})	53
2-12.	Heat Treatment - HIP Experiment, Knoop Hardness (HK_{50})	54
3-1.	Knoop Hardness (HK_{50}) CVD ZnS Before and After HIP	57
3-2.	Flexural Strength, CVD ZnS, Before and After HIP (PSI)	58
3-3.	Material Toughening Matrix	60
3-4.	Knoop Hardness (HK_{50}) of Thermal Tempered, Water-Clear ZnS	63
3-5.	Knoop Hardness (HK_{50}) Cd Diffusion Experiment	64
3-6.	Knoop Hardness (HK_{50}) Cd Diffusion Experiment	67
3-7.	Knoop Hardness (HK_{50}) Cd Diffusion Experiment	68
3-8.	Cd Coating Diffusion Experiment	69
3-9.	Cd Coating Diffusion Experiment 50 g Vickers (HK_{50}) and Knoop (HK_{50}) Hardness	73
3-10.	Vickers Hardness (HV_{50}) of Water-Clear ZnS from ZnS/CdS Diffusion Couple	76
3-11.	Knoop Hardness (HK_{50}) SiO_2 Coated Water-Clear ZnS	78
3-12.	Knoop Hardness (HK_{50}) Cubic BN Coated Water-Clear ZnS	81
3-13.	Knoop Hardness (HK_{50}) Cubic BN Coated Water-Clear ZnS	84
3-14.	Knoop Hardness (HK_{50}) of Sulfur Ion Implantation into Water-Clear ZnS	89

LIST OF TABLES (cont.)

Table		Page No.
3-15.	Knoop Hardness (HK_{50}) of Iodine Ion Implantation into Water-Clear ZnS	92
3-16.	Knoop Hardness (HK_{50}) of Aluminum Ion Implantation into Water-Clear ZnS	93
3-17.	Knoop Hardness (HK_{50}) of Cadmium Ion Implantation into CVD (As Deposited and Water-Clear) ZnS	96
3-18.	Knoop Hardness (HK_{50}) of Lithium Ion Implantation into CVD (As Deposited and Water-Clear) ZnS	101
3-19.	Knoop Hardness (HK_{50}) of Ion Implantation/Diffusion by PEBA and HIP	102
3-20.	Knoop Hardness (HK_{50}) of Lithium Ion Implantation into Water-Clear ZnS	104
3-21.	Scanning Auger Microscopy of AF-4 Water-Clear ZnS	107
3-22.	Predeposition Surface Preparation CVD ZnS/Water-Clear ZnS Composite	108
3-23.	Knoop Hardness (HK_{50}) of CVD ZnS/Water-Clear ZnS Composite	109
4-1.	Material Validating Measurements and Tests	116
4-2.	Effective Absorption Coefficients* x 10^{-3} of Water-Clear ZnS	120
4-3.	MTF of Water-Clear ZnS 8-12 μm	127
4-4.	Thermo-optic Coefficients of Water-Clear ZnS	128
4-5.	Mechanical, Thermal and Electrical Properties of Water-Clear ZnS	134
4-6.	CVD ZnS Rain Erosion Data	135-138

1.0 INTRODUCTION

Chemical vapor deposition (CVD) is a manufacturing process in which a chemical reaction of vapors forms a solid material. It is generally used when the desired material is difficult to fabricate by conventional techniques such as crystal pulling, hot pressing and casting. Materials that have been made by the CVD process include refractories, e.g., tungsten, boron nitride, silicon carbide, ceramics, e.g., aluminum oxide, magnesium oxide, and, more recently, infrared materials such as zinc selenide and zinc sulfide and a zinc sulfide/zinc selenide sandwich. The process has several intrinsic advantages, notably its ability to produce large pieces of high purity materials in high volume and of low cost. Since the materials are deposited upon a substrate (mandrel), arbitrary size and shapes may be formed during the deposition process. The CVD process is also widely employed in semiconductor technology to produce a variety of thin films.

In the CVD process for ZnS, zinc vapor is reacted with H_2S gas:

$$Zn(v) + H_2S(g) \rightarrow H_2(g) + ZnS(s)$$

Typical deposition conditions are 670 C with a total pressure of about 40 torr. Zinc vapor is generated by maintaining a uniform inert-gas flow over the surface of liquid zinc which is kept at a temperature just below its boiling point. Hydrogen sulfide is a gas at standard conditions. Because CVD is a dynamic process, the manufacturing equipment must be capable of continuously and safely injecting, reacting and exhausting gases over long periods of time.

Figure 1-1 schematically shows a typical CVD apparatus. The furnace is a large electrically heated vacuum chamber with a continuous flow system. The Zn vapor and H_2S are injected into the reaction chamber where the deposition takes place. Unreacted and product gases are exhausted through traps to remove toxic substances. Figure 1-2 shows a cross section of a 36 inch diameter CVD furnace presently in use at CVD Incorporated. The only limitations on the process are imposed by the chamber size and deposition rate. Current chambers are 48 inches in diameter, and can produce plates up to 40 by 30 inches across and as much as 1-inch thick. To attain one-inch thickness, the chemical reaction must be accurately monitored and continuously controlled for almost three weeks.

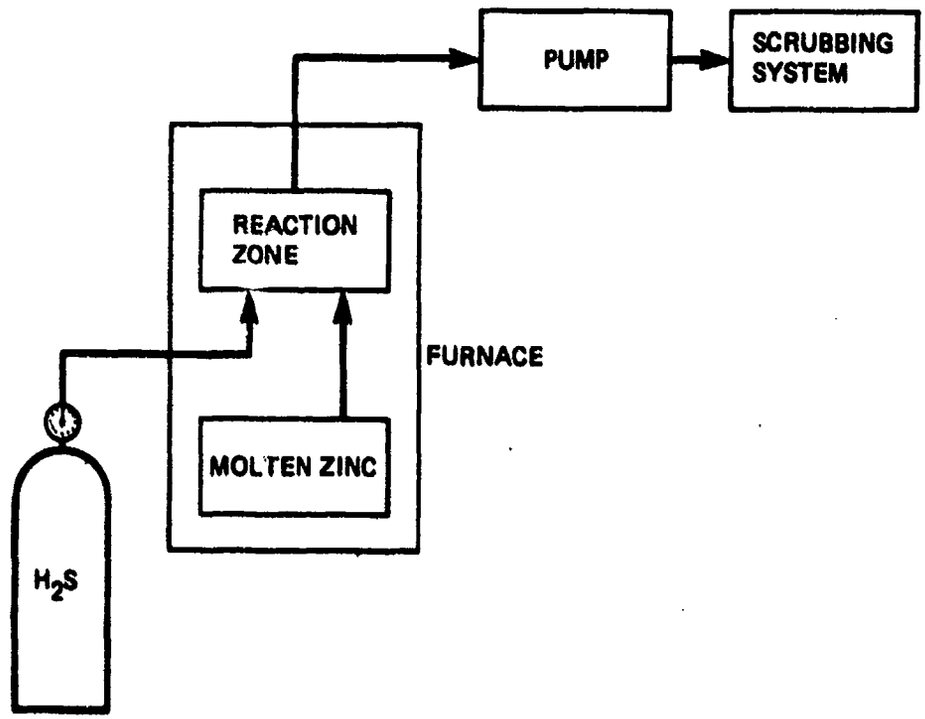

Figure 1-1. Schematic of Chemical Vapor Deposition Process

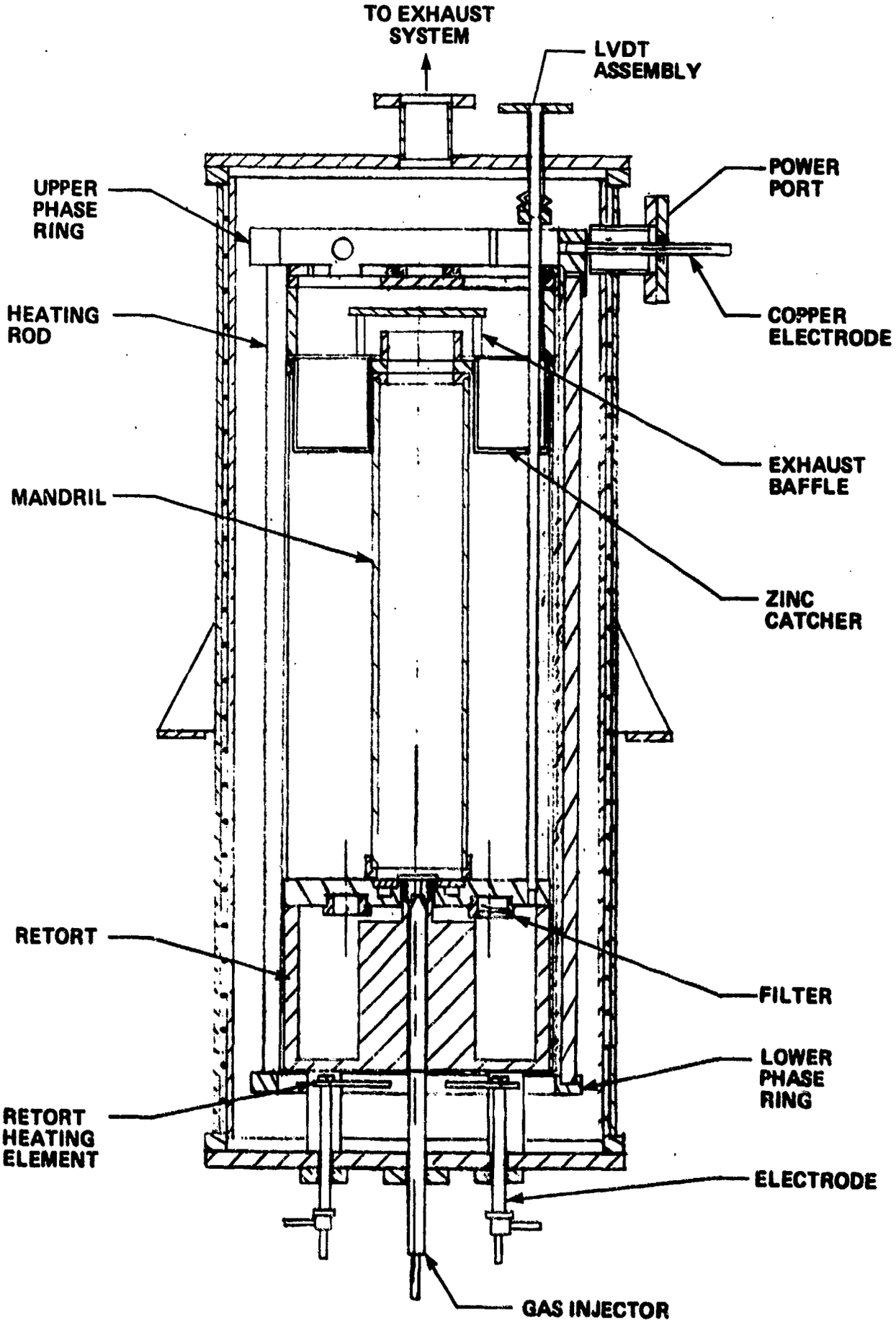

Figure 1-2. Cross Sectional View of a Typical CVD Furnace in Use at CVD Incorporated.

CVD ZnS has become a very useful infrared transmissive optical material. Visible and infrared transmission curves are shown in Fig. 1-3. In the LWIR spectral region (8-12 μm), ZnS has reasonably good transmission. It should be noted that the transmission values of about 70% shown in Fig. 1-3 can be improved to greater than 95% by the use of suitable anti-reflection coatings. The excellent transmission combined with reasonable rain erosion resistance, mechanical and physical properties has led to the use of CVD ZnS in domes for heat-seeking missiles and as windows in many other infrared military systems. The companion CVD product material, ZnSe, has better infrared optical properties but its weaker mechanical strength have restricted is use to benign environmental applications.

As is seen from Fig. 1-3, the transmission of CVD ZnS degrades toward the shorter wavelengths and the material possesses little or no useful transmission in the near infrared and visible spectral regions. This fact is intrinsic to CVD produced ZnS; the theoretical transmission limit for ZnS is in the near ultraviolet. Several years ago CVD Inc. was able to demonstrate the production of a ZnS with vastly superior visible optical properties. This water-clear ZnS was made by subjecting CVD ZnS to a post deposition hot isostatic processing (HIP) at high temperature and pressure (HIP is described later in this report). A transmission curve of this material is shown in Fig. 1-4, and comparison with Fig. 1-3 indicates the improved short wavelength optical properties. A dome made with water-clear ZnS is shown in Fig. 1-5 and compared to one fabricated from normal CVD ZnS. Unfortunately, the high temperatures used in producing water-clear ZnS also lead to significant grain growth and a weakening of the mechanical properties of the material. Thus, water-clear ZnS no longer possesses the good environmental characteristics of CVD ZnS.

The purpose of this program was severalfold: (i) To optimize the conditions under which water-clear ZnS is produced. In particular, an attempt was made to find conditions of CVD and HIP to produce good optical material while retaining as much of the intrinsic strength of the CVD ZnS as possible. Also, more cost effective approaches to produce the material were investigated. (ii) Since it was not thought possible to produce water-clear ZnS without some loss in mechanical characteristics, research was conducted to find some

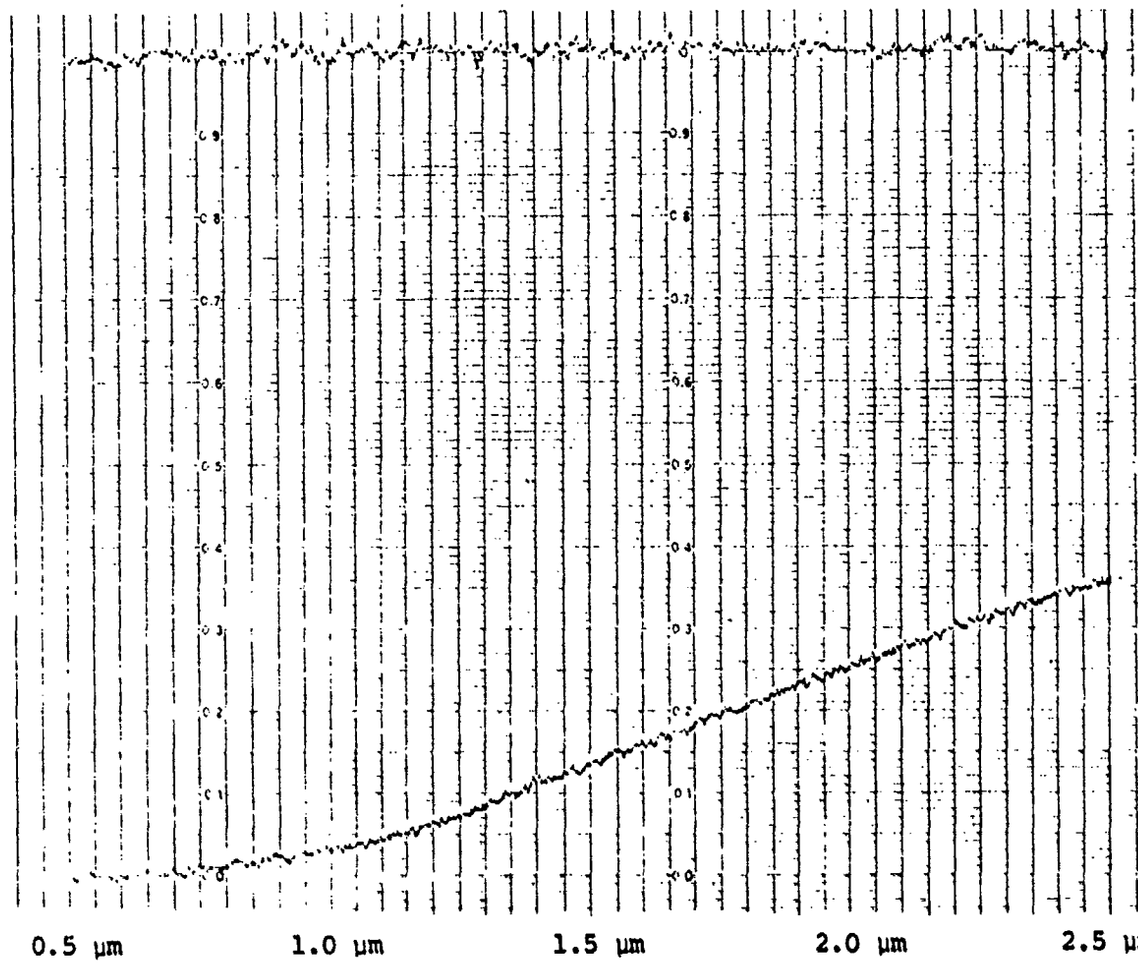

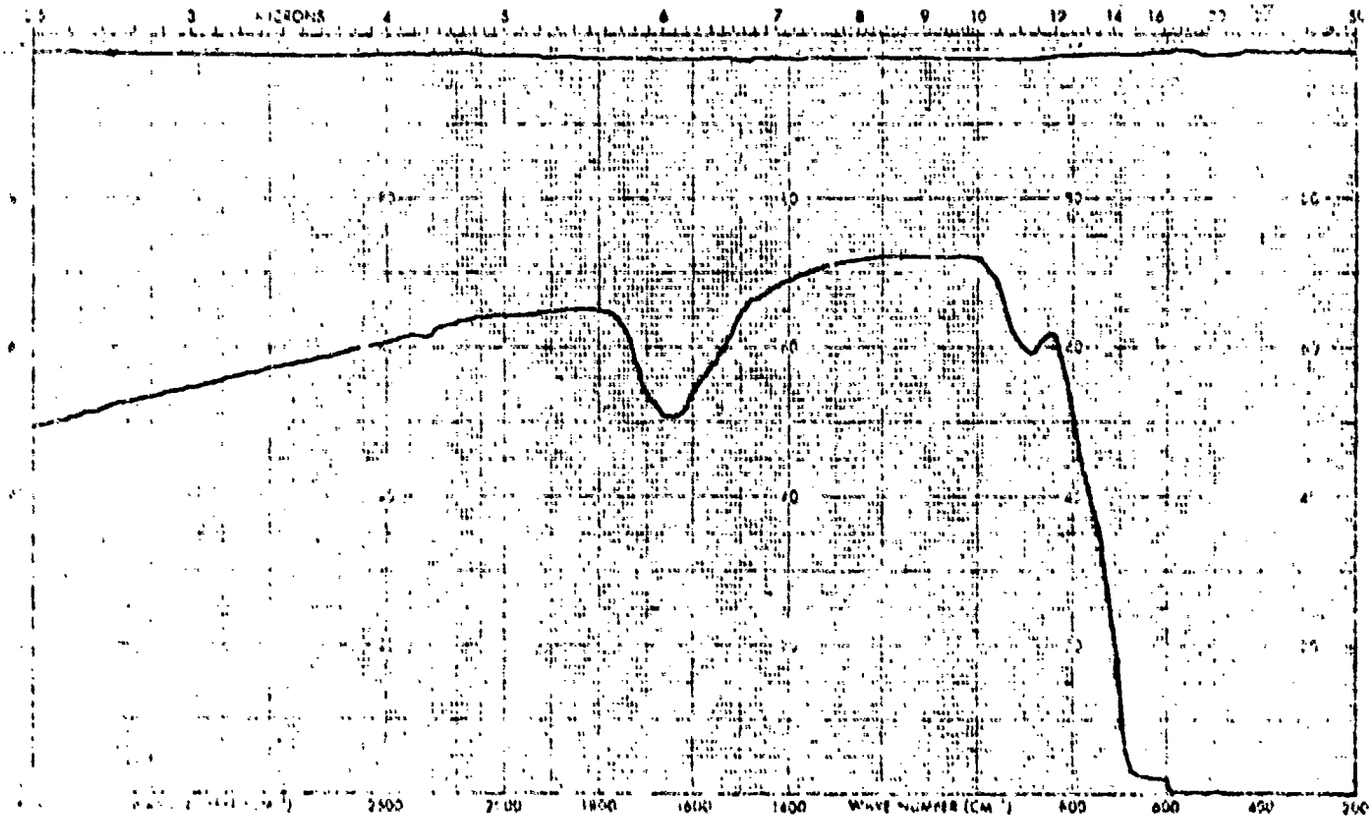

Figure 1-3. Visible-Near Infrared (top) and Infrared (bottom) Transmittance of As Deposited CVD ZnS.

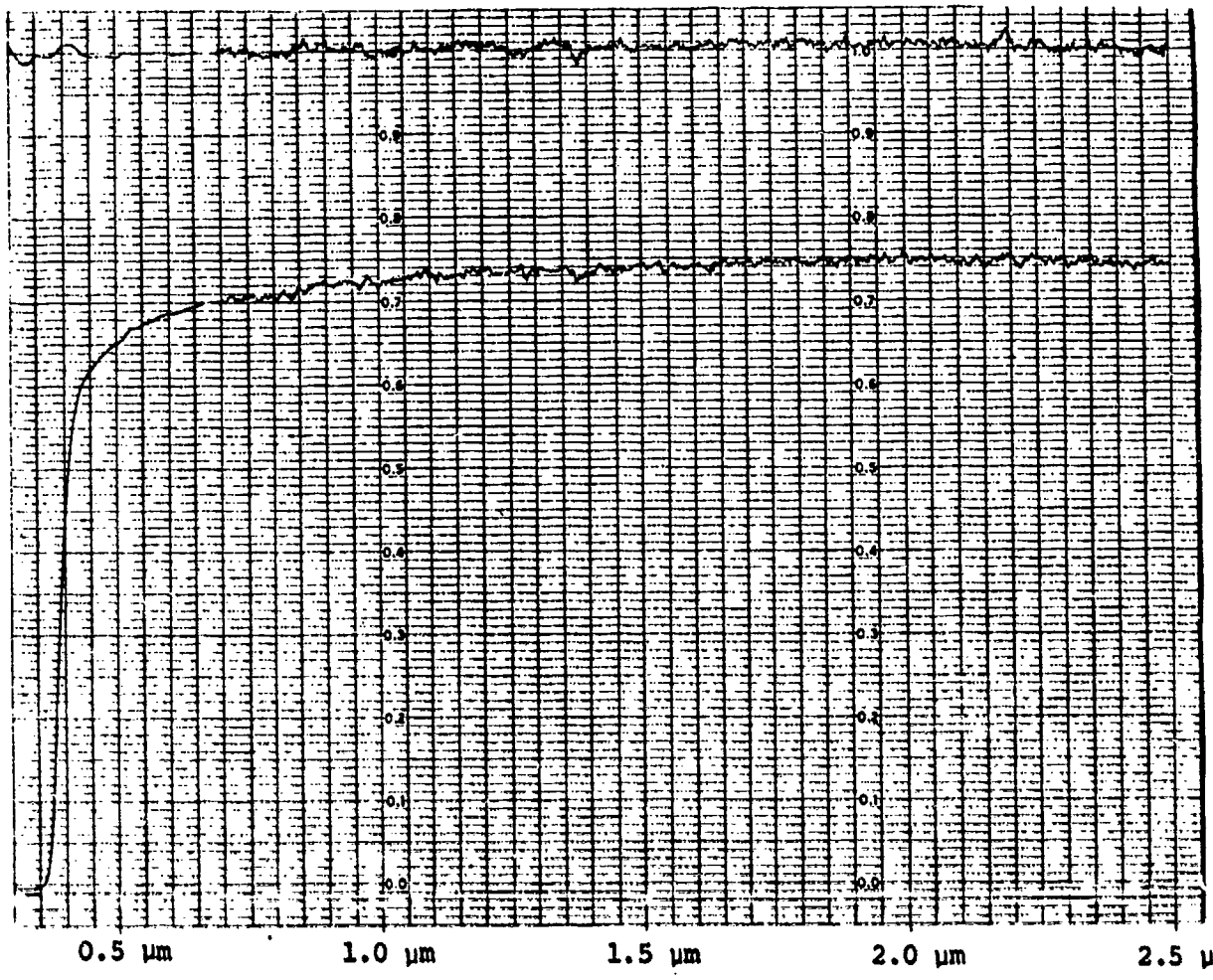

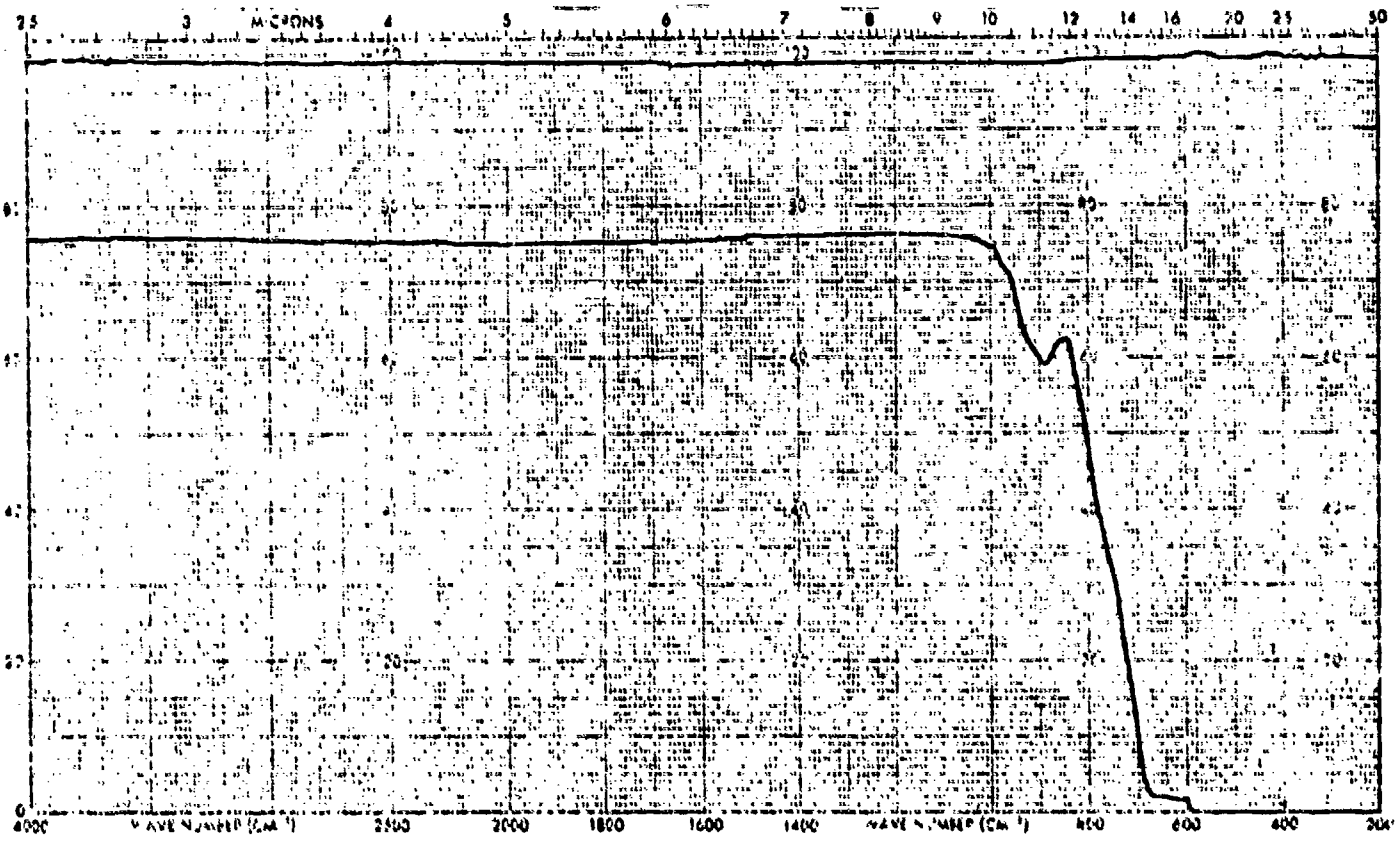

Figure 1-4. Visible-Near Infrared (top) and Infrared (bottom) Transmittance of Water-Clear CVD ZnS.

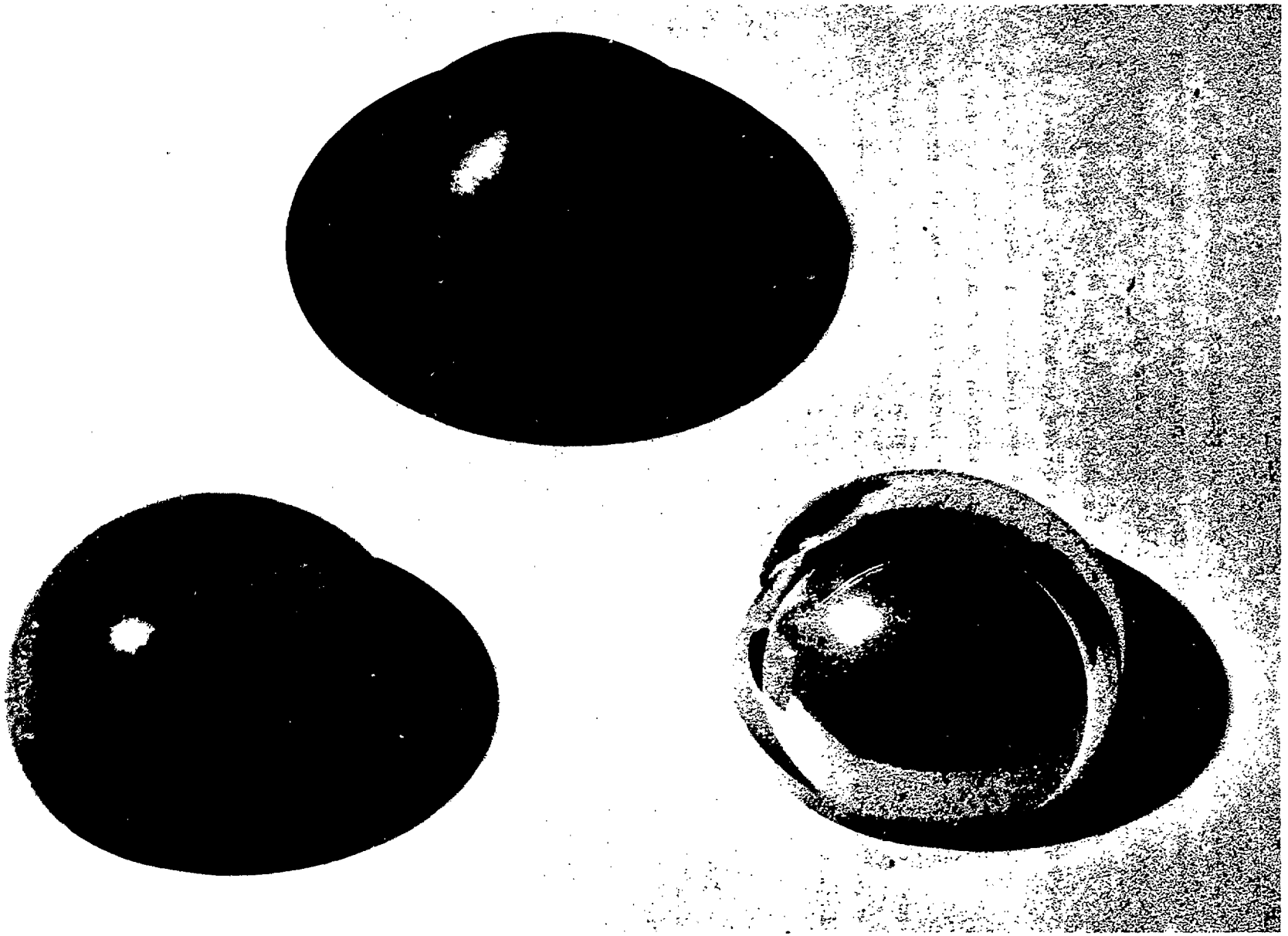

Figure 1-5. Photograph of ZnS Dome Before and After Hip Treatment

technique to increase the rain erosion resistance of the material as produced in (i) above. (iii) Finally, important optical, mechanical and physical constants of the water-clear ZnS were obtained and documented.

The overall program plan is shown in the matrix of Fig. 1-6. The optimization of the process parameters was investigated in branches (1)-(3). Material toughening experiments are indicated in branches (4) and (5). Additional approaches to improve rain erosion resistance that are not shown in Fig. 1-6 were also tried. Finally, in branch (6) the overall process is demonstrated in the generation of 10 x 10 x 1/2 inch blanks of water-clear ZnS. The details of this investigation are described in the sections that follow.

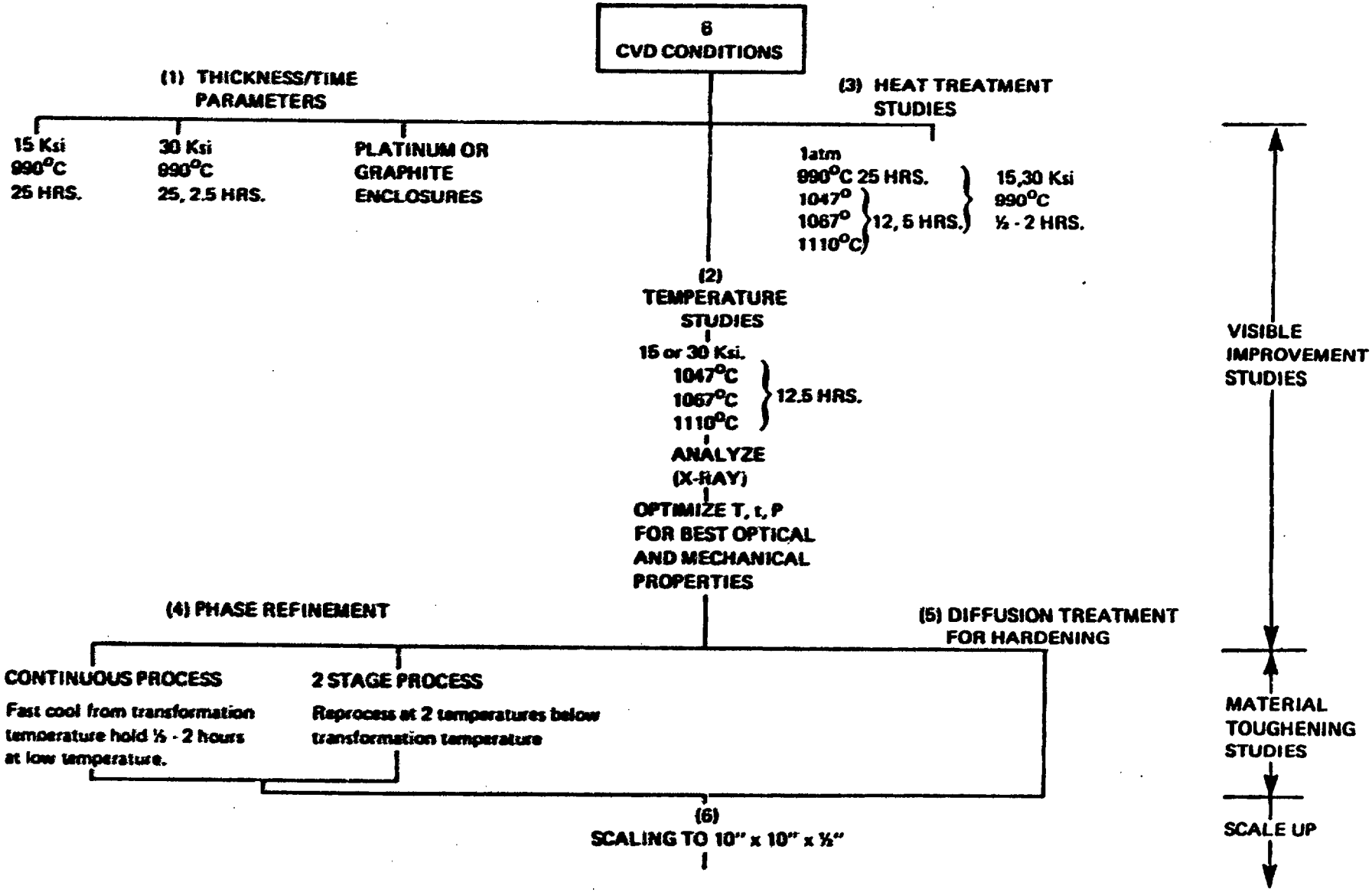

Figure 1-6. Process Optimization Matrix Ladder

2.0 TASK I - OPTIMIZATION OF GROWTH AND TREATMENT PROCESS

2.1 Introduction

The objective of this first task was to establish the optimum set of process parameters to produce water-clear ZnS. It was known at the start of the program that a water-clear ZnS could be produced from standard CVD ZnS by a subsequent HIP treatment. However, there are a large number of process variables from both the initial CVD process and the subsequent HIP treatment which can affect the optical and mechanical properties of the final water-clear ZnS. In addition, it was hoped that by starting with ZnS material produced outside of the standard CVD condition, it might be possible to obtain water-clear material by the most cost effective combination of treatments.

There are a large number of process parameters which can be varied in both the CVD and HIP steps. Therefore, it was not possible to vary each parameter independently. Rather, those parameters judged most critical were varied and only a limited range of variation was attempted.

The method of making colorless ZnS is a two step process involving (1) chemical vapor deposition of ZnS and (2) hot isostatic pressing (HIP) of the CVD ZnS in a separate chamber. The HIP technique applies a combination of inert gas pressure and temperature to a body to do useful work. Figure 2-1 shows a schematic of a typical HIP unit.

In the HIP process, the material is placed in containers which are enclosed in a heated pressure vessel. The material is generally wrapped with some foil (Pt is typically used) to prevent any contamination or chemical interaction with the container. In addition, this wrapping can also act as a gettering agent for species which outgas during the HIP treatment. The working fluid is generally an inert gas - Ar. Pressures of up to 30,000 psi and temperatures of 2000 C are attainable in HIP chambers currently available. The size of these chambers is also increasing with the demand to process larger parts. Currently available chambers have up to a 38 inch working diameter.

Hot isostatic pressing is a proven, cost effective and energy efficient technique used in many metallurgical and ceramic applications.

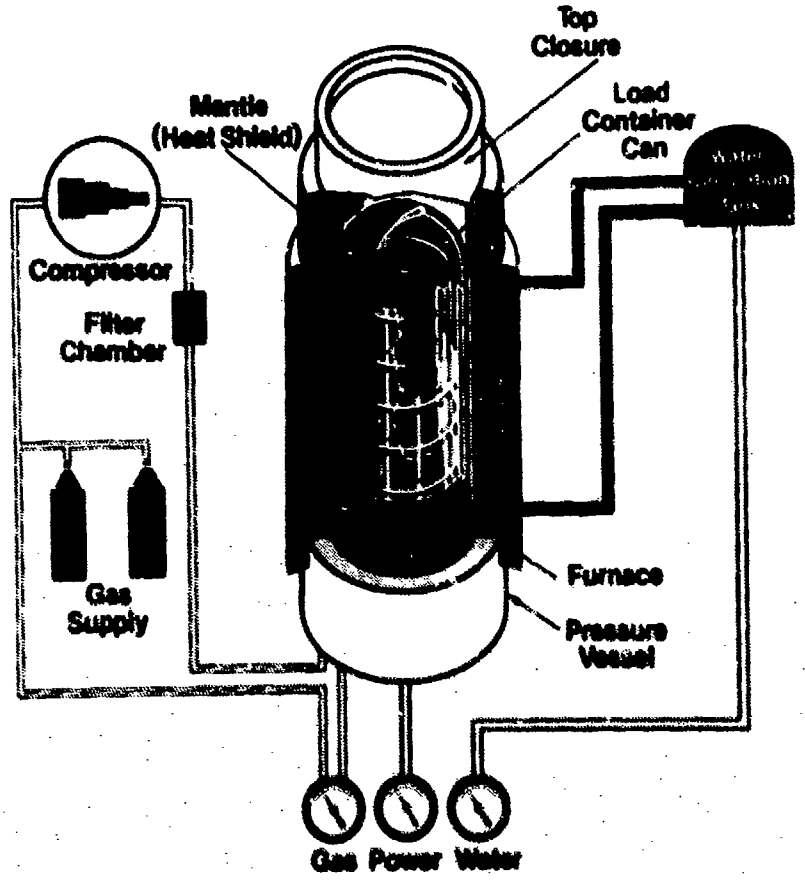

Figure 2-1. HIP Unit Schematic
(Courtesy of Dr. Peter Price of INT Inc.)

HIP processing is used in the manufacture of dies and composite parts, significantly improving the performance and service life of high wear parts. HIP allows materials with widely disparate coefficients of expansion to be bonded in a one step procedure. HIP processing is extensively used in the manufacture of high performance super alloys and similar materials from powder compacts. In a single operation, super alloy powders can be consolidated into a 100% dense material, with the capability of producing complex internal and surface geometries. Other uses of HIP processing include rejuvination of turbine blades and components, and densification of castings. Strength deterioration of turbine blades can be essentially reversed with HIP processing, greatly extending the useful life of these components and reducing replacement. Previously 'uncastable' materials are HIP processed to increase yields and material properties by healing casting flaws that often result in poor high temperature creep strength, lower strength and ductility.

2.2 Phase I - CVD Deposits

During this phase of Task I, six varieties of CVD ZnS were produced for use in the HIP treatment. Chemically vapor deposited ZnS can vary in optical and mechanical properties, depending primarily upon deposition temperature, pressure, stoichiometry and deposition rate. A matrix of six CVD ZnS deposits was planned (Table 2-1) to produce various quality CVD ZnS which was in turn to be used as baseline material for the subsequent HIP processing. Table 2-2 shows the actual deposition conditions followed for this matrix. The first deposit (ZnS AF-1) represents standard CVD conditions for producing ZnS. In the second deposit (AF-2), the molar ratio of H_2S/Zn was increased from 0.7 to 1.0, with remaining conditions unchanged. This was done by lowering the Zn vapor pickup rate (rate of Zn evaporation) while keeping the H_2S gas injection rate the same. The third ZnS deposition (AF-3) represents a low temperature deposit, i.e., a standard ZnS deposit with a lower overall deposition temperature. Conversely, AF-4 represents a high temperature run. In AF-5 the deposition rate was doubled by increasing the partial pressure of reactants (H_2S and Zn) while keeping the standard stoichiometry (H_2S/Zn) of 0.7. Finally, AF-6 represents a Zn rich deposit, i.e., ratio of $H_2S/Zn = 0.3$. The Zn pickup rate was increased from 675 to 1223 g/hr. while the H_2S was injected at 2 1 ℓ/min (down from 2.7).

TABLE 2-1

CVD ZnS Deposition Parameter Matrix

Deposition No.	Deposition Temperature (°C)	Molar Ratio (S/Zn)	Deposition Rate (in/h)
1*	670	0.7	0.003
2	670	1.0	0.003
3	620	0.7	0.003
4	720	0.7	0.003
5	670	0.7	0.006
6	670	0.3	0.003

* Standard CVD ZnS manufactured according to CVD Incorporated Process Specification CVD-ZNS-680.

TABLE 2-2

CVD ZnS Deposition Conditions

Run No.	Deposition Temperature (°C)	H_2S (l/min)	Zn (g/h)	Furnace Pressure (Torr)	Deposition Time (h)
ZnS-AP1	670	2.7	675	38	125.5
ZnS-AP2	670	2.7	470	38	117
ZnS-AP3	620	2.7	675	38	120
ZnS-AP4	720	2.7	675	38	125
ZnS-AP5	670	3.9	974	35	66.5
ZnS-AP6	670	2.1	1223	38	137

As is evident from the infrared transmittance curves of these 6 ZnS materials (Figs. 2-2 to 2-7), the optical quality of the ZnS is affected by the deposition conditions, most noticeably the short wavelength scatter and the intensity of the impurity absorption band at 6.3 μm. AF-2 and 4 ZnS material display appreciable short wavelength scatter in comparison to the other deposits. AF-3 and 5 ZnS exhibit a very broad, strong absorption band at 6.3 μm in contrast to AF-4, which displays a very shallow absorption. AF-6 displays the best overall transmittance for ZnS. It shows a fairly well defined doublet at 6.3 μm, whereas the remaining runs show a flat (AF-1, 3 and 5) or rounded (AF-2 and 4) singlet peak.

The Knoop hardness of these six deposits also show variations, as can be seen from Table 2-3, with values ranging from a minimum of 216 to a maximum of 256. These extremes can be explained by the deposition temperatures and corresponding crystal structure. The hardest material (AF-3) was deposited at the lowest temperature, yielding relatively small grained material (Fig. 2-8a) whereas, the softest material (AF-4) was deposited at the highest temperature resulting in a large grained structure (Fig. 2-8b).

These six materials were then HIP processed as described in the next section to determine the optimum overall CVD/HIP conditions to produce the best water-clear ZnS.

2.3 Phase II - Hot Isostatic Pressing

In Phase II, a series of HIP runs was conducted to quantitatively investigate the effects of time, temperature, pressure and wrapping (enclosure) material on the optical and mechanical properties of the water-clear ZnS produced. All six CVD deposits produced from Phase I were used in each HIP treatment. Various atmospheric heat treatment experiments were also performed to determine their effectiveness to relax or eliminate the HIP treatment. The matrix of parameters is shown in Fig. 1-6 in steps (1)-(3).

A matrix of twelve HIP treatment runs was investigated, as shown in Table 2-4, to determine the optimum HIP conditions to render the CVD ZnS clear. The first three HIP runs were conducted at 990 C, the HIP processing temperature used at the inception of this program. Parameters of time, pressure, and wrapping material were varied at constant temperature. Three higher

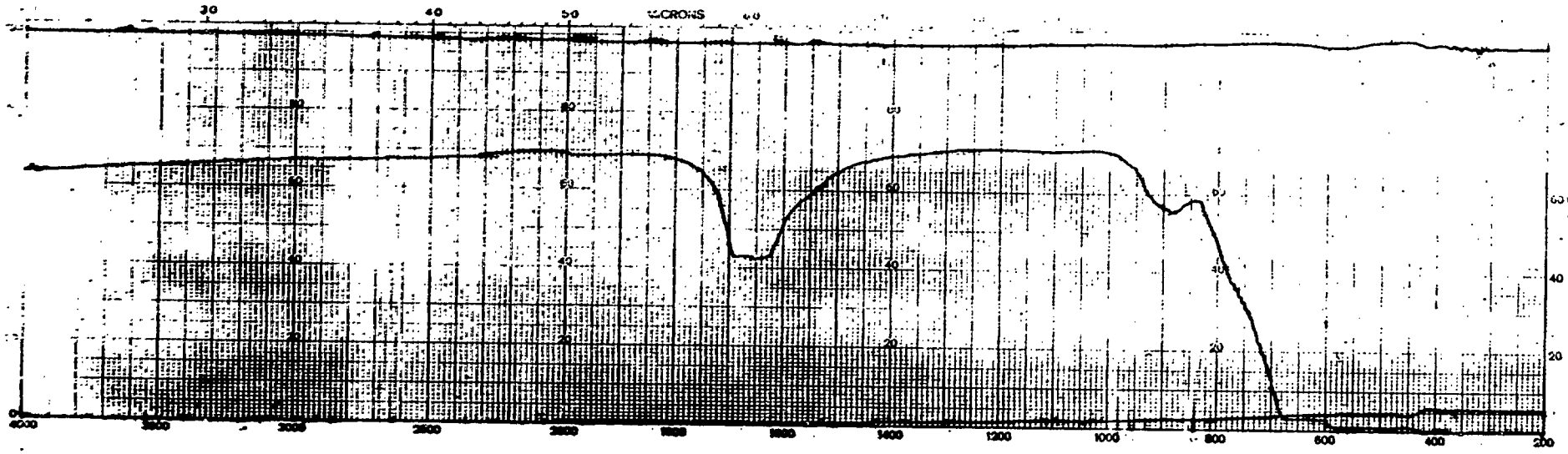

Fig. 2-2. Infrared Transmittance of CVD ZnS AF-1, As Deposited.

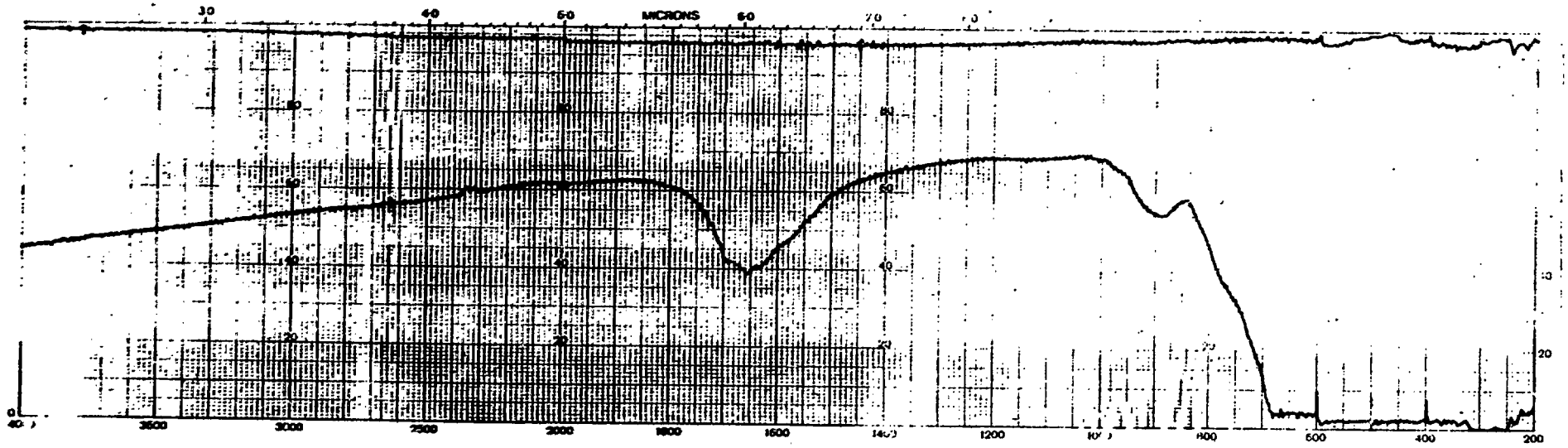

Fig. 2-3. Infrared Transmittance of CVD ZnS AF-2, As Deposited.

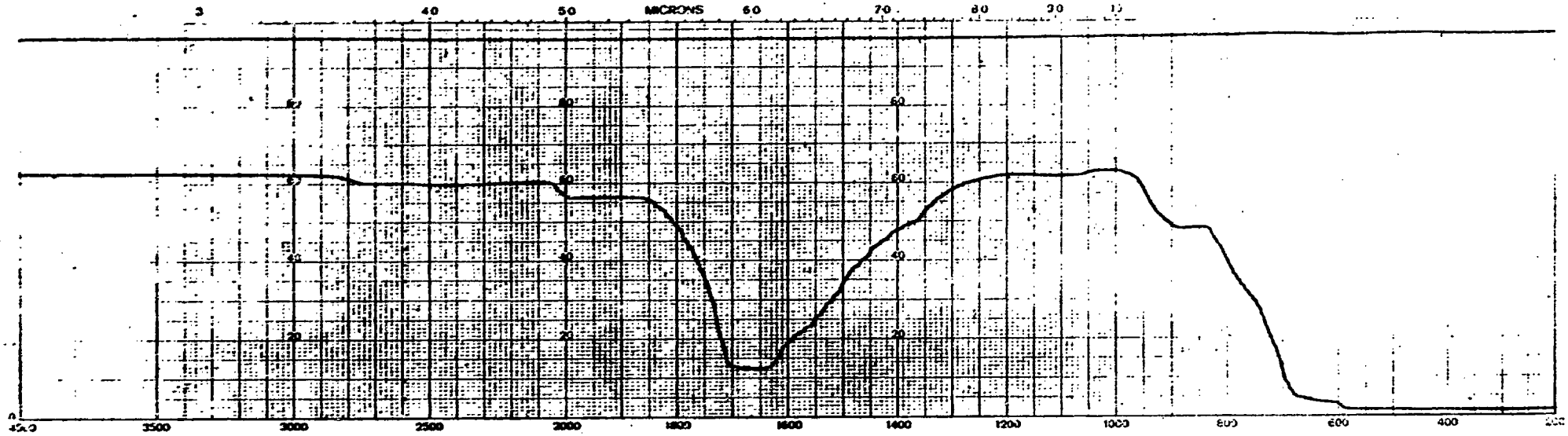

Fig. 2-4. Infrared Transmittance of CVD ZnS AF-3, As Deposited.

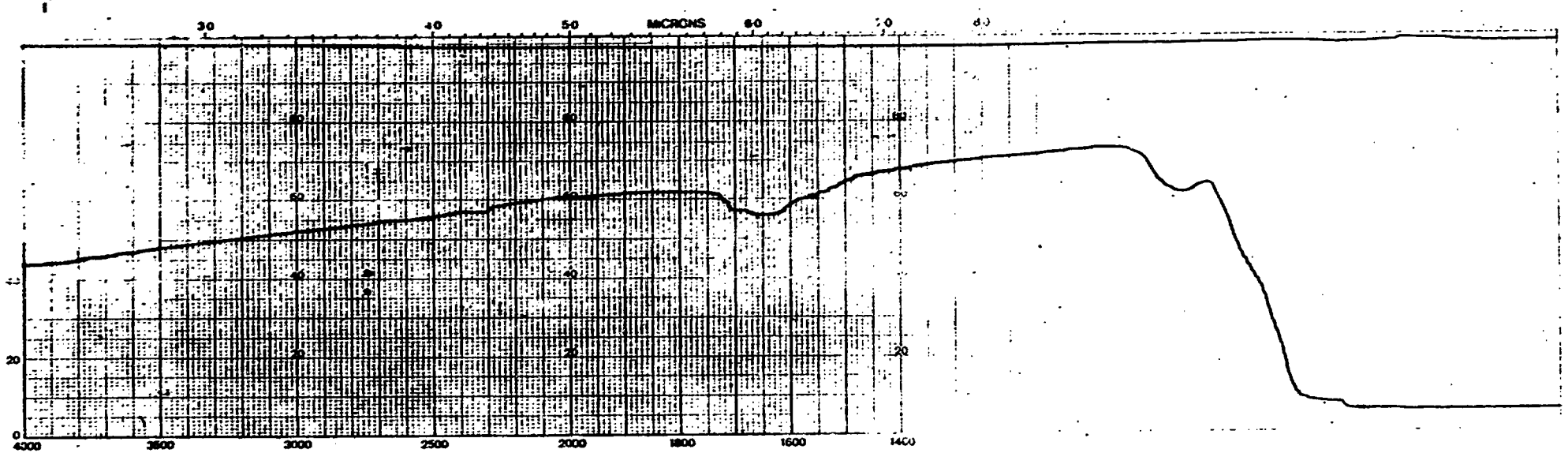

Fig. 2-5. Infrared Transmittance of CVD ZnS AF-4, As Deposited.

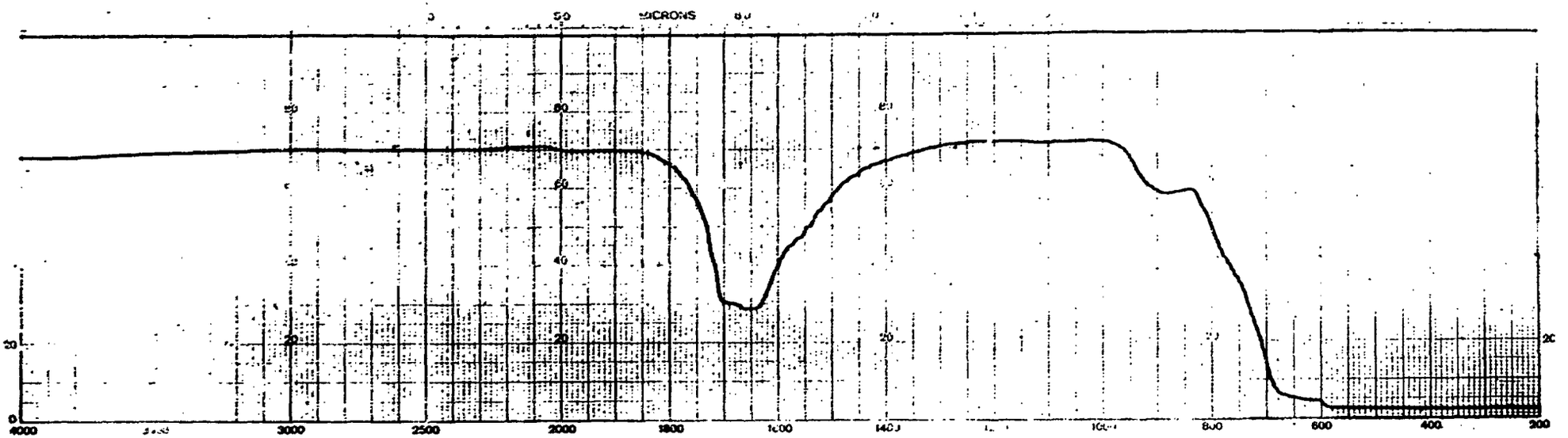

Fig. 2-6. Infrared Transmittance of CVD ZnS AF-5, As Deposited.

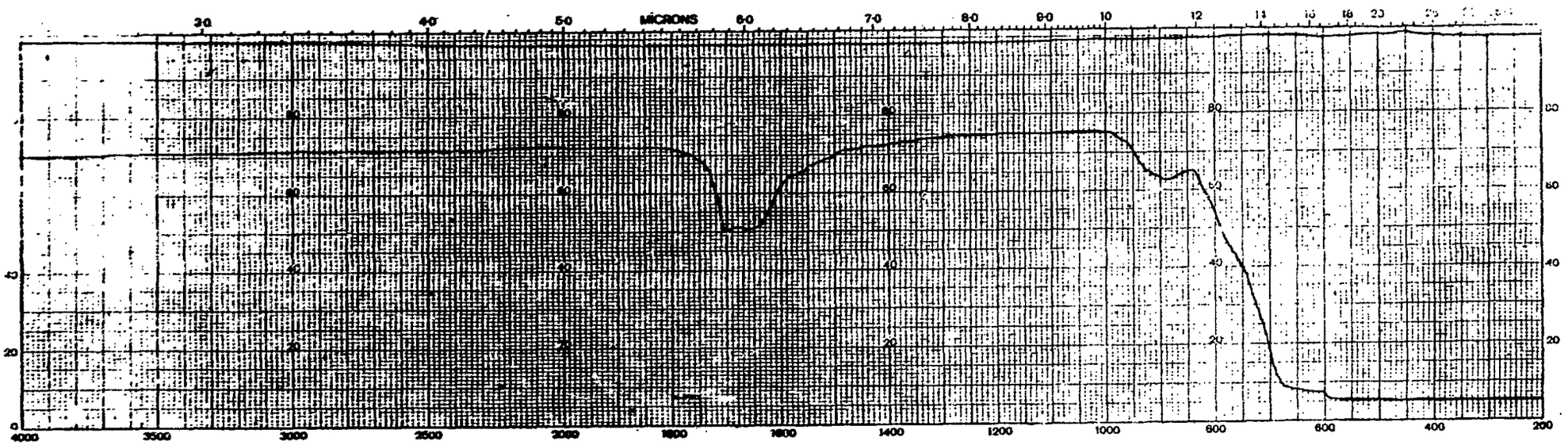

Fig. 2-7. Infrared Transmittance of CVD ZnS AF-6, As Deposited.

TABLE 2-3

Knoop Hardness (HK_{50}) CVD ZnS

Run No.	HK_{50}
ZnS AF-1	220
ZnS AF-2	230
ZnS AF-3	256
ZnS AF-4	216
ZnS AF-5	252
ZnS AF-6	247

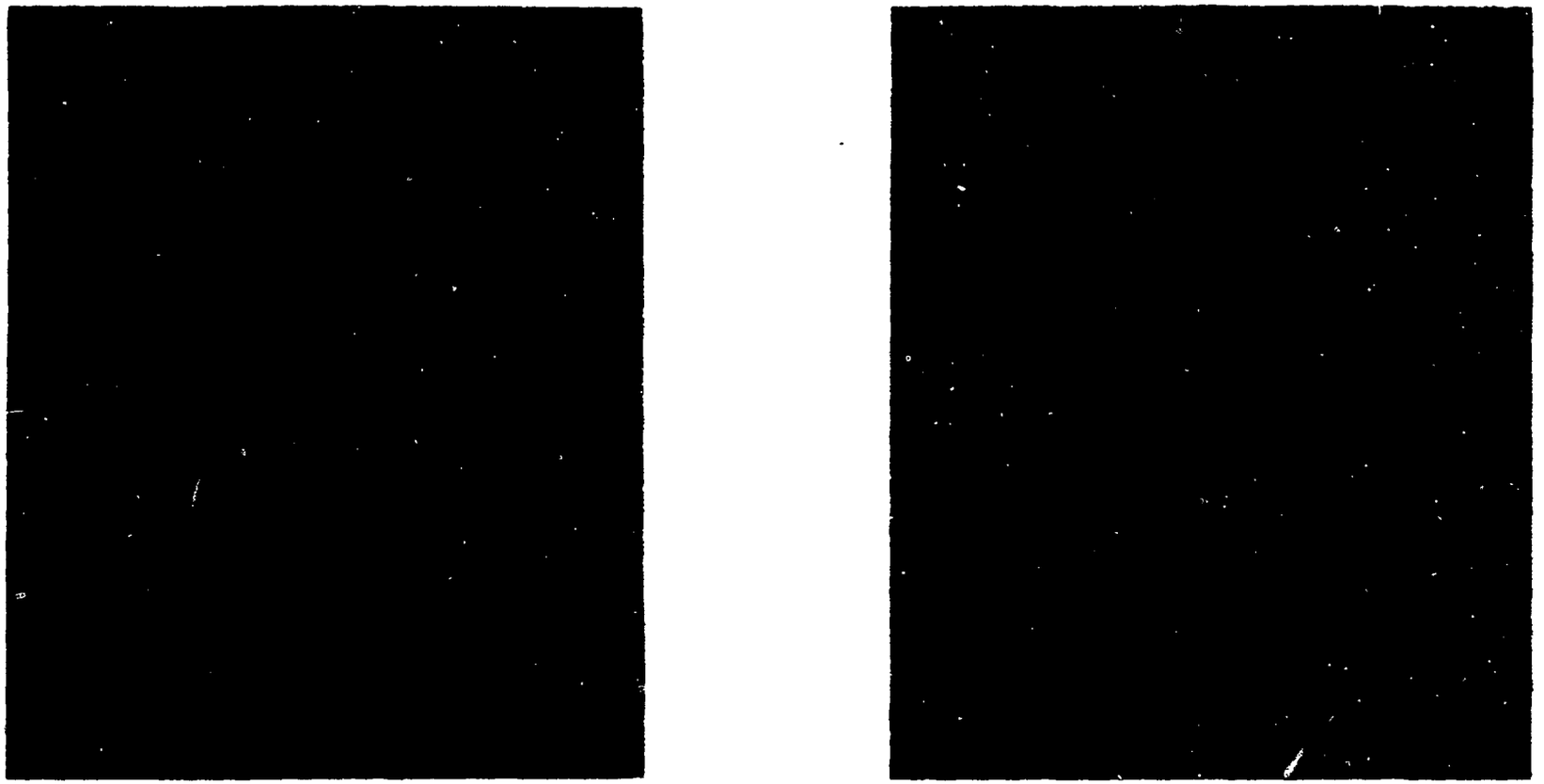

(a) (b)

Figure 2-8. Photomicrographs of Etched Surface of CVD ZnS AF-3 (a) and AF-4 (b), 250x.

TABLE 2-4

Hot Isostatic Pressing Parameters

Run No.	Temperature °C	Pressure psi x 10^3	Time h	Enclosure
HIP-I	990	15	25	platinum
HIP-II	990	30	25	platinum & graphite
HIP-III	990	30	2.5	platinum
HIP-IV	1047	15	12.5	graphite
HIP-V	1047	30	12.5	graphite
HIP-VI	1067	15	12.5	graphite
HIP-VII	1067	30	12.5	graphite
HIP-VIII	1110	15	12.5	graphite
HIP-IX	1110	30	12.5	platinum
HIP-X	1047	15	12.5	platinum
HIP-XI	1047	30	12.5	platinum

temperatures were used in the HIP treatment matrix to determine trends with increasing temperature. Temperatures of 1047, 1067 and 1110 C were selected to double the diffusion rate above the baseline temperature of 990 C. These values are based on three assumed values for the activation energy of diffusion of 20, 30 and 40 kcal/mol K.

The edges and faces of the six samples from HIP I were polished and inspected for residual visible banding or stria normally observed in standard CVD ZnS. Samples from AF-5 revealed a light hazy band which could be observed from an edge view. Material from AF-3 was the only deposit showing a dark scattering core at the center of the sample and displaying short wavelength scatter not observed in the other material. Infrared transmission traces of the six samples are shown in Figs. 2-9 to 2-14. As is evident from the photomicrographs (250x) of the etched surface of CVD ZnS before and after HIP (Figures 2-15a and b), there is a substantial increase in grain size after the high temperature processing.

HIP II was performed at 990 C, 30 ksi, 25 h with both platinum and graphite enclosures. Edge views of the material wrapped in platinum revealed a slight residual scattering core in all samples except for AF-3, which was severe. Samples from AF-3 were significantly milky and translucent in appearance, similar to the previous HIP run. Qualitatively, it appears that there are more scattering layers present in the material processed at 30 ksi than at 15 ksi. In Figs. 2-16 through 2-27, visible transmittance curves confirm quantitatively that material HIP processed at 15 ksi has superior visible optical properties. Samples from HIP II were also processed without platinum, using a graphite enclosure. All samples show residual scatter sites in the form of dark networking or texture. It is evident that material wrapped in platinum from HIP II has superior visible transmittance than material processed with graphite.

A 2.5 hour HIP (HIP III) was conducted at 990 C, 30 ksi with platinum enclosures. This run was designed to indicate the time/thickness relationship for HIP processing of CVD ZnS. Visual evaluation shows removal of nearly all color/scatter centers in AF-4 and AF-6; while the remaining samples display a large amount of color/scatter to be present.

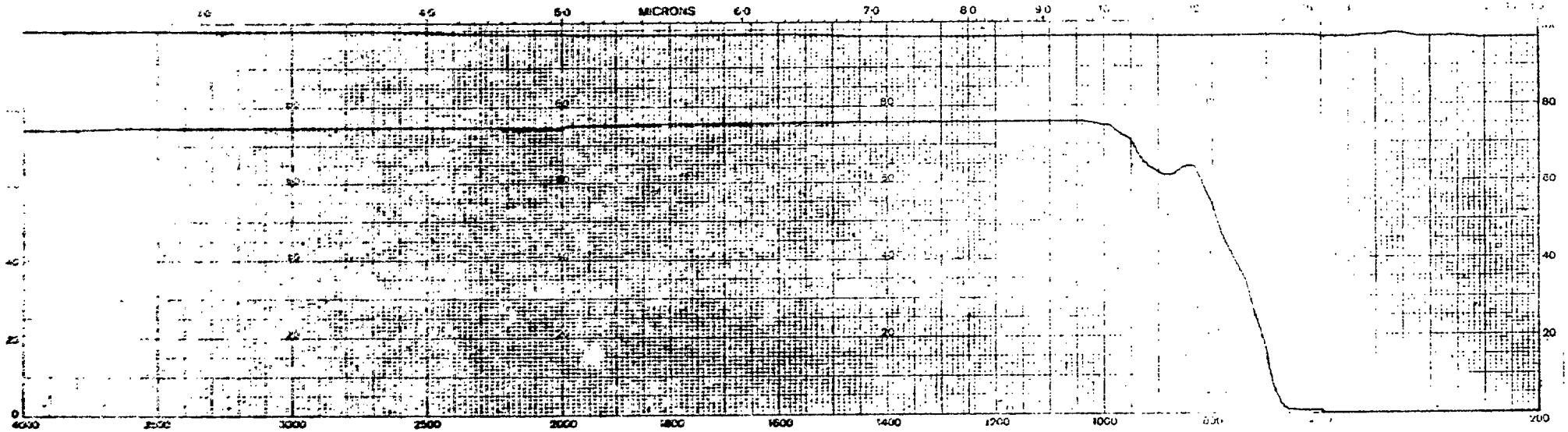

Fig. 2-9. Infrared Transmittance of CVD ZnS AF-1 HIP Processed at 990 C, 15 ksi for 25 h, Pt Wrapped.

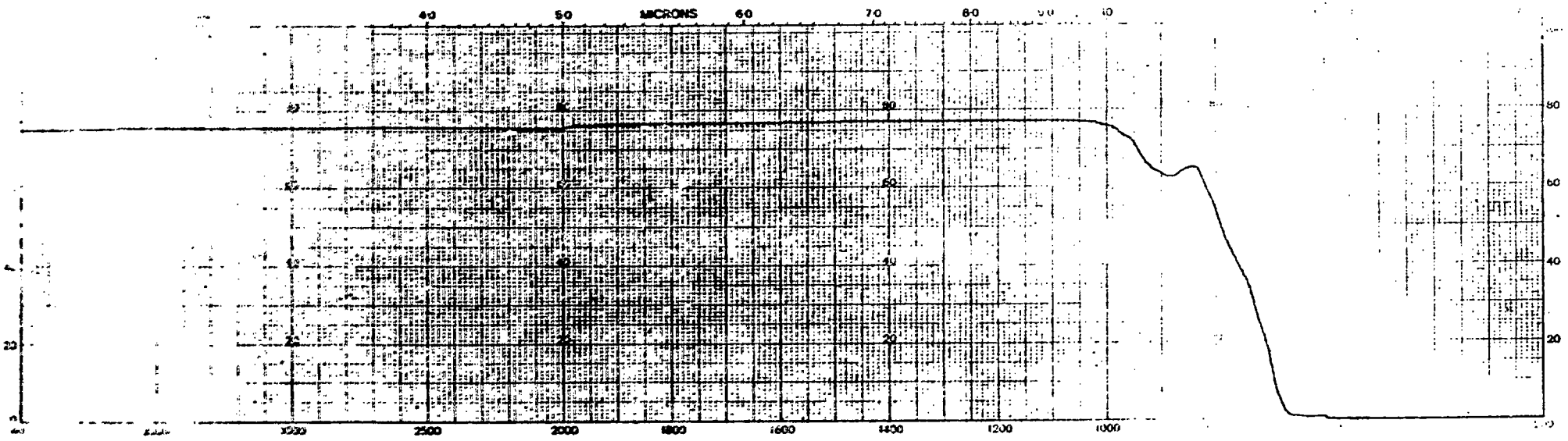

Fig. 2-10. Infrared Transmittance of CVD ZnS AF-2 HIP Processed at 990 C, 15 ksi for 25 h, Pt Wrapped.

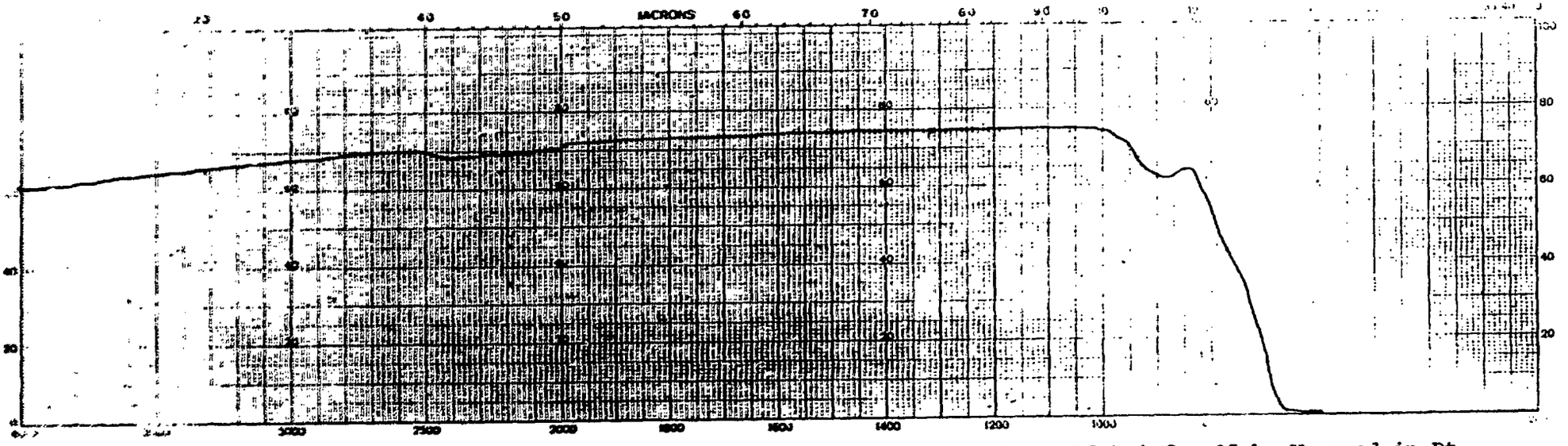

Fig. 2-11. Infrared Transmittance of CVD ZnS AF-3, HIP Processed at 990 C, 15 ksi for 25 h, Wrapped in Pt.

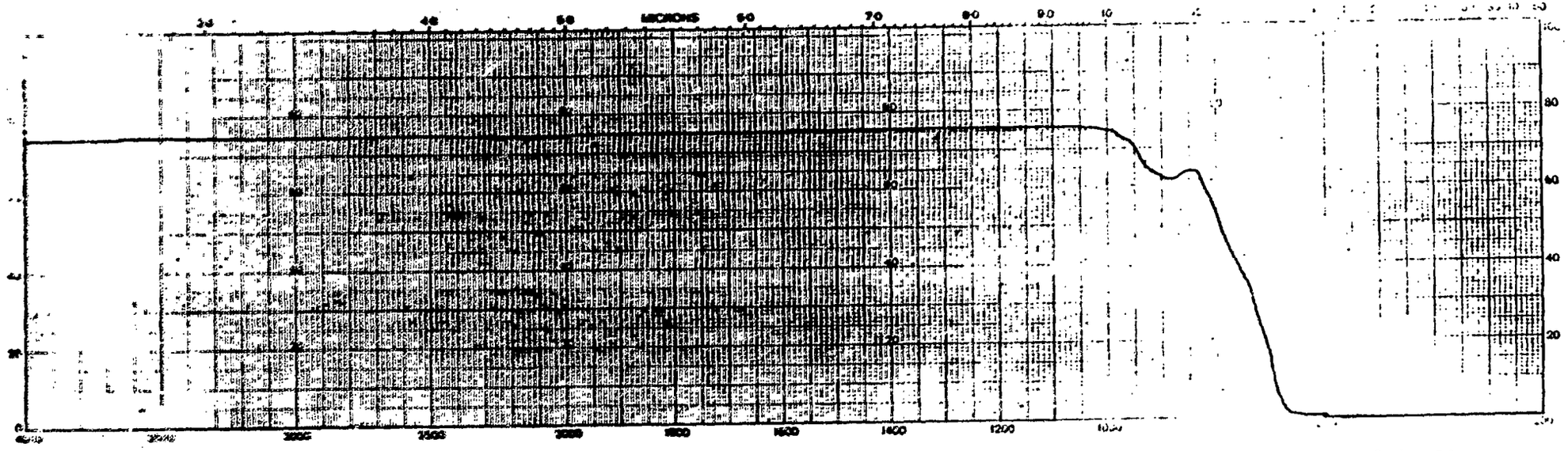

Fig. 2-12. Infrared Transmittance of CVD ZnS AF-4, HIP Processed at 990 C, 15 ksi for 25 h, Wrapped in Pt.

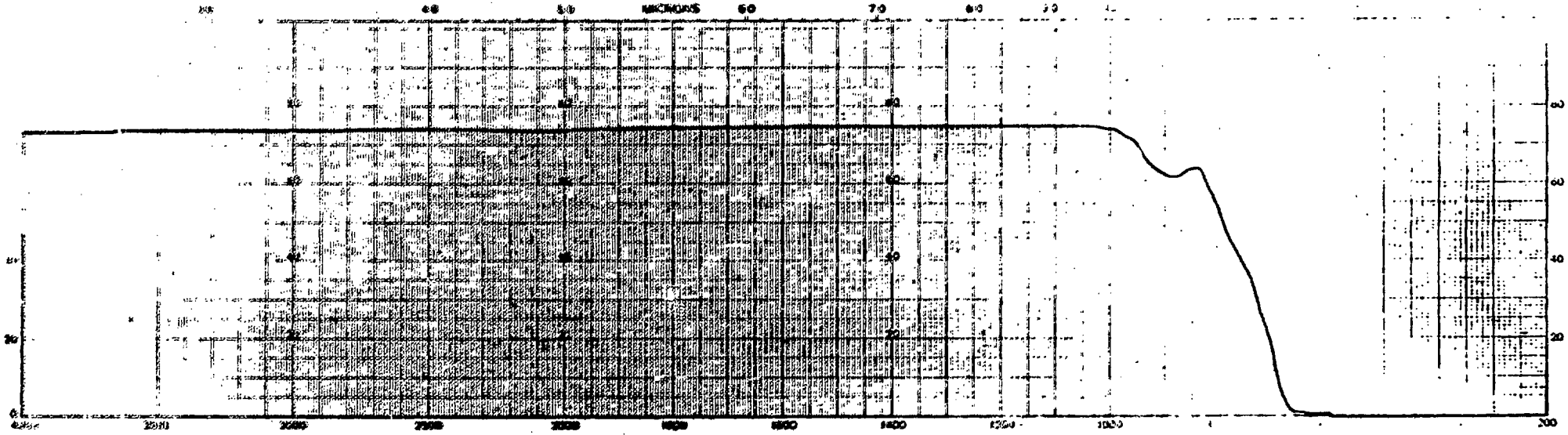

Fig. 2-13. Infrared Transmittance of CVD ZnS AP-5, HIP Processed at 990 C, 15 ksi for 25 h, Pt Wrapped.

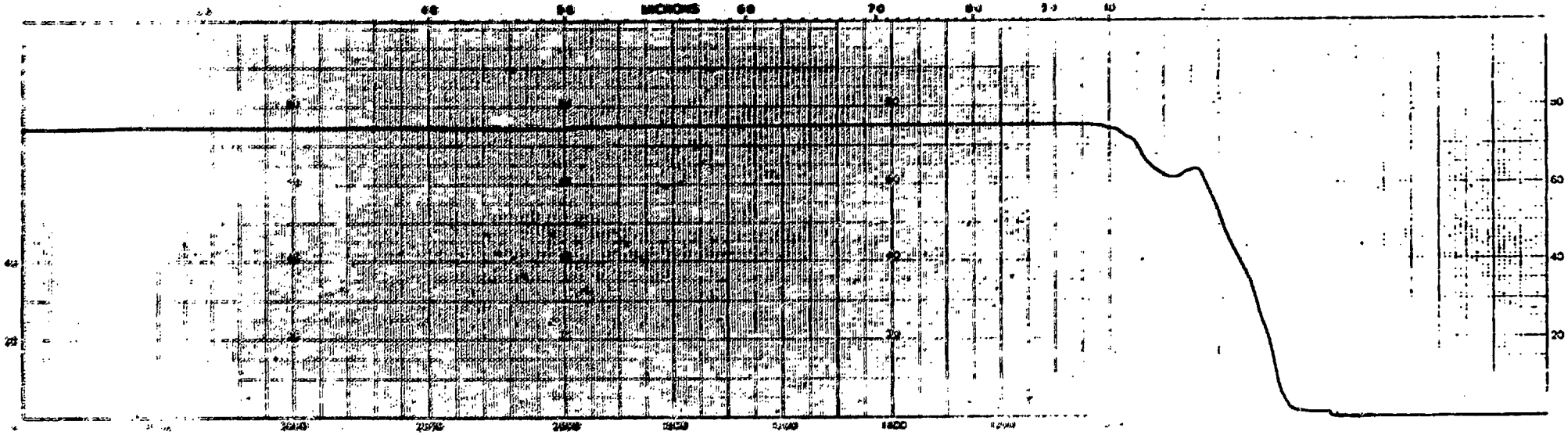

Fig. 2-14. Infrared Transmittance of CVD ZnS AP-6, HIP Processed at 990 C, 15 ksi for 25 h, Pt Wrapped.

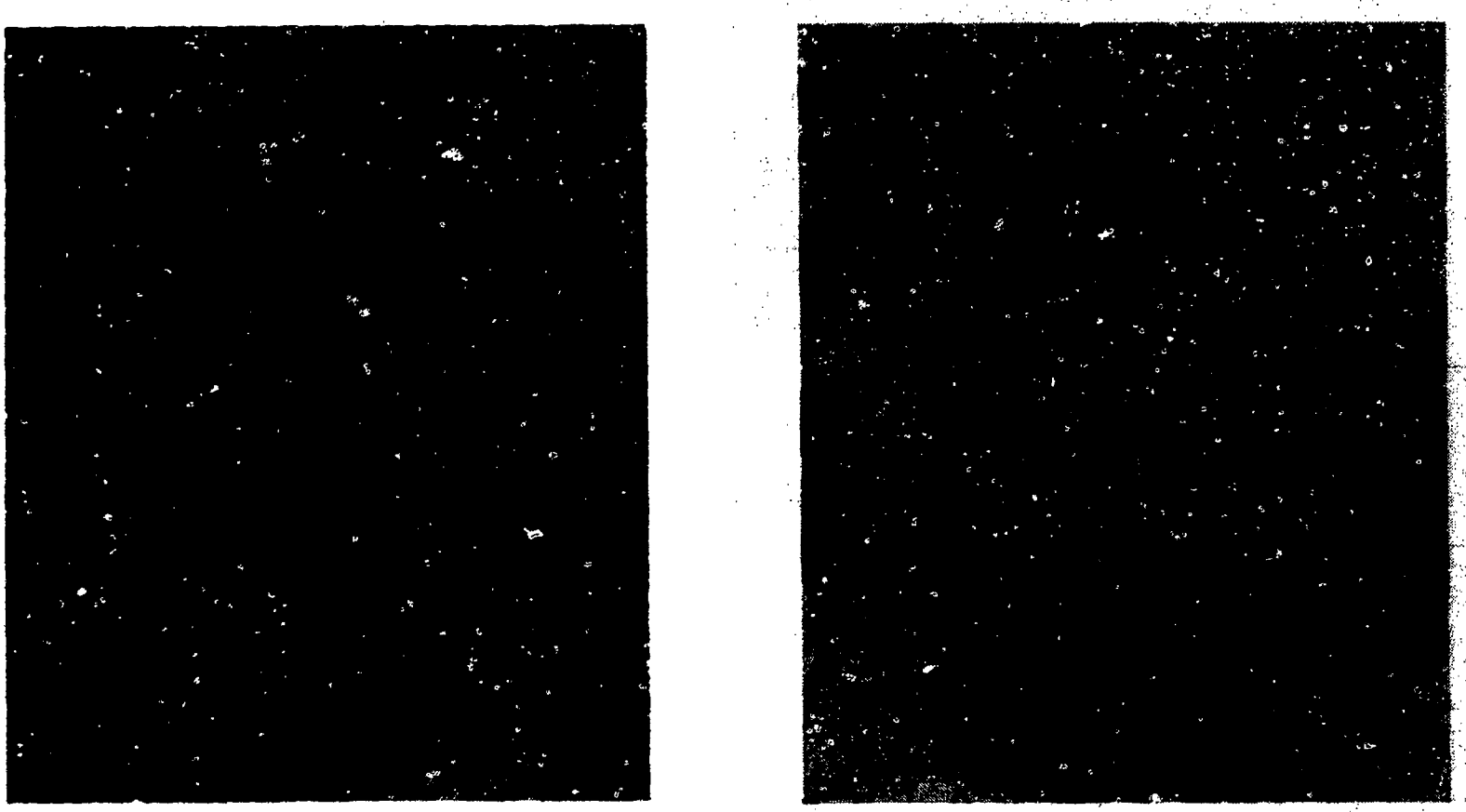

(a) (b)

Figure 2-15. Photomicrographs of Etched Surface of CVD ZnS AF-4 as Deposited (a) and HIP Processed (b), 250x.

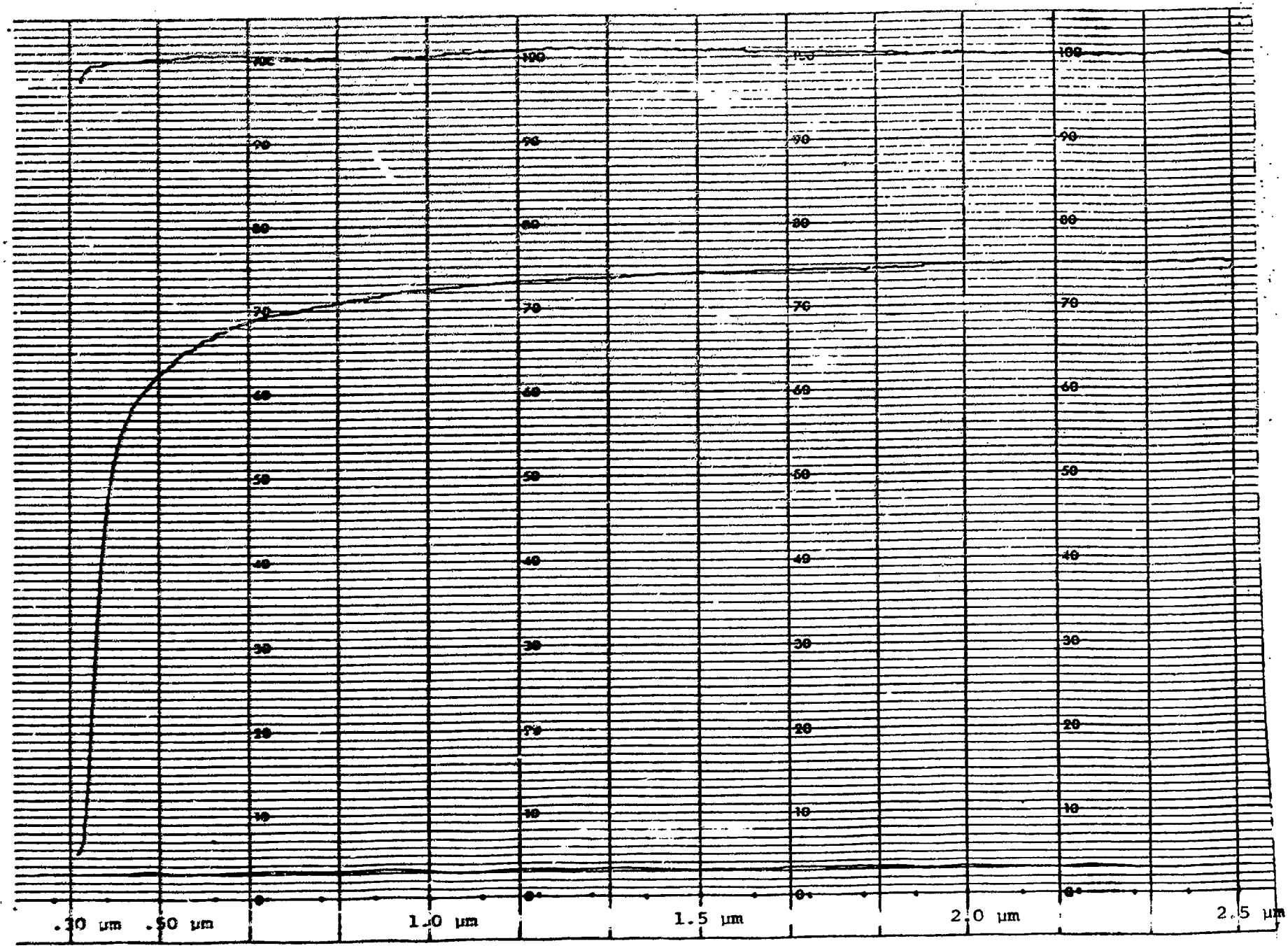

Fig. 2-16. Visible-Near Infrared Transmittance of ZnS AF-1 HIP Processed at 990 C,

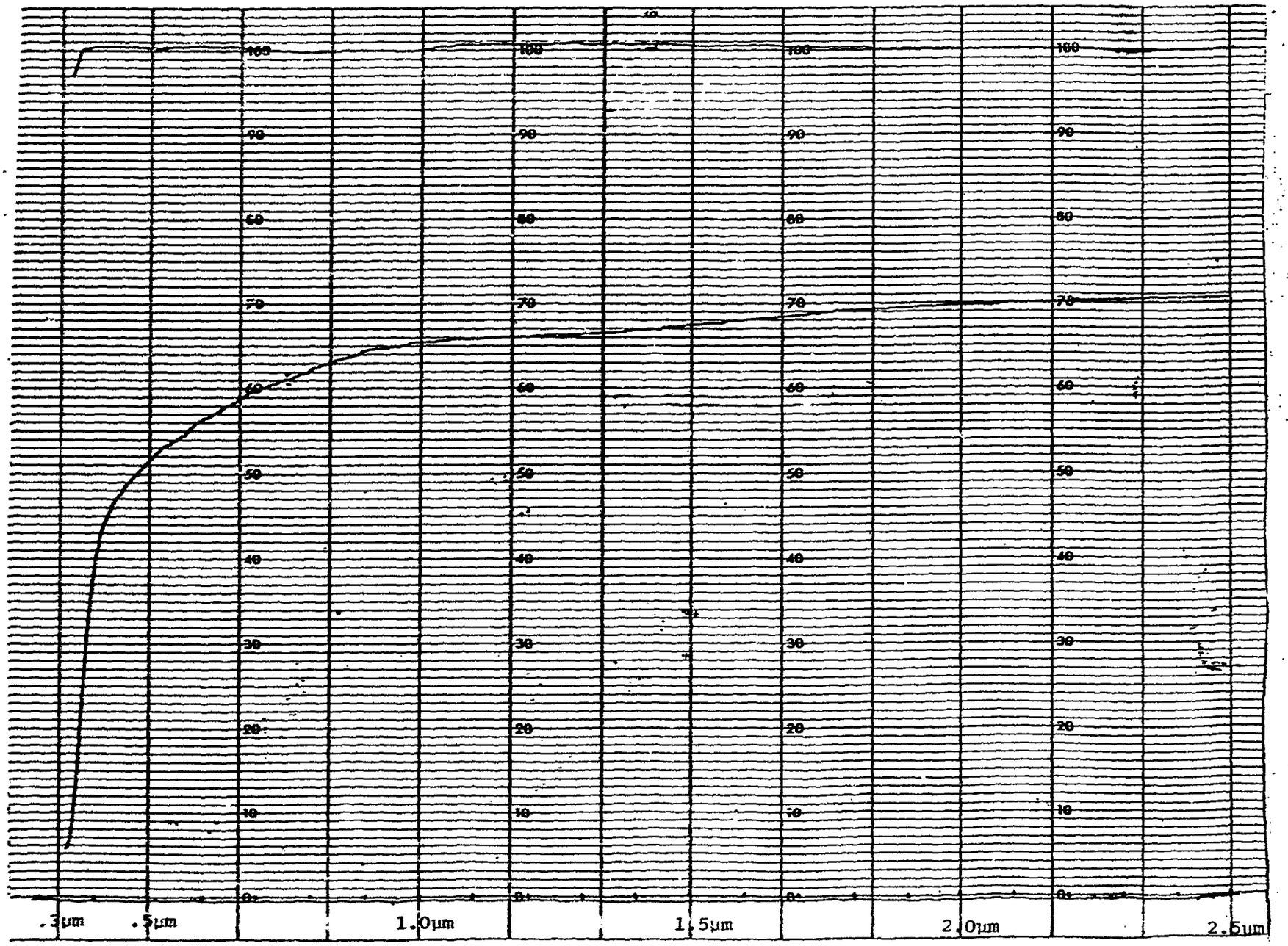

Fig. 2-17. Visible-Near Infrared Transmittance of ZnS AF-1 HIP Processed at 990 C, 30 ksi for 25 h, Pt Wrapped.

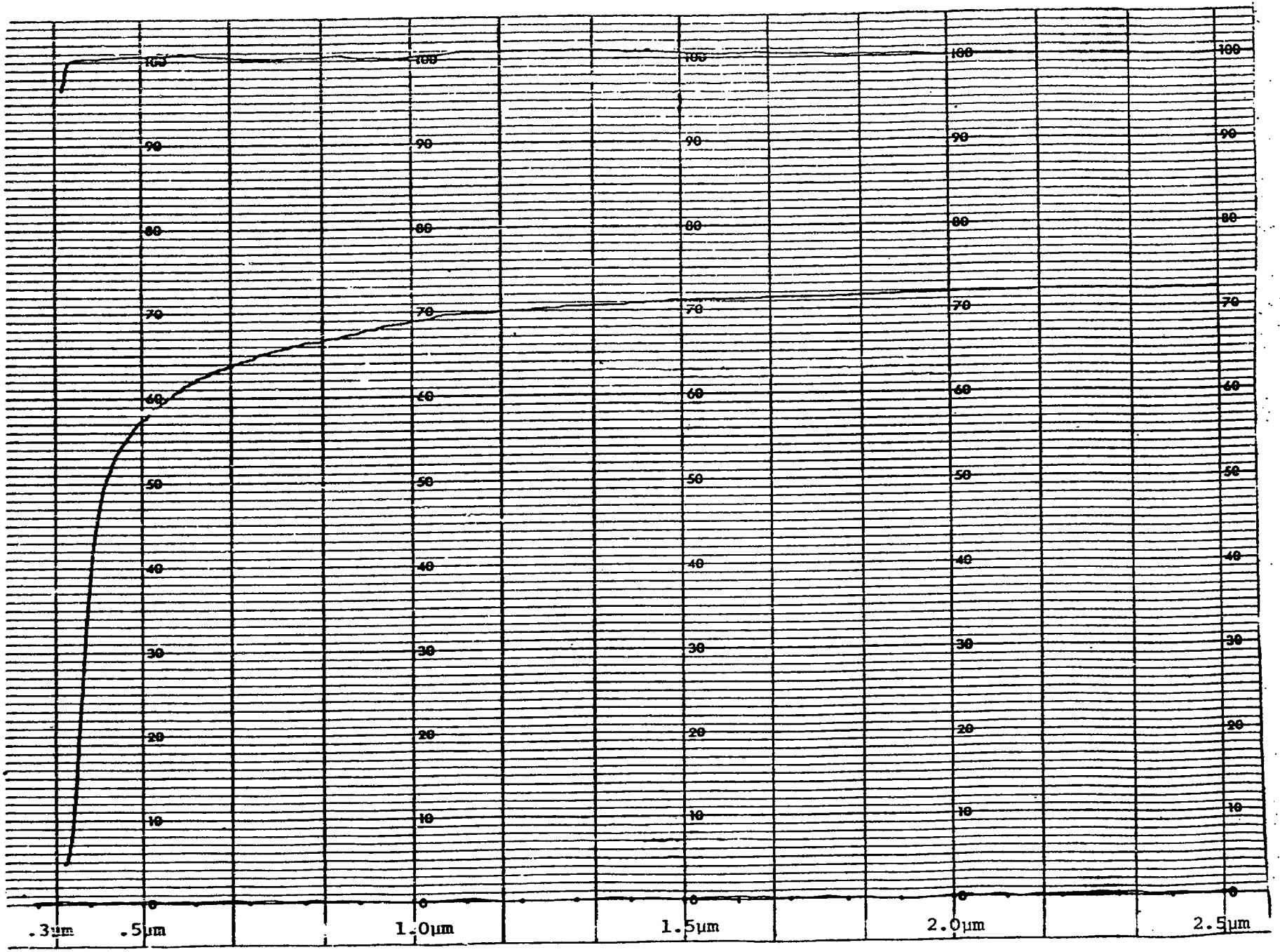

Fig. 2-18. Visible-Near Infrared Transmittance of ZnS AF-2 HIP Processed at 990 C, 15 ksi for 25 h, Pt Wrapped.

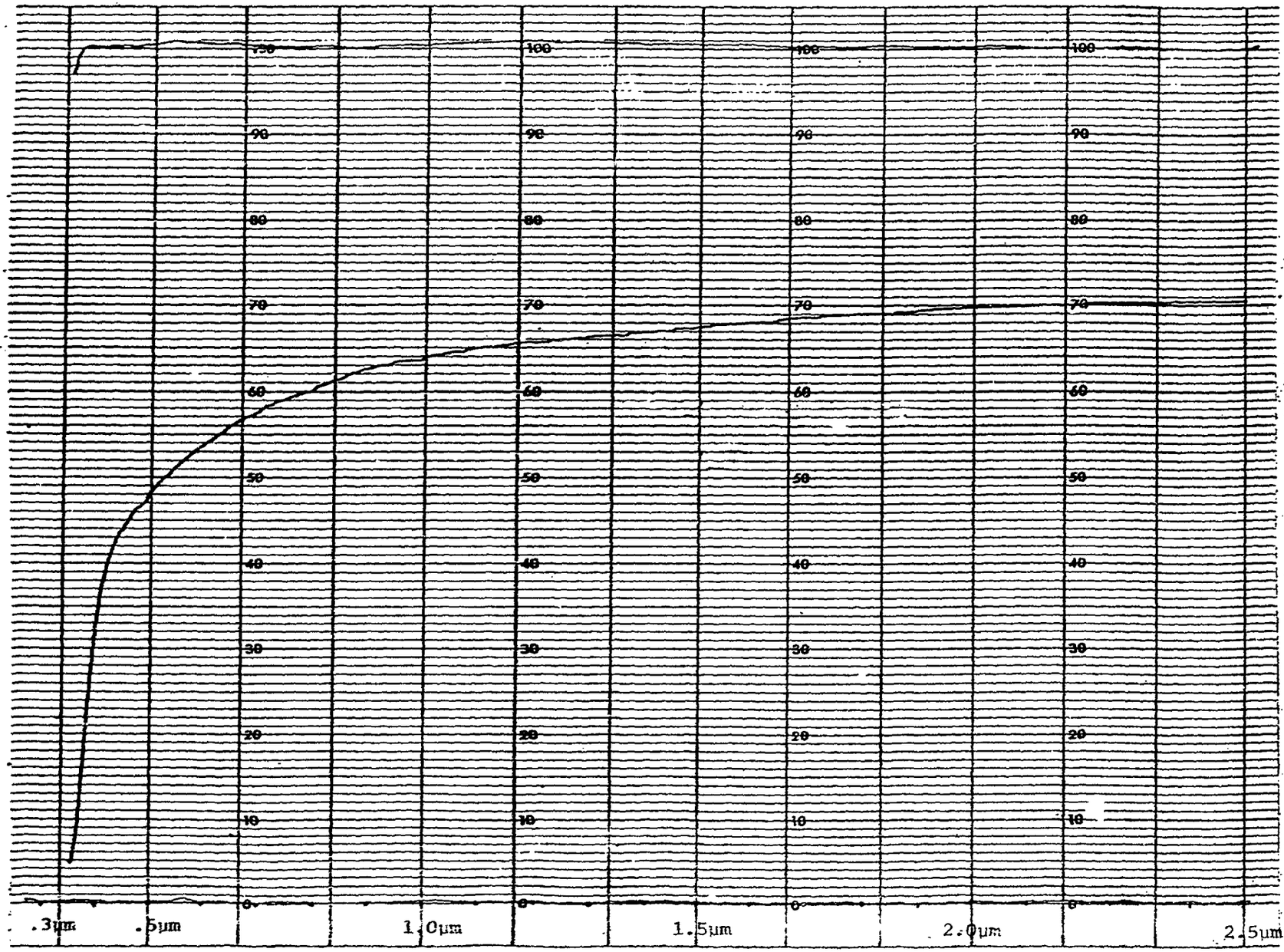

Fig. 2-19. Visible-Near Infrared Transmittance of ZnS AF-2 HIP Processed at 990 C, 30 ksi for 25 h, Pt Wrapped.

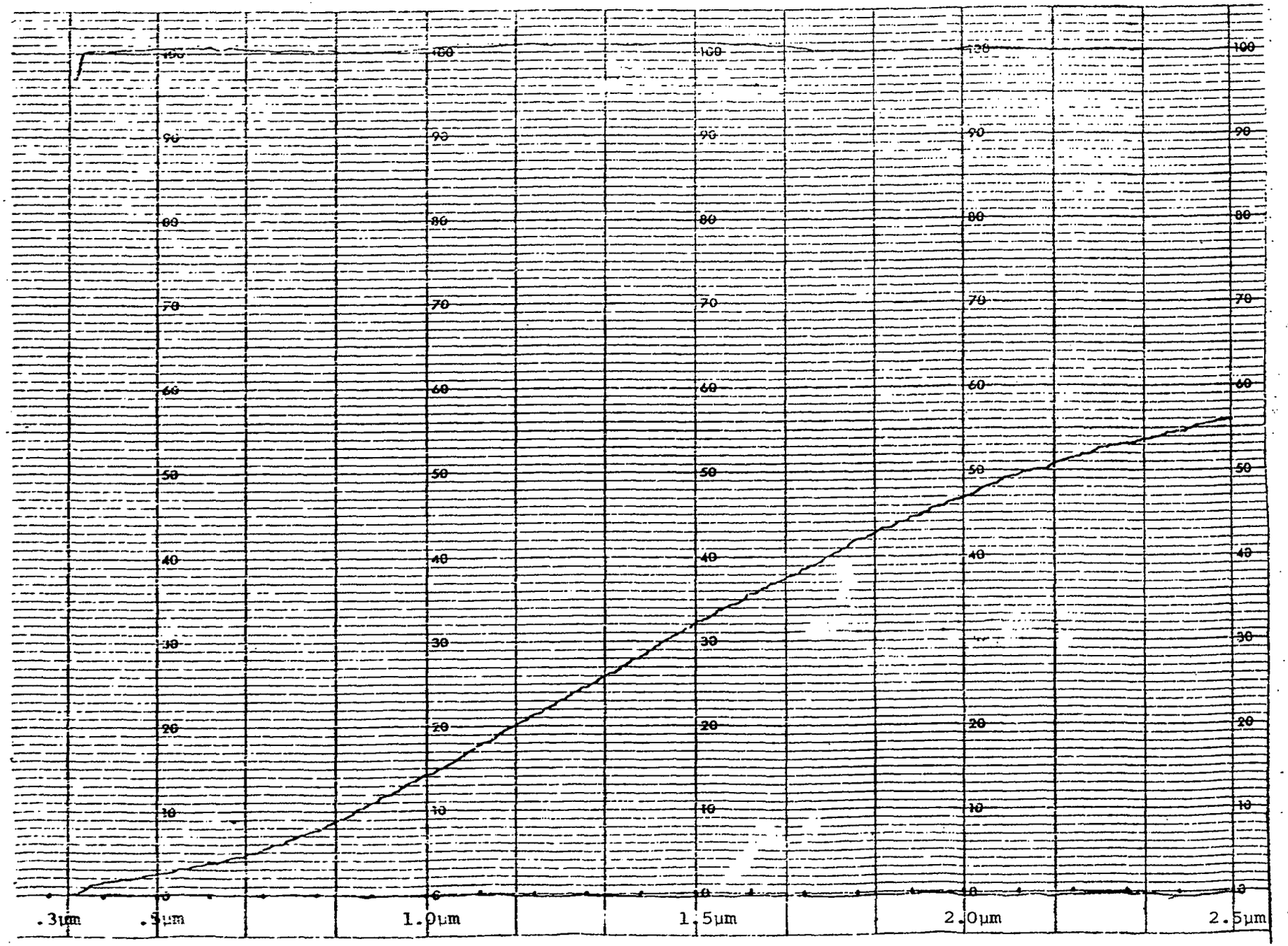

Fig.2-20. Visible-Near Infrared Transmittance of ZnS AF-3 HIP Processed at 990 C, 30 ksi for 25 h, Pt Wrapped.

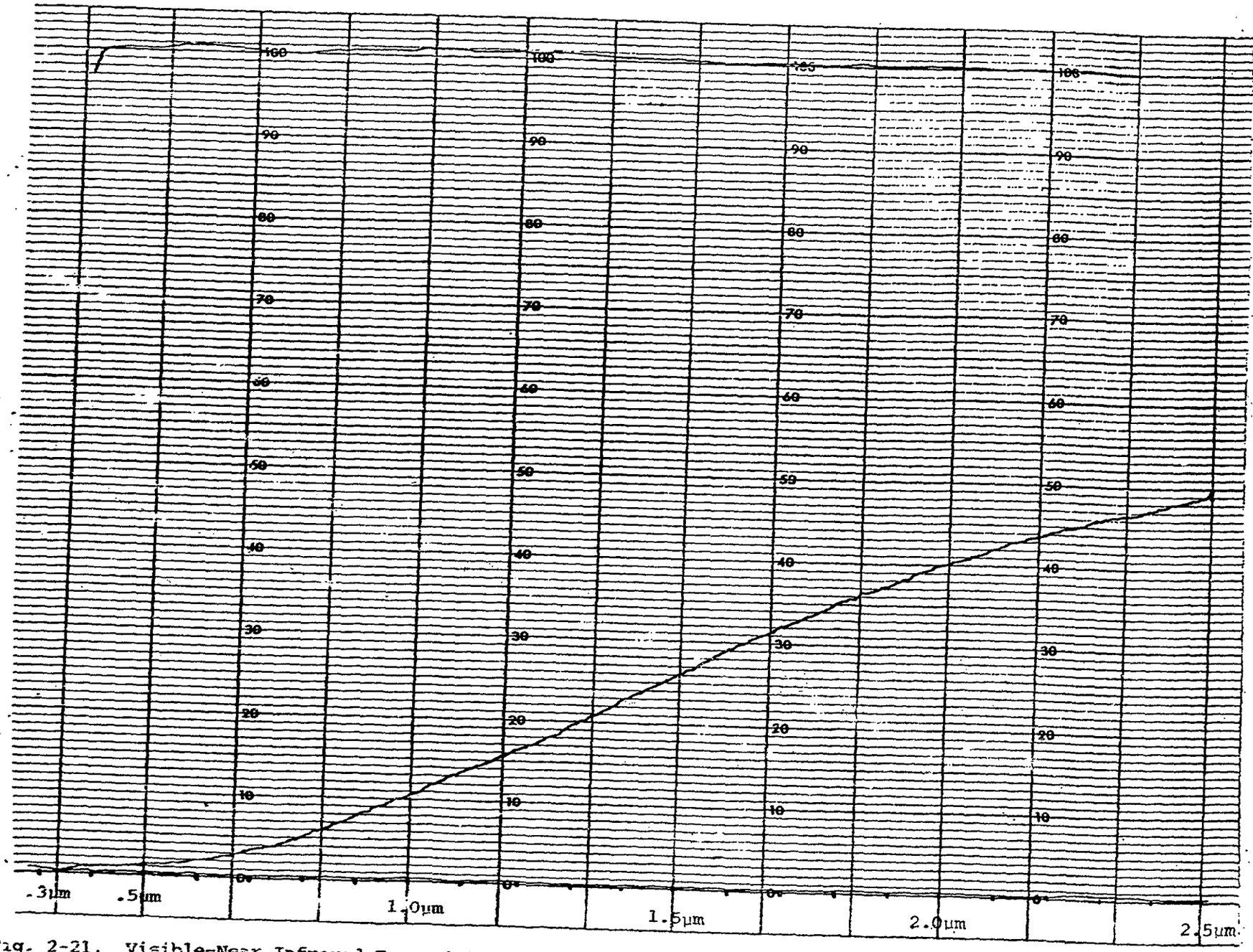

Fig. 2-21. Visible-Near Infrared Transmittance of ZnS AF-3 HIP Processed at 990 C, 15 ksi for 25 h, Pt Wrapped.

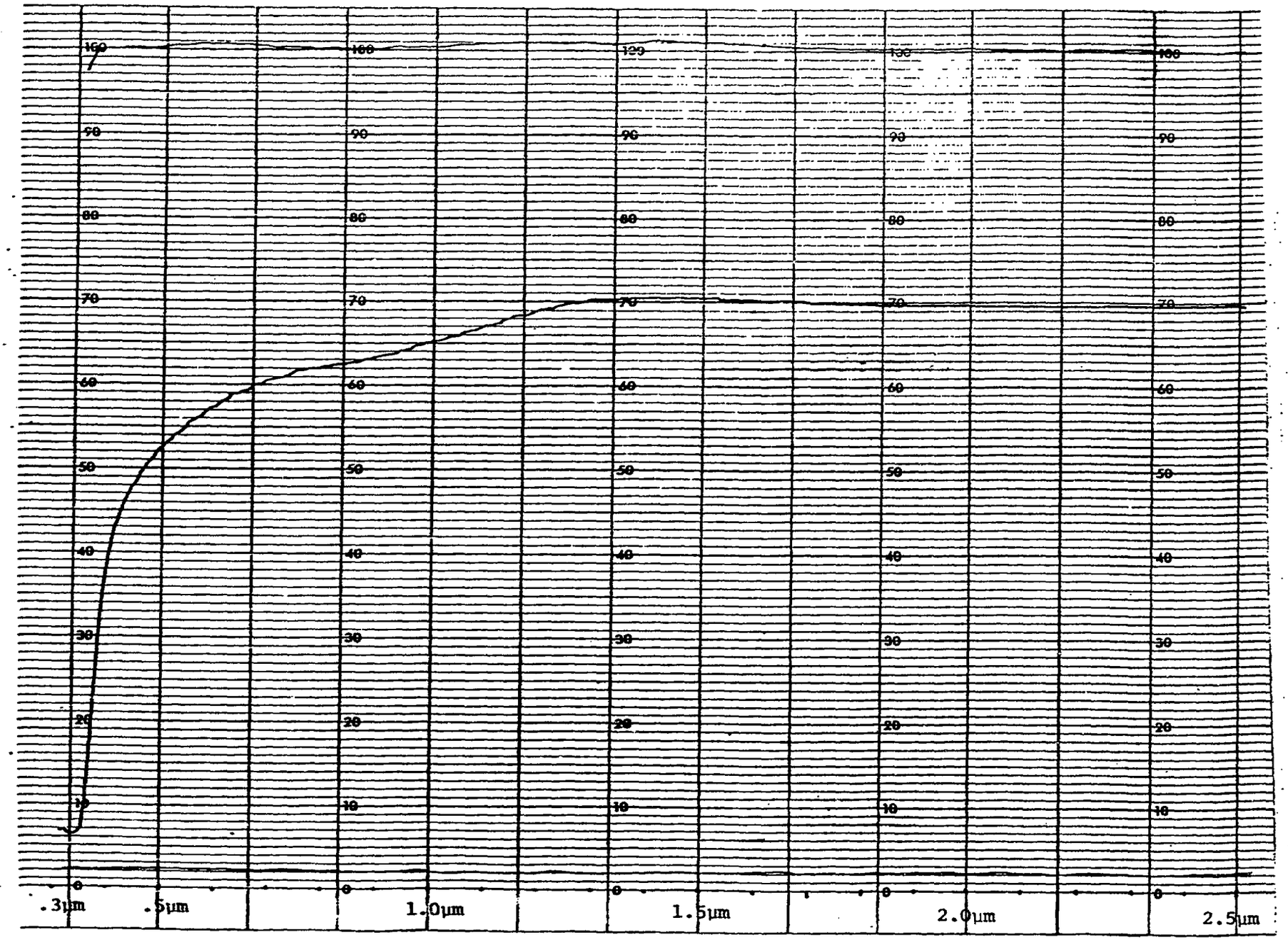

Fig. 2-23. Visible-Near Infrared Transmittance of ZnS AF-4 HIP Processed at 990 C, 30 ksi for 25 h, Pt Wrapped.

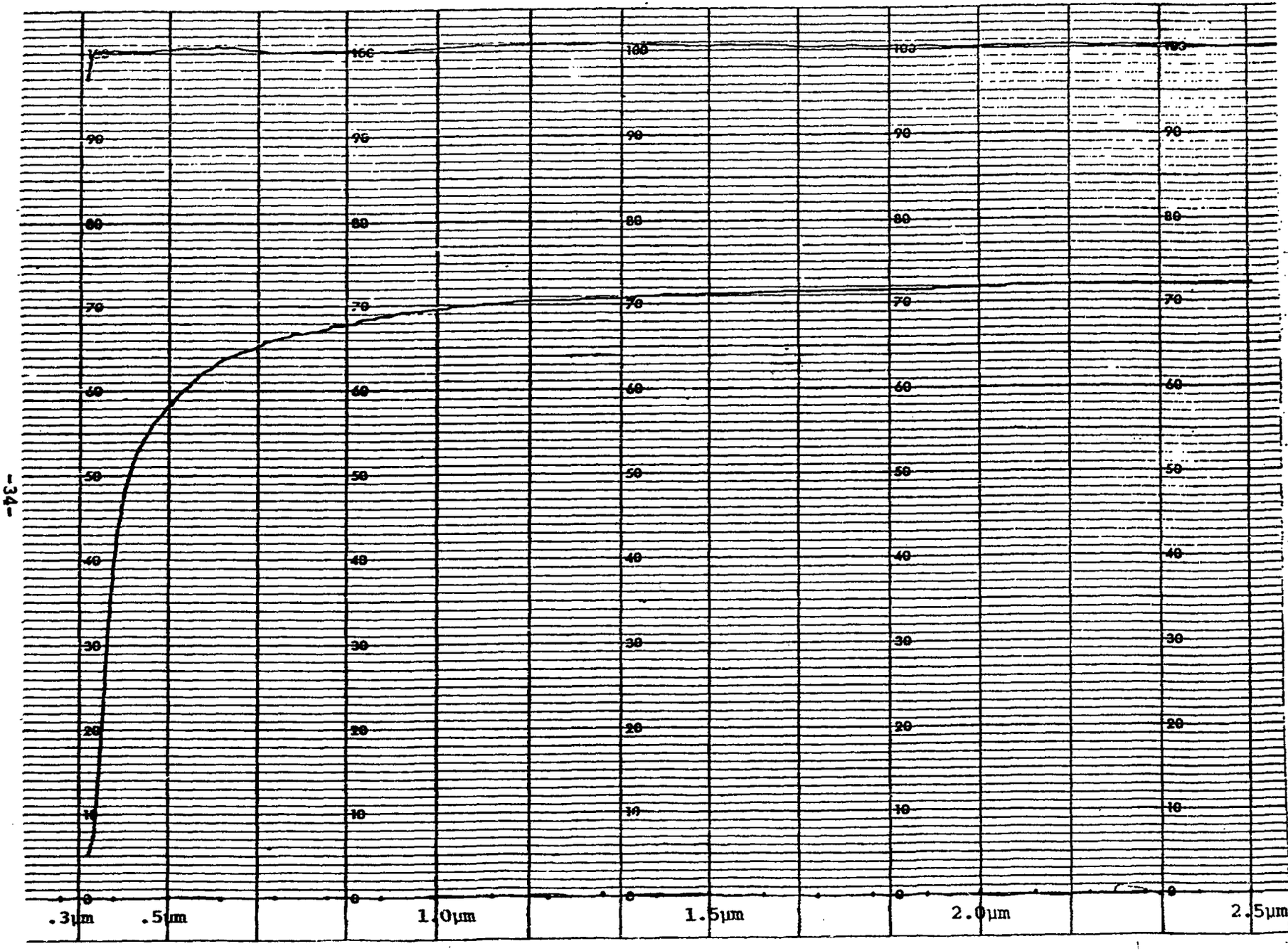

Fig. 2-22. Visible-Near Infrared Transmittance of ZnS AF-4 HIP Processed at 990 C, 15 ksi for 25 h, Pt Wrapped.

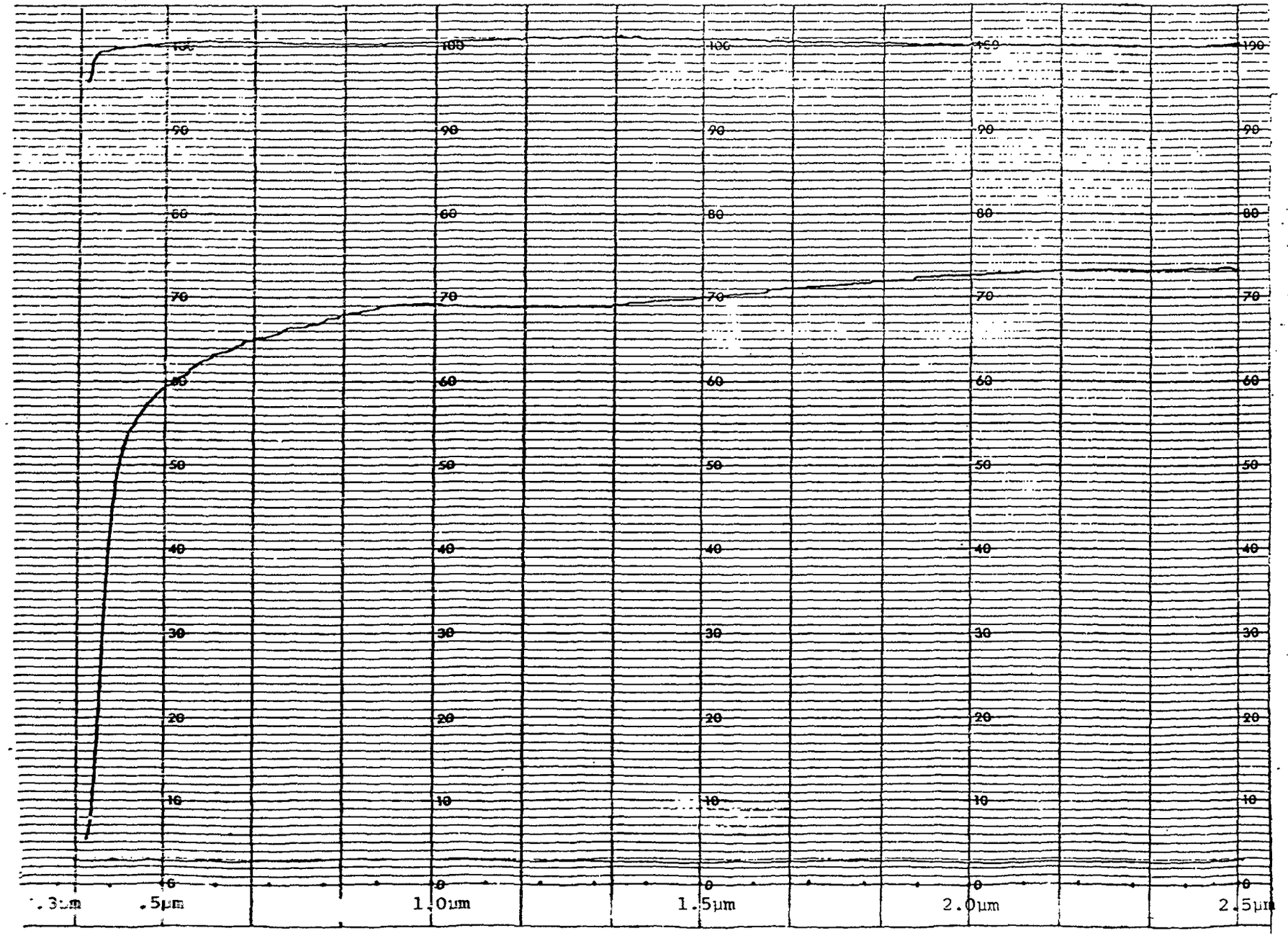

Fig. 2-24. Visible-Near Infrared Transmittance of ZnS AF-5 HIP Processed at 990 C, 15 ksi for 25 h, Pt Wrapped.

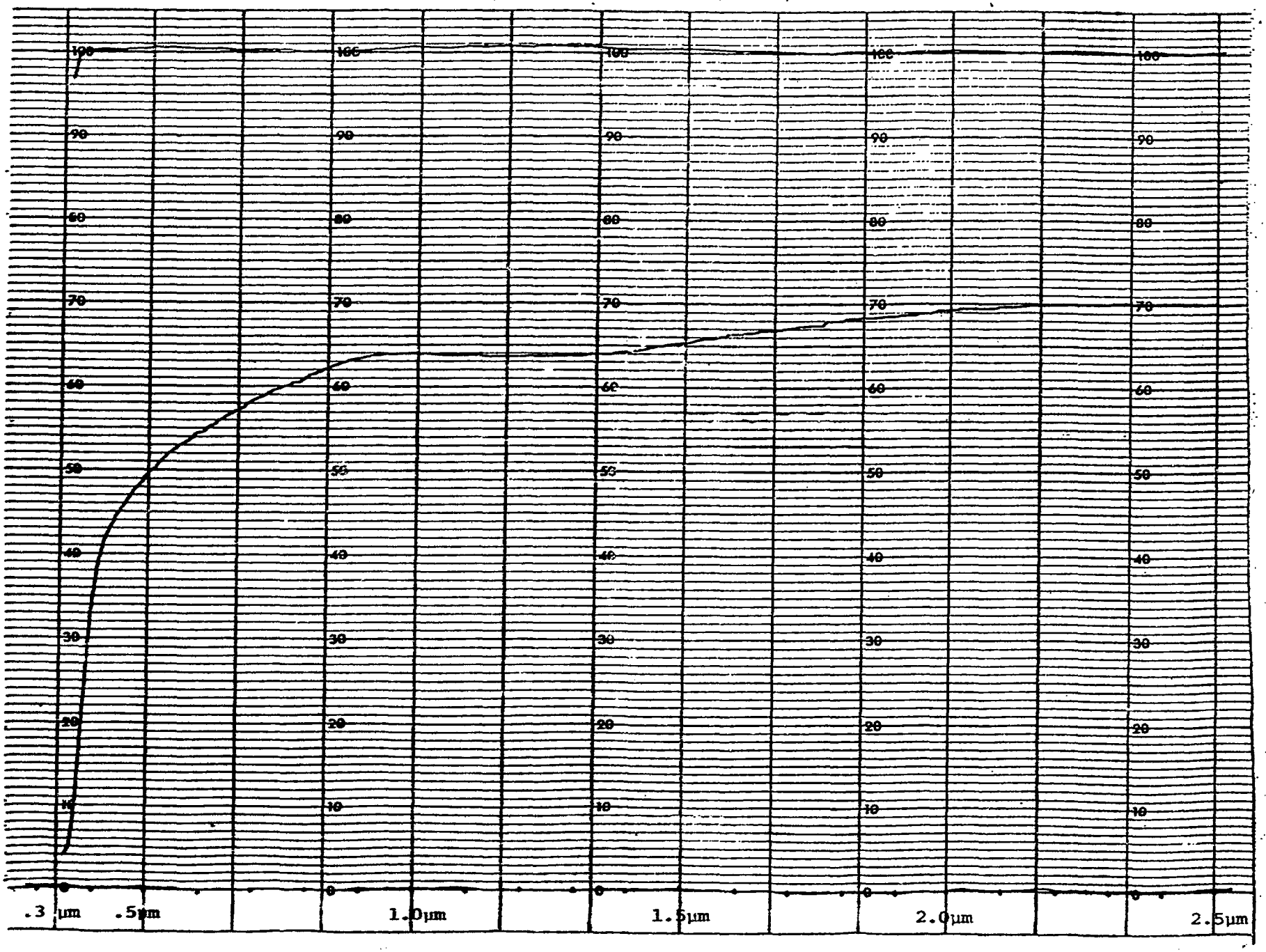

Fig. 2-25. Visible-Near Infrared Transmittance of ZnS AF-5 HIP Processed at 990 C, 30 ksi for 25 h, Pt Wrapped.

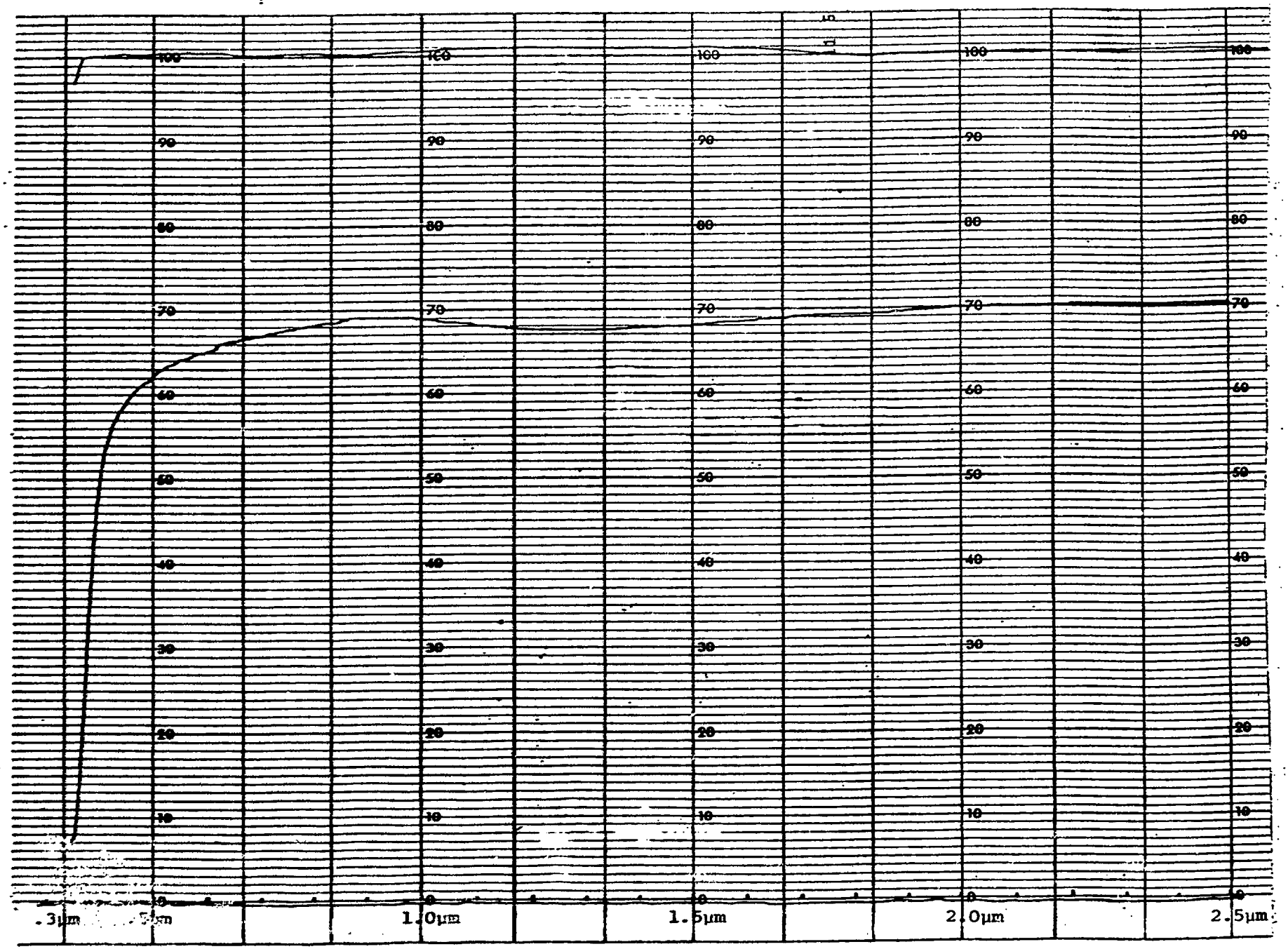

Fig. 2-26. Visible-Near Infrared Transmittance of ZnS AF-6 HIP Processed at 990 C, 15 ksi for 25 h, Pt Wrapped.

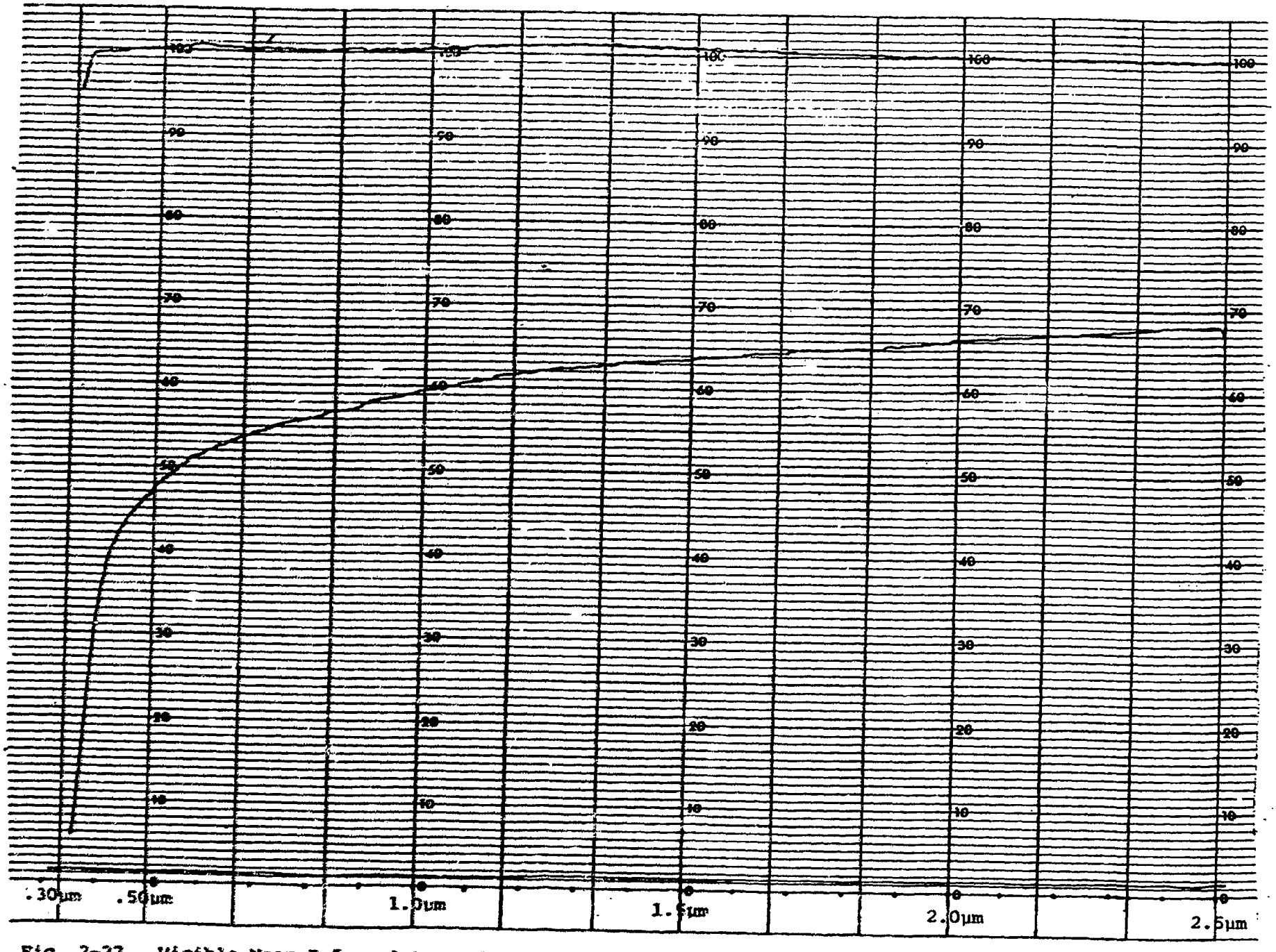

Fig. 2-27. Visible-Near Infrared Transmittance of ZnS AF-6 HIP Processed at 990 C, 30 ksi for 25 h, Pt Wrapped.

HIP runs IV, V, X and XI were processed at 1047 C using different pressures and enclosures. This increase in processing temperature caused a large crystal growth in the material, leaving a grainy surface difficult to optically fabricate. This material displays an increased scatter at shorter wavelengths when compared with material processed at 990 C. This degradation is in part due to the large crystals and resultant poor surface figure. Although the previous HIP runs performed at 990 C yielded material which showed consistently higher transmission when wrapped in platinum, such was not the case with material HIP processed at 1047 C. As can be seen from a comparison of the infrared transmittance curves of AF-4 (Figs. 2-28 and 2-29), HIP processed at 1047 C, 15 ksi, and 12.5 h, the graphite enclosed ZnS displays a higher transmittance in the near infrared than material processed with platinum. The Knoop hardness of material HIP processed at 1047 C is similar to material processed at 990 C (Table 2-5). ZnS processed from HIP XI has a relatively high Knoop hardness average of 184 but also exhibited a large variation in values.

The remaining HIP processing runs were performed at 1067 C and 1110 C with differing wrapping material and pressure. As was expected, there was large grain growth (Fig. 2-30a) with some of the crystallites approaching one cm in diameter. The material also exhibited cracking along grain boundaries (Fig. 2-30b), especially prevalent in the material processed at 1110 C. Table 2-6 shows the Knoop hardness values for the material processed at high temperatures, and as can be seen, a few values are quite high, e.g., 257 and 260. It appears that as the HIP temperature increases, so do the corresponding Knoop hardness values. It is thought that this may be due to boundary effects and does not necessarily represent a typical hardness of the material. There is also considerable scatter in the Knoop hardness values for these samples processed at high temperatures. In any event, the large grains and cracks which form at these high HIP processing temperatures preclude those conditions from any practical usage of this material in optical applications. The added short wavelength scatter evident from these samples along with the difficulty in fabricating an adequate optical surface eliminate these high processing temperatures from any further consideration.

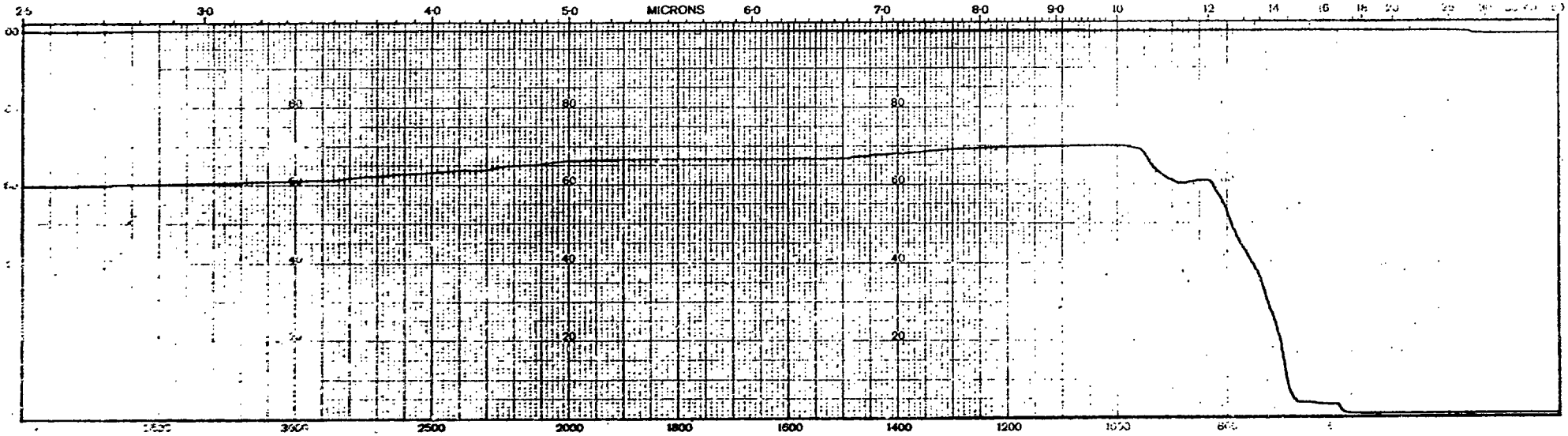

Fig. 2-28. Infrared Transmittance of CVD ZnS AF-4, HIP Processed at 1047 C, 15 ksi for 12.5 h, Pt Wrapped.

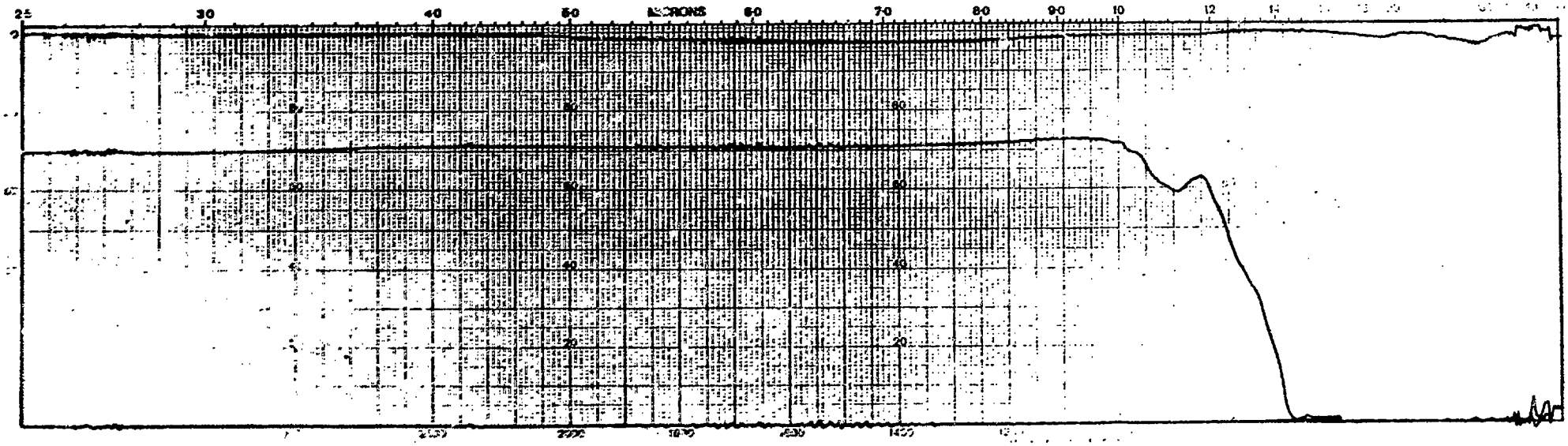

Fig. 2-29. Infrared Transmittance of CVD ZnS AF-4, HIP Processed at 1047 C, 15 ksi for 12.5 h, Graphite Enclosed.

TABLE 2-5

Knoop Hardness (HK_{50}) Water-Clear ZnS

Run	HIP I 990 C 15K 25h Pt	HIP II 990 C 30K 25h Pt	HIP III 990 C 30K 2.5h Pt	HIP IV 1047 C 15K 12.5h Graphite	HIP V 1047 C 30K 12.5h Graphite	HIP X 1047 C 15K 12.5h Pt	HIP XI 1047 C 15K 12.5h Pt
AP-1	176	169	174	161	159	173	189
AP-2	175	161	168	169	168	172	177
AP-3	177	170	180	165	182	177	202
AP-4	160	153	163	169	155	180	175
AP-5	159	172	168	166	170	174	181
AP-6	164	168	168	176	165	181	177

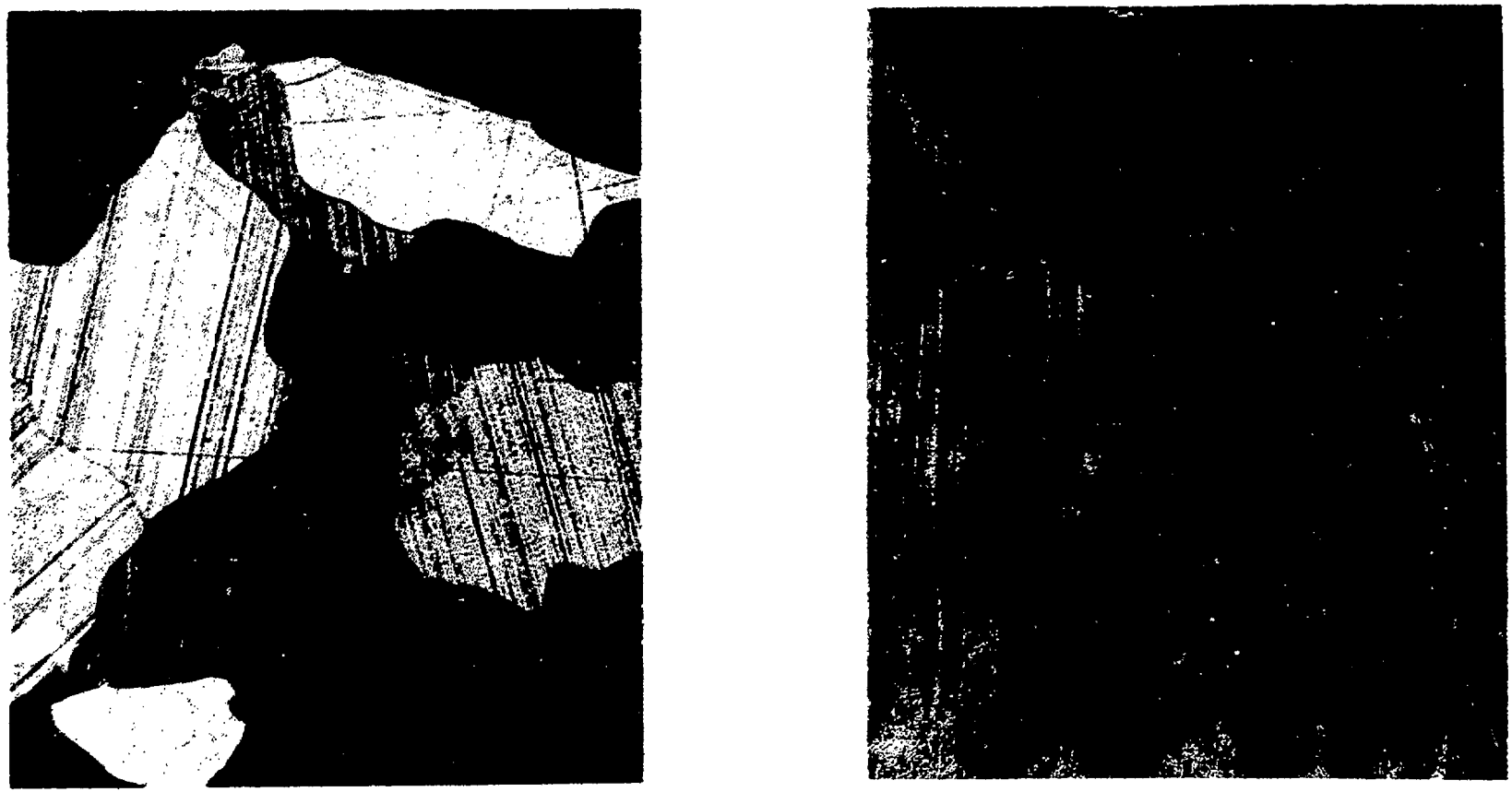

(a) (b)

Figure 2-30. Photomicrograph of CVD ZnS After HIP Processing at 1067 C (a) and 1110 C (b), 30 ksi for 12.5 h, Pt wrapped, 100x.

TABLE 2-6

Knoop Hardness (HK_{50}) Water-Clear ZnS

Run	HIP VI 1067 C 15 ksi 12.5 h Graphite	HIP VII 1067 C 30 ksi 12.5 h Graphite	HIP VIII 1110 C 15 ksi 12.5 h Graphite	HIP IX 1110 C 15 ksi 12.5 h Graphite
AF-1	177	180	173	194
AF-2	182	195	257	188
AF-3	176	173	175	170
AF-4	192	183	168	260
AF-5	181	187	---	215
AF-6	190	198	219	171

Although comparative ranking of the water-clear ZnS produced from the various combinations of CVD and HIP was generally possible by visual inspection, a more quantitative method was desired. For this purpose, the attenuation coefficient of the material was calculated from the visible transmission curves from the relationship:

$$I_M = I_T \, e^{-\alpha t}$$

where

I_M = measured transmittance

I_T = total theoretical external transmittance assuming only reflectance losses

$= \frac{2n}{n^2 + 1} = .73$; $n = 2.30$ at 0.7 μm

α = attenuation coefficient (cm^{-1})

t = thickness (cm)

0.7 μm was selected as the wavelength for this calculation, because it occurs in a sensitive region of the transmission curve. Attenuation coefficients calculated as described above are shown in Table 2-7 for the first three HIP conditions for all 6 CVD ZnS samples.

As is evident from the data of Table 2-7, material from AF-1, 4 and 6 produced the best water-clear ZnS. In addition, the optimum HIP conditions appear to be a temperature of 990 C, pressure of 15 ksi, platinum wrap and processing from 12-24 hours depending upon the thickness of the material. Water-clear ZnS was produced at these optimum conditions from AF-1, 4 and 6 and optically fabricated for quantitative optical testing. Visible transmission spectra were obtained and calorimetric absorption measurements made at 1.3, 2.7, and 3.8 μm on these three samples. The transmission spectra are compared in Fig. 2-31 and the absorption data are listed in Table 2-8. It is obvious from these data that material produced from AF-4 provides superior optical quality.

TABLE 2-7

Attenuation Coefficients for HIP Processed Samples

ZnS Run No. Sample No.	HIP Run	I_M at 0.7μm,%	Thickness (cm)	Attenuation (cm^{-1})
AF1-10	II*	43	0.406	1.310
AF1-12	II	60	0.437	0.453
AF1-15	III	26	0.516	2.006
AF1-19	I	69	0.513	0.109
AF2-1	II*	36	0.401	1.766
AF2-17	I	64.5	0.517	0.244
AF2-19	II	58	0.437	0.531
AF2-20	III	42.5	0.376	1.444
AF3-2	II*	0	0.610	---
AF3-4	I	3.5	0.401	7.574
AF3-6	II	5	0.406	5.229
AF3-8	III	0	0.513	---
AF4-6	III	62.5	0.516	0.305
AF4-16	II*	57.5%	0.422	0.570
AF4-18	II	59	0.386	0.556
AF4-20	I	66	0.516	0.199
AF5-A	II	58.8	0.378	0.576
AF5-A1	II*	16.5	0.373	3.988
AF5-A2	I	62.5	0.424	0.370
AF5-A3	III	5.5	0.574	4.508
AF6-B	II	53.5	0.445	0.703
AF6-B1	II*	25.2%	0.419	2.542
AF6-B2	I	67	0.422	0.203
AF6-B3	III	61.8	0.518	0.325

* HIP processed in graphite crucible only.

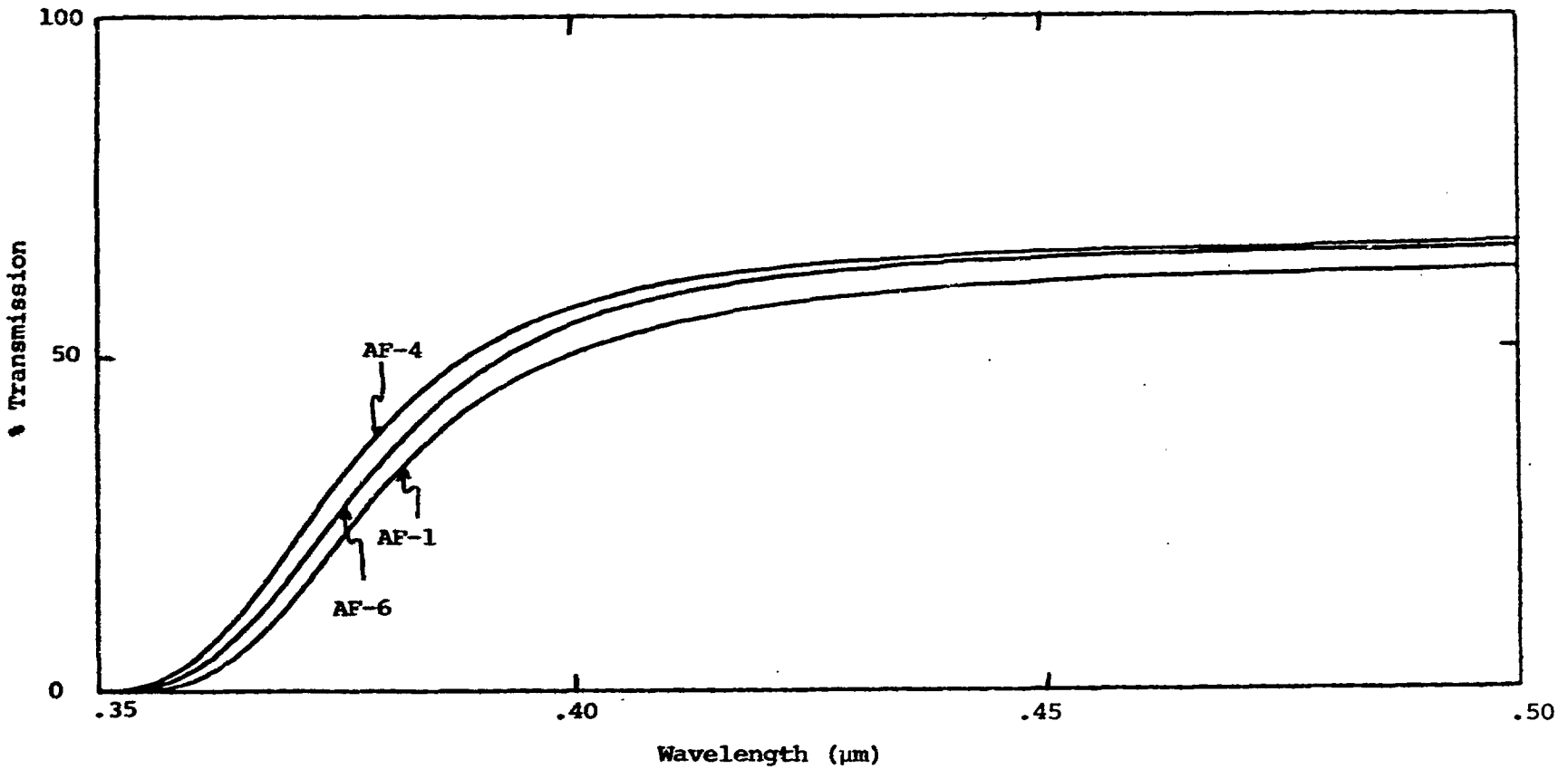

Fig.2-31. Visible Transmittance AF-1, 4, and 6 Water-Clear ZnS

TABLE 2-8

Effective Absorption Coefficient, Water-Clear ZnS*

$\beta_{eff} \times 10^{-3}$ cm^{-1}

Sample	1.3 μm	2.7 μm	3.8 μm
AF-1A	13.6	17.1	16.4
AF-1B	16.2	21.3	20.7
AF-4A	3.15	5.16	2.91
AF-4B	2.98	5.33	2.29
AF-4C	2.62	---	---
AF-4D	0.956	---	---
AF-6A	5.88	15.7	7.63
AF-6B	10.0	21.6	9.23

*Effective absorption includes surface losses

Flexural strength measurements were also performed on water-clear ZnS HIP processed at 990 C, 15 ksi, 12.5 h. and Pt wrapped from AF-1, 4 and 6. As can be seen from Table 2-9, AF-4 has a slightly higher flexural strength than AF-1 and 6, although this difference is within the scatter of the data.

Various atmospheric pressure heat treatment experiments were performed, followed by HIP processing. Table 2-10 shows the process conditions. To avoid surface oxidation, the heat treatments were carried out in one atmosphere of argon. The optical quality of the heat treated material displayed substantial increases in scatter and absorption at all processing temperatures. The heat treated material has a milky white appearance and is non-transmissive in the visible spectrum. Figs. 2-32 and 2-33 show the infrared transmittance of the best optical heat treated ZnS. In following the trend of all post deposition, high temperature processes, there is a substantial increase in grain size and corresponding softening typical of material HIP processed at similar temperatures.

The heat treated ZnS was next subject to HIP processing at 990 C 15 and 30 ksi, 25 h and wrapped in platimum. As is evident from infrared transmittance curves (Figs. 2-34 and 2-35) which represent the best results, the optical quality has been improved over the non-Hip processed, heat-treated ZnS, but still remains well below the optimum water-clear ZnS. Apparently the heat treatment locks in the scatter sites making subsequent HIP treatments less effective. Predictably, the Knoop hardness of the heat treated and HIP processed material did not degrade further as can be seen from Tables 2-11 and 2-12.

TABLE 2-9

Flexural Strength Water-Clear ZnS

HIP 990 C, 15 ksi, 12.5 h, Pt

Run	HIP Conditions	Flexural Strength (psi)
AF-1	990°C 15 ksi 12.5 h Pt	8300 ± 1600
AF-4		8700 ± 700
AF-6		8300 ± 1000

TABLE 2-10

Heat Treatment Conditions, 1 Atmosphere Argon

Run	Temperature °C	Time h	Enclosure
HT-1	990	25	Platinum
HT-2	990	25	Graphite
HT-3	1047	12.5	Platinum
HT-4	1047	12.5	Graphite
HT-5	1067	12.5	Platinum
HT-6	1067	12.5	Graphite
HT-7	1110	12.5	Platinum
HT-8	1110	12.5	Graphite

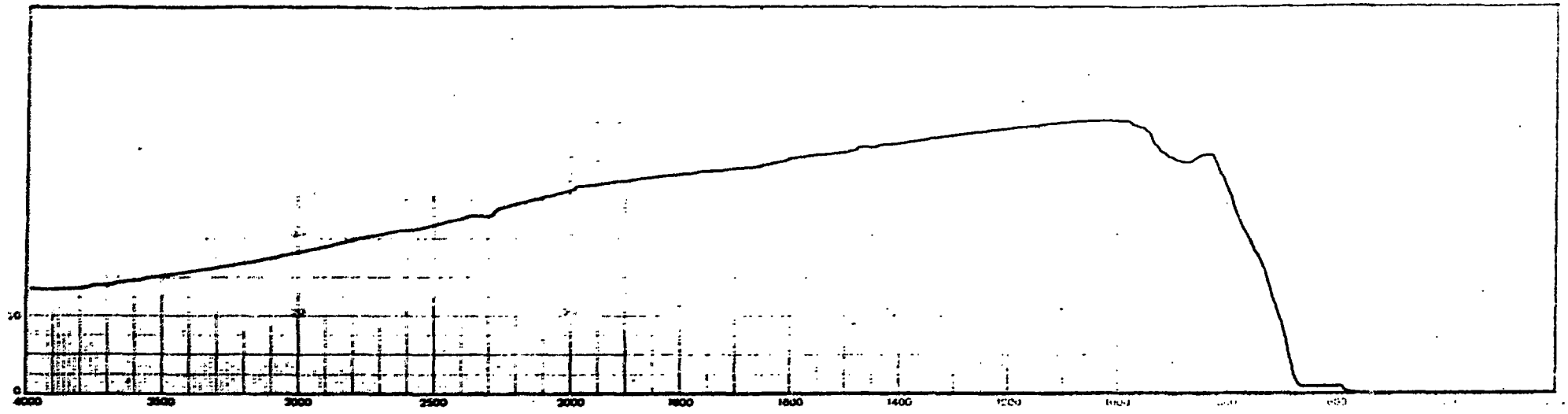

Fig. 2-32. Infrared Transmittance of CVD ZnS AF-4, Heat Treated at 990 C, 1 atm, for 25 h, Pt Wrapped.

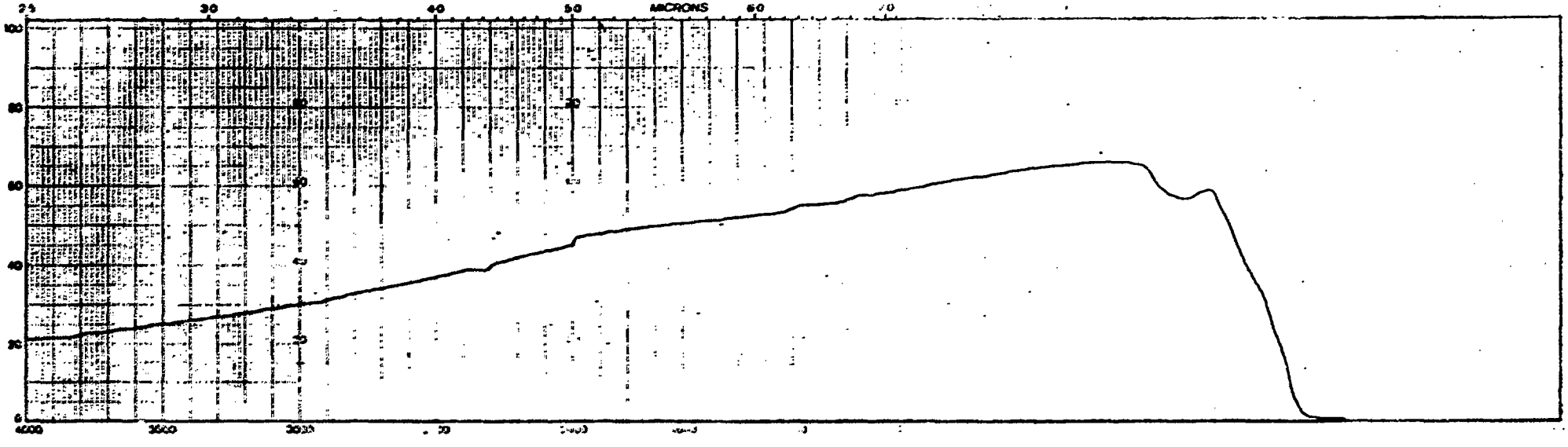

Fig. 2-33. Infrared Transmittance of CVD ZnS AF-4, Heat Treated at 1047 C, 1 atm, for 12.5 h, Pt Wrapped.

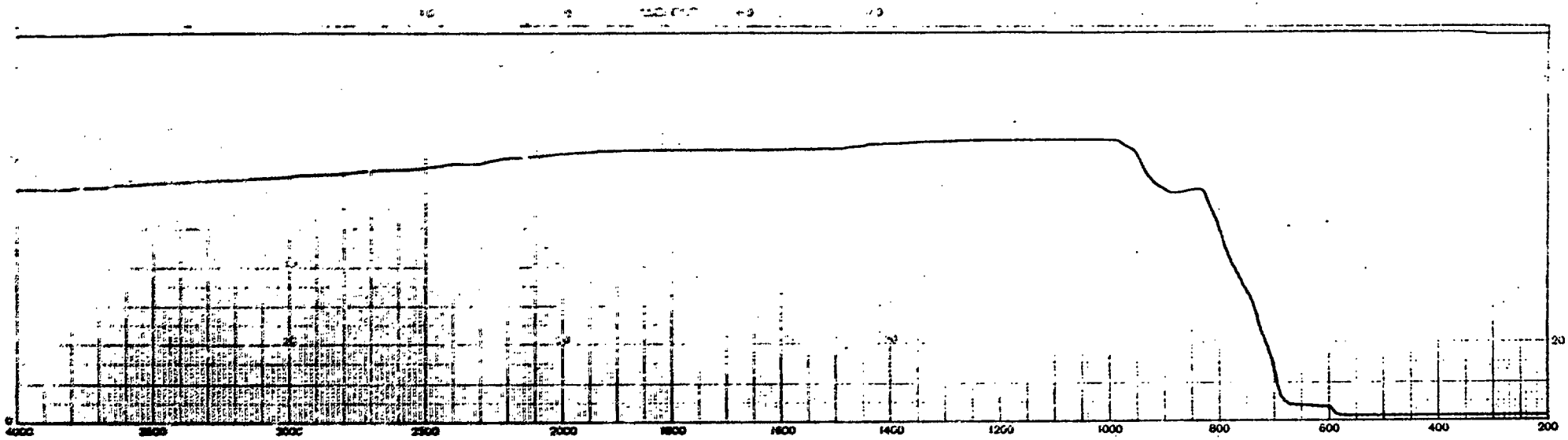

Fig. 2-34. Infrared Transmittance of CVD ZnS AF-4, Heat Treated at 990 C, 1 atm, for 25 h, Pt Wrapped, then HIP Processed at 990 C, 15 ksi, for 25 h, Pt. Wrapped.

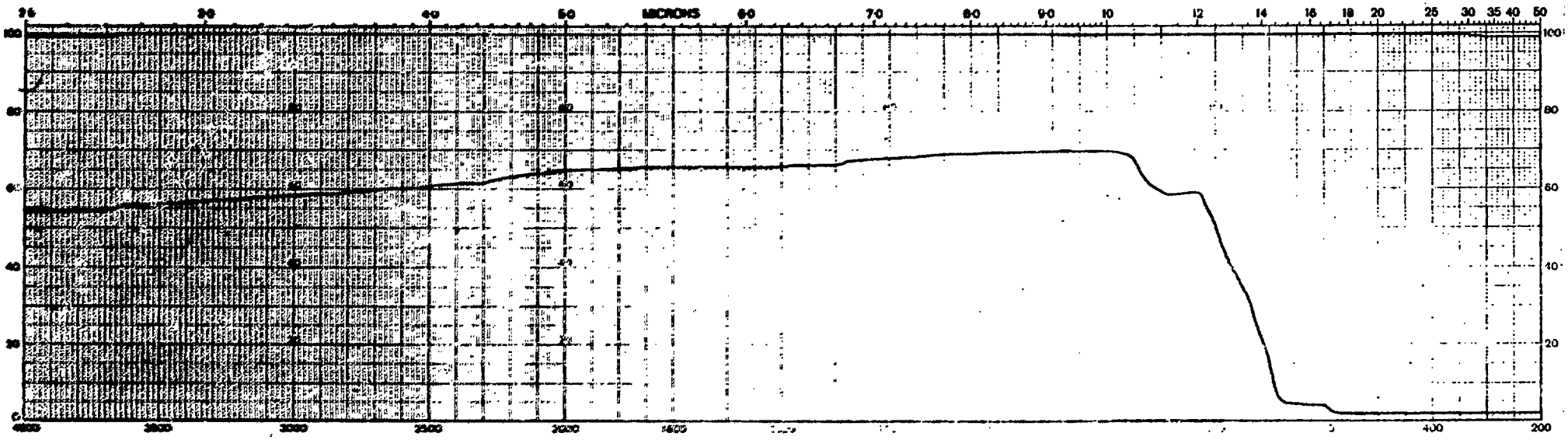

Fig. 2-35. Infrared Transmittance of CVD ZnS AF-4, Heat Treated at 1047 C, 1 atm, for 12.5 h, Pt Wrapped, then HIP Processed at 990 C, 15 ksi, for 25 h, Pt Wrapped.

TABLE 2-11

Heat Treatment - HIP Experiment, Knoop Hardness (HK_{50})

Run	Heat Treatment Conditions	HK_{50} Before HIP	HK_{50} After HIP 990°C, 15 ksi 25 h, Pt
AF-1	990 C	166	167
AF-4	1 atm	155	166
AF-6	25 h	152	155
	Pt		
AF-4	1047 C	156	161
	1 atm		
AF-6	12.5 h	172	151
	Pt		
	1067 C		
	1 atm		
	12.5 h		
AF-4	Pt	182	180
	1110 C		
AF-4	1 atm	189	186
	12.5 h		
AF-6	Pt	190	179

TABLE 2-12

Heat Treatment - HIP Experiment, Knoop Hardness (HK_{50})

Run	Heat Treatment Conditions	HK_{50} Before HIP	HK_{50} After HIP 990°C, 30 ksi 25 h, Pt
	990 C		
	1 atm		
AF-1	25 h	166	156
AF-6	Pt	152	143
AF-1	1047 C	182	157
	1 atm		
AF-4	12.5 h	156	154
AF-6	Pt	172	147
	1067 C		
	1 atm		
AF-6	12.5 h	193	191
	Pt		
	1110 C		
AF-1	1 atm	172	171
AF-4	12.5 h	183	168
	Pt		

2.4 Summary and Conclusions - Task I

It has been demonstrated that a "water-clear" ZnS infrared optical material can be produced by a combination of "standard" CVD ZnS which is subsequently hot isostatically pressed. This water-clear material exhibits good optical transmission from the first optically allowed electronic transition at about 3400Å to the multiphonon edge at 11 μ and, therefore, is useful in a variety of multispectral applications.

The optimum conditions for producing this water-clear ZnS have been shown to consist of a high temperature CVD combined with HIP treatment at 990 C and 15 ksi using Pt foil wrapping. The time for HIP treatment is thickness dependent with a 24 h processing necessary for 0.5-inch thick material. HIP processing at temperatures higher than 1000 C leads to large crystallites and pronounced grain boundaries. Such material is not useful in optical applications because of cracking and difficulty of fabrication. The effect of CVD temperatures in excess of 720 C was not investigated. However, it is known that as the deposition temperature increases, CVD ZnS becomes clearer. Therefore, it might be possible to produce water-clear ZnS directly in the CVD process and avoid the HIP treatment. Lewis(1) has claimed to have demonstrated this, but the appropriate conditions have not been published.

An attempt to replace or ameliorate the HIP treatment by a low pressure, heat treatment was unsuccessful. It appears that the heat treatment "locked in" the scattering sites, making any subsequent HIP ineffective.

No definitive mechanism for clearing CVD ZnS was established in this program. However, the totality of data strongly suggests that the initial scattering sites are microscopic (< 1 μm) diameter lattice dislocations which are healed by the HIP treatment. There is also some evidence that removal of impurities or excess zinc may also occur. For example, the 6.3 μm "impurity band", seen in CVD ZnS, is removed. Such diffusional processes would have to occur along grain boundaries to be effective for the times and distances involved.

Finally, every combination of CVD and HIP processes that produces an optically optimum water-clear ZnS, also produces larger grains and a softer material than CVD ZnS. This is a serious disadvantage to the water-clear material and attempts to provide a harder material by subsequent treatment are discussed in the following sections.

3.0 TASK II - MATERIAL TOUGHENING TECHNIQUES

3.1 Introduction

Water-clear ZnS, as produced in Task I, displays excellent optical transmittance from the visible to LWIR wavelengths. However, the grain growth which occurs during the HIP (clearing) process leads to mechanically weak and soft material as compared with standard CVD ZnS. The reductions in hardness and strength are shown in Tables 3-1 and 3-2 respectively. As a result, the rain erosion resistance of the water-clear ZnS has been considerably lowered. Figure 3-1, which shows the infrared transmittance curves of water-clear and as deposited ZnS before and after exposure to a simulated high speed rainfall, graphically illustrates this point. The objective of Task II, is to increase the rain erosion resistance of water-clear ZnS to at least the level of standard CVD ZnS, while retaining the excellent multi-spectral qualities inherent in the clear material.

The material toughening experiments tried in this program included both bulk material and surface treatments. Table 3-3 displays the various material toughening techniques which were tried on water-clear ZnS. The technical details and results of these experiments are discussed in the sections which follow.

3.2 Grain Size Refinement

Analogous to metallurgical systems, grain size refinement was investigated as a technique to provide increased bulk hardening. Literature indicates a phase transition in ZnS from cubic to hexagonal at approximately 1020 C (2-4). Hexagonal material is optically undesirable due to scattering effects from anisotropic refractive indices. The goal of this approach was to heat the water-clear ZnS to above this transition point to provide a cubic to hexagonal transformation. Then the material would be cooled to a temperature slightly below the transition temperature to 1) anneal any stresses obtained during the cubic → hexagonal transformation and 2) to recrystallize the hexagonal material to a fine grained, cubic structure. This fine grained material should display better strength characteristics than the larger grained starting material.

Two experimental procedures were proposed to obtain a small grained, cubic structure. The first experiment involved CVD ZnS which was HIP processed

TABLE 3-1

Knoop Hardness (HK_{50}) CVD ZnS Before and After HIP

Run	CVD ZnS	HK_{50} Water-Clear ZnS
*AF-1	220	176
AF-4	216	160
AF-6	247	164

*Standard CVD Deposition Conditions

TABLE 3-2

Flexural Strength, CVD ZnS, Before and After HIP (PSI)

Run	CVD ZnS	Water-Clear ZnS
*AF-1	14,600	8,700
AF-4	--	8,600
AF-6	--	8,300

*Standard CVD deposition conditions

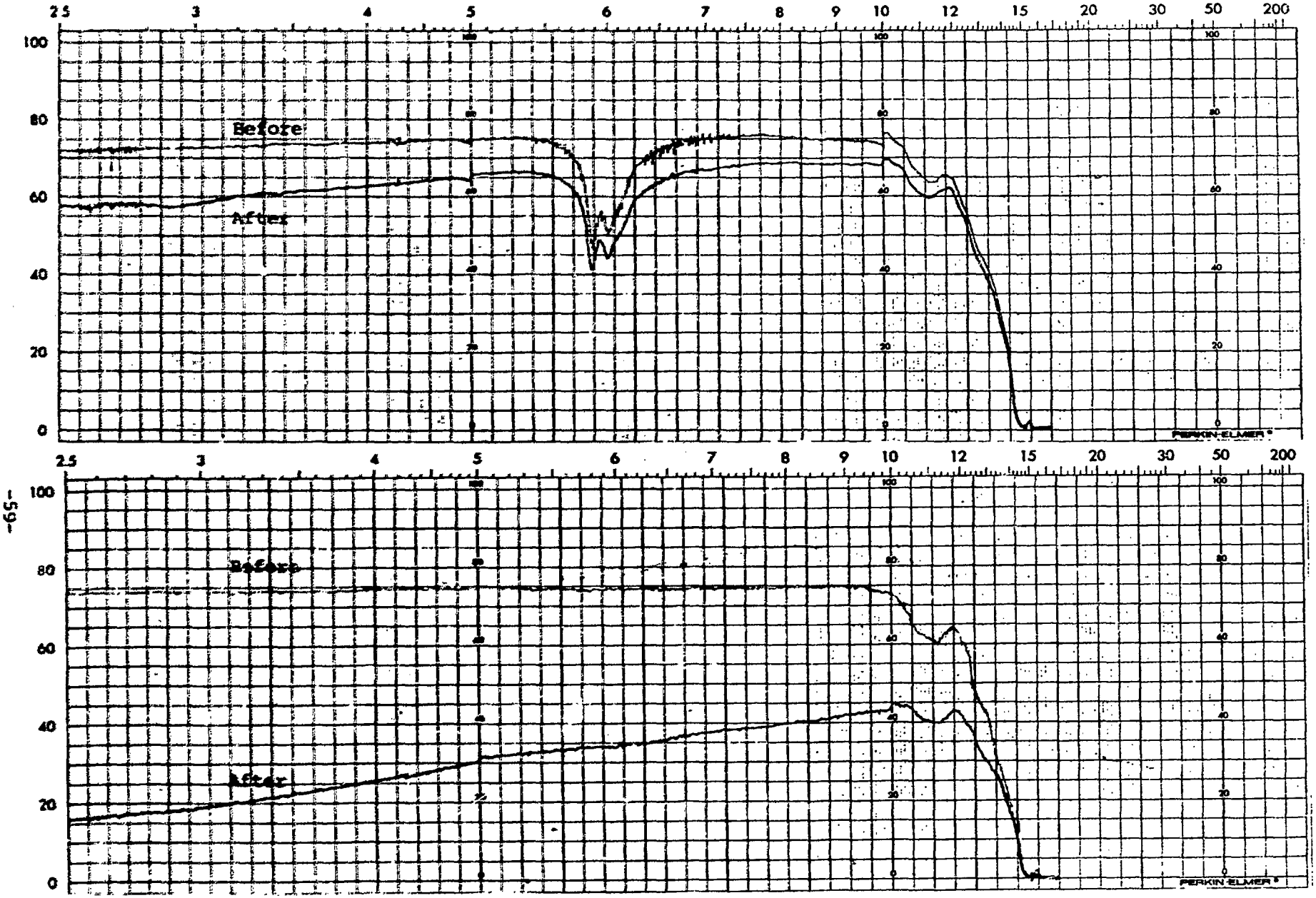

Fig. 3-1. Infrared Transmittance of CVD ZnS (Top) and Water-Clear ZnS (Bottom), Before (Top Trace) and After (Bottom Trace) Rain Erosion Testing at 475 mph, 90° Impact Angle, 1 inch/h Rainfall, 30 min Exposure.

TABLE 3-3

Material Toughening Matrix

Process	Variables	Treatment Depth
Grain Size Refinement and Phase Transformation	Temperature, Time Cooling Rate	Bulk
Thermal Tempering	Temperature, Quench Rate	Bulk
Thermal Diffusion	Dopant Species, Temperature, Time Pressure	Surface
Thin Film Coating	Material, Thickness	Surface
PEBA	Dose, Pulse Width	Surface
Ion Implantation	Dopant Species, Ion Flux, Acceleration Energy, Annealing	Surface

at high temperatures (> 1047 C). This material was expected to display a significant (> 30%) amount of hexagonal material, as the rapid cooling (to room temperature) from the high processing temperature should have precluded an appreciable hexagonal → cubic recrystallization. The ZnS would then be heated to a nucleation temperature below the transition temperature for a few hours. It was expected that complete nucleation of the cubic phase would occur, without accompanied grain growth. In the second approach, the HIP and grain refinement were to be carried out in one sequence in which the ZnS would be rapidly cooled from the HIP temperature to the refinement temperature and held for the nucleation period.

X-ray diffraction measurements were performed on standard untreated CVD ZnS and both HIP processed and heat treated materials. Only trace amounts of hexagonal phase material were revealed even after heat treatment exposures as high as 1110 C. It was determined that there was insufficient hexagonal phase present to effect the grain structure, even assuming a complete, fine grained cubic recrystallization. In addition, material that was subjected to these high temperature (> 1000 C) processes exhibited large grains, cracking along grain boundaries and occasional grain boundary separation. The conclusion is that either there is no cubic-hexagonal transition in the temperature range studied or that such a transition is kinetically limited and, therefore, is too slow for grain refinement. Due to these negative results, further bulk grain refinement experiments were discontinued.

3.3 Thermal Tempering

In another attempt to increase the overall bulk strength of water-clear ZnS, various thermal tempering experiments were performed(5). In the production of safety glass, residual compressive stresses are intentionally induced in the surface regions through nonuniform temperature profiles, followed by a controlled cooling procedure (6,7).In the experiments with water-clear ZnS, two quenchants were used to study the effects of different quench rates. Water was used as a fast quenchant, and oil for slower quench rates. Water provides a more rapid quench because the conversion of water to steam at the surface of the heated ZnS absorbs a large quantity of heat due to the high latent heat of vaporization of water. Quenches in oil lead to less distortion because of lower thermal gradients.

Table 3-4 shows the thermal tempering test parameters. Room temperature air cooling (natural convection) was used for comparitive purposes. As is evident from these data, no significant increase in hardness was observed. Water-clear ZnS quenched in water severely cracked at both temperatures.

Material quenched in oil slightly cracked at 600 C, but did not crack at 300 C. There was no evidence of cracking in ZnS cooled in ambient air. Because of the lack of positive indicators, further thermal tempering experiments were abandoned.

3.4 Surface Diffusion

A number of surface diffusion experiments were performed on water-clear ZnS to increase its rain erosion resistance. A proven technique to impart a hard surface layer in metals is to diffuse into the metal an appropriate impurity atom. If this impurity atom is of the proper size, it will cause a lattice strain in the metal and result in a compressive stress in the surface layer. In the present case, the impurity species must diffuse into the ZnS lattice, be of sufficiently different size from the host ions to produce lattice strain, but not cause significant optical degradation of the material. Based on theoretical calculations a species whose atomic radius is about 15% larger (or smaller) than the host ions appears to be the most optimum (8). Cd fits this requirement. Several different techniques were tried to diffuse Cd into the ZnS.

In the first approach, ZnS (both water-clear and as deposited) was heated to 1100 C in a Cd vapor atmosphere. Table 3-5 displays the Knoop hardness of CVD ZnS subjected to Cd vapors at 1100 C, 1 atm pressure for 3 h in a graphite crucible. As is evident from these data, the hardness was substantially increased in three out of the four samples treated. Figure 3-2 is an infrared transmittance curve of the treated materials showing the substantial short wavelength scatter. This scatter is largely due to surface degradation, as the samples showed substantial etching and pitting from the Cd vapor and high heat. The Cd-doped pieces were then repolished and new IR transmittance curves were generated (Fig. 3-3). As is evident, the material continues to exhibit some short wavelength scattering. The doped ZnS also has a cloudy appearance, and one sample (AF4-CD) shows some internal cracking along grain boundaries. Knoop hardness

TABLE 3-4

Knoop Hardness (HK_{50}) of Thermal Tempered, Water-Clear ZnS

Sample	Initial HK_{50}	300 C Quench, HK_{50}		600 C Quench, HK_{50}	
A	159	*Water,	157	-----	
B	161	*Oil	160	-----	
C	158	Air	158	-----	
D	164	-----		*Water	169
E	166	-----		Oil	152
F	153	-----		Air	171

*Samples cracked

TABLE 3-5

Knoop Hardness (HK_{50}) Cd Diffusion Experiment

Sample	Initial Conditions	HK_{50} Before Diffusion	HK_{50} After Diffusion 1110 C, 3 h 1 Atm, Graphite
AF4-00	As Deposited	216	213
AF4-44	As Deposited	206	258
AF4-21	Water-Clear	160	188
AF4-20	Water-Clear	162	245

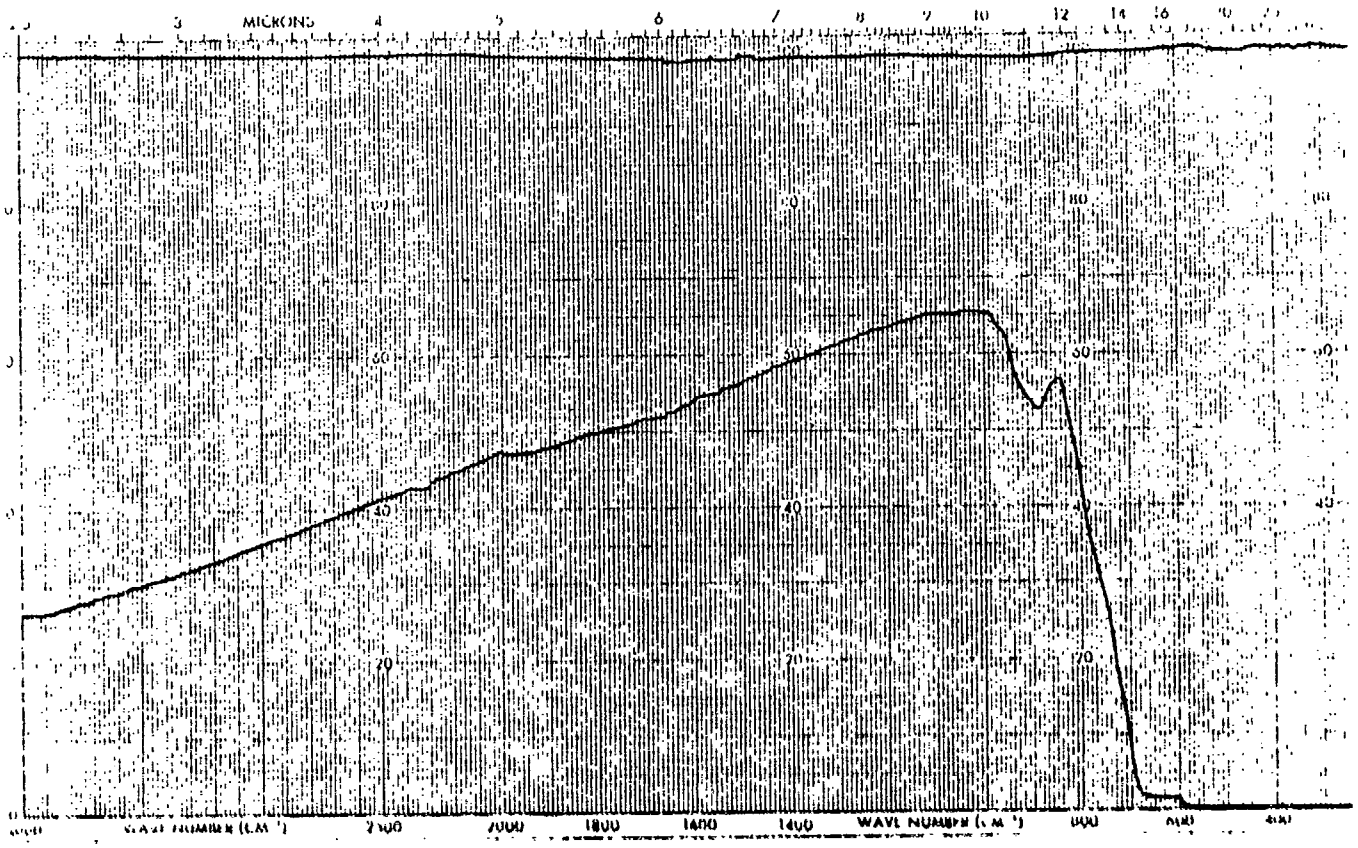

Fig. 3-2. Infrared Transmittance of AF-4 Water-Clear ZnS Exposed to 1110 C, Cd Vapor, 3 h, 1 atm.

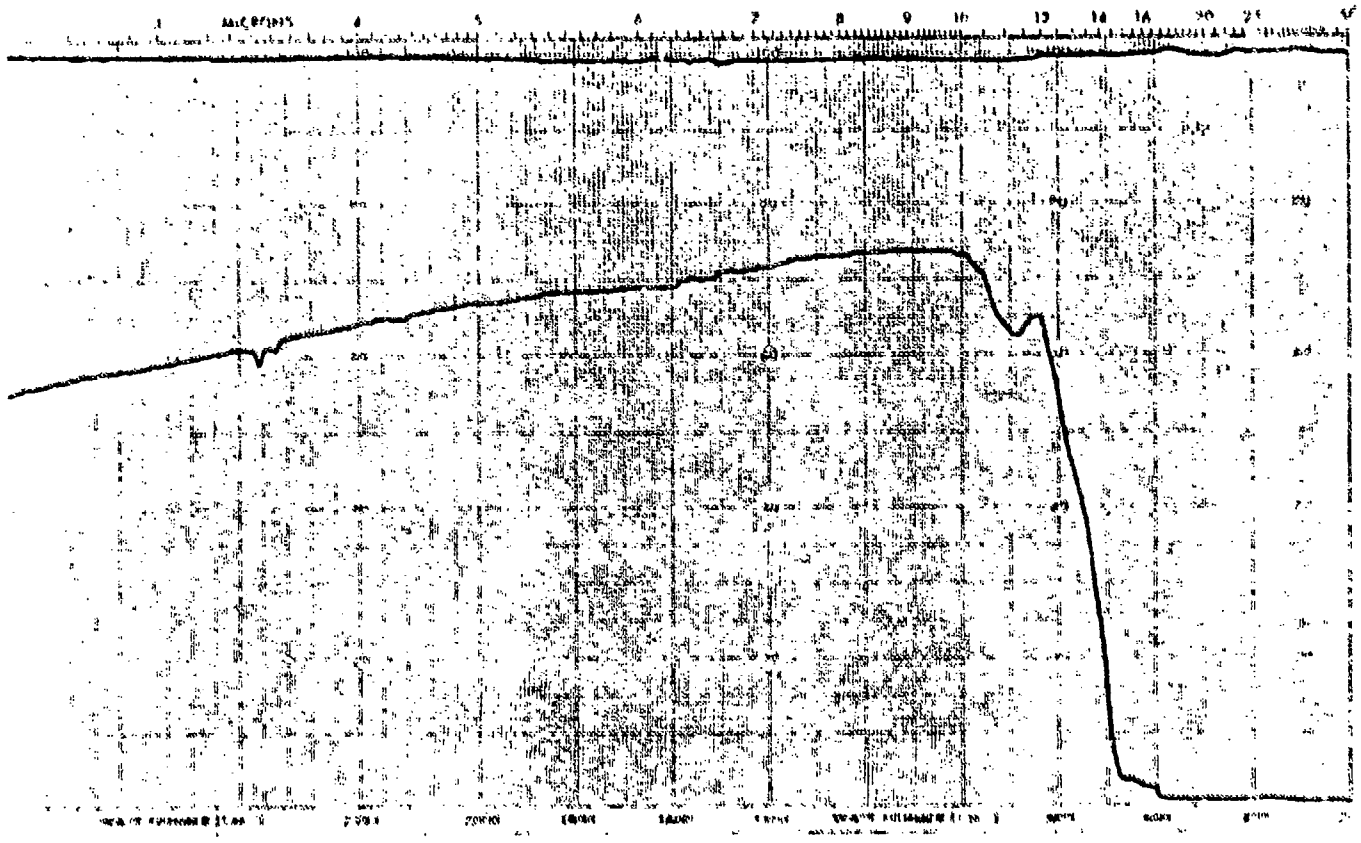

Fig. 3-3. Infrared Transmittance of AF-4 Water-Clear ZnS Exposed to 1110 C, Cd Vapor, 3 h, 1 atm, Repolished.

measurements were made on these repolished pieces, with the results shown in Table 3-6. Approximately 0.005 inches of material was removed in the repolishing, and as is evident from the data, the hardness was not appreciably effected by this fabrication step.

In an attempt to repeat these results, another similar Cd thermal diffusion experiment was performed. However, as is evident from the data shown in Table 3-7, no apparent increase in hardness was observed. As a result of this inconsistency, the added short wavelength scatter and grain growth/grain boundary cracking, no further Cd diffusion experiments were performed using this technique. However, this technique merits further detailed investigation, because it did yield a significant improvement in surface hardness.

Another experiment was performed to thermally diffuse Cd into ZnS by a different technique. Samples of both as deposited and water-clear ZnS were coated with an approximate 1000 Å thick Cd film, stacked between alternating layers of graphite foil, placed in graphite load cans, then HIP processed at 750 C, 15 ksi for 12 hours. The lower HIP temperature was chosen because of the low boiling point of Cd. Unfortunately, the use of graphite foil during HIP processing produced a rough surface finish making Knoop hardness measurements difficult and uncertain. As a result, this experiment was repeated with minor packing changes.

These new Cd coated samples (both CVD and water-clear ZnS) were HIP processed in graphite load cans (two samples per can) with both samples in close proximity but not touching each other. As is evident from the results (see Table 3-8), sample AF4-1S shows a substantial increase in hardness. In this experiment, the two samples fell together during HIP processing with the coated surface of AF4-1S pressed to the back (uncoated) side of the other sample. In this contact region, a single Knoop hardness reading of 558 was observed. Hardness measurements of AF4-1S away from this "hard band" showed values more typical of untreated CVD ZnS. This large difference was responsible for both the large Knoop hardness average (373) and standard deviation (158) of this sample.

Also evident from the results of Table 3-8 is the large deviation of the net change in hardness after Cd diffusion by HIP processing. Along with

TABLE 3-6

Knoop Hardness (HK_{50}) Cd Diffusion Experiment

Sample	HK_{50} After Treatment	HK_{50} After Polish
AF4-CD	213	---
AF4-44	258	236
AF4-21	188	187
AF4-20	245	235

TABLE 3-7

Knoop Hardness (HK_{50}) Cd Diffusion Experiment

Sample	Initial Conditions	HK_{50} Before Diffusion	HK_{50} After Diffusion 1110 C, 3 h 1 Atm, Graphite
4-H1	Water-Clear	158±6	170±6
4-H3	Water-Clear	163±6	166±17

TABLE 3-8

Cd Coating Diffusion Experiment

Sample	Initial Condition	HK_{50} Before Diffusion	After Diffusion 1000 Å Cd Film HIP 990 C 15 ksi, 12 h	Change in Hardness
AF4-1S	As Deposited	214±5	373±158	+159
AF4-2S	As Deposited	216±7	262±18	+ 46
AF4-3S	As Deposited	216±5	248±31	+ 32
AF4-4S	As Deposited	218±4	210±11	- 8
AF4-R13	HIP	159±6	149±35	- 10
AF4-R14	990 C	161±8	180±13	+ 19
AF4-R15	16 ksi	155±4	167±6	+ 12
AF4-R16	12 hours	159±5	210±21	+ 51
	Pt			

large increases in hardness, there are two samples that actually decreased in hardness. Again, there was a problem of inconsistent hardness measurement due to surface damage from HIP processing. This damage also degraded the short wavelength infrared transmittance (Figs. 3-4 to 3-7). Samples were repolished, and the Knoop hardness was more typical of untreated material.

In another experiment, a series of as deposited ZnS samples were given a sputtered CdS coating. Both 200 Å and 1000 Å thick coatings were applied, and these samples were then HIP processed at 830 C, 15 ksi, 12.5 h in a graphite crucible. Due to the frequent difficulty in reading the Knoop hardness indentations, independent Vickers hardness measurements were made to confirm our measurements. The hardness measurements are reported in Table 3-9. It can be seen that the hardness of the CdS sputtered and HIP processed material remains largely unchanged. However, the CdS material has only diffused into the ZnS lattice a short distance. Subsequent repolishing of the material, which removed approximately 0.002 inches, removes the CdS and reduces the hardness to the range of uncoated material. The data from these polished samples are also shown in Table 3-9. In addition, the material treated by this process has degraded optical quality and visually exhibits a gray appearance.

A final ZnS/CdS diffusion experiment was performed in a HIP unit to study the effects of diffusion of Cd into the ZnS lattice. Alternating 0.875-inch diameters of ZnS (both as deposited and water-clear) were stacked between diameters of CVD CdS, double wrapped in platinum foil, then placed in a single outer wrap of tantalum foil before enclosing in a titanium can. The Ta wrapper was used to prevent any interaction between the CVD material and the titanium can. Titanium caps were then e-beam welded on either end, and the billet (Fig. 3-8) was then HIP processed at 845 C, 30 ksi for 25 h. The end plugs were cut off and approximately one quarter of the billet was ground and polished, exposing the alternating layers of ZnS and CdS (Fig. 3-9). Vickers hardness measurements were made on the water-clear ZnS in a traverse from the ZnS/CdS interface out to approximately 500 μm, with readings every 25-50 μm (Fig. 3-10 and Table 3-10). As can be seen, the first Vickers indentation (closest to the interface) gave the highest hardness, which then decreased to approximately 200 HV_{50}. The polished surface was then etched in a fuming, dilute HCl solution.

Fig. 3-4. Infrared Transmittance of CVD ZnS AF-4, Before Cd Diffusion Experiment.

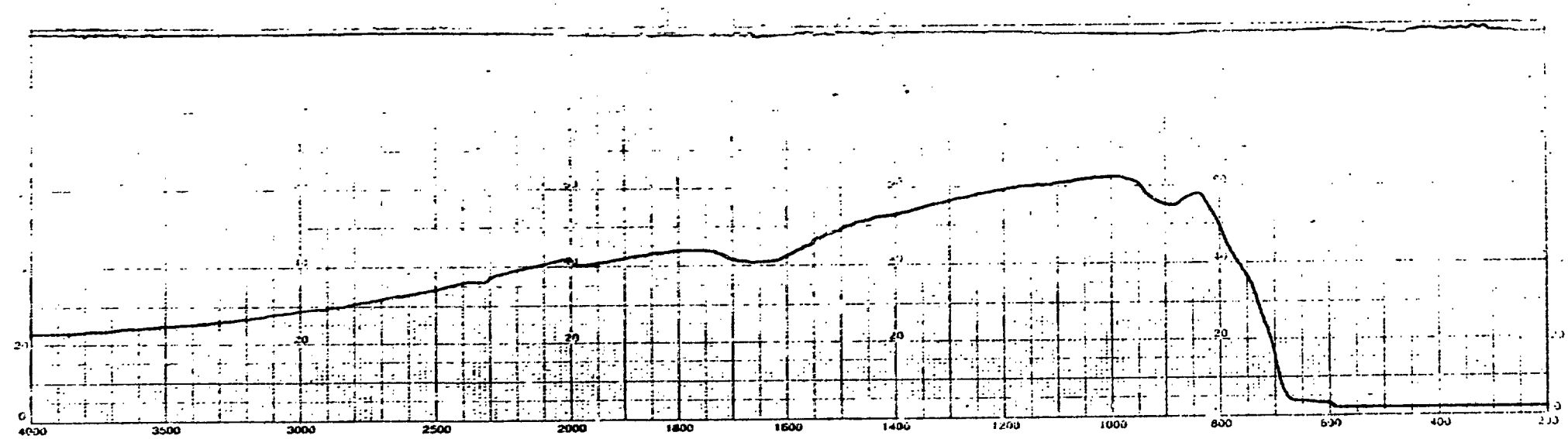

Fig. 3-5. Infrared Transmittance of CVD ZnS AF-4, After Cd Coating and HIP Processing at 750 C, 15 ksi for 12 h.

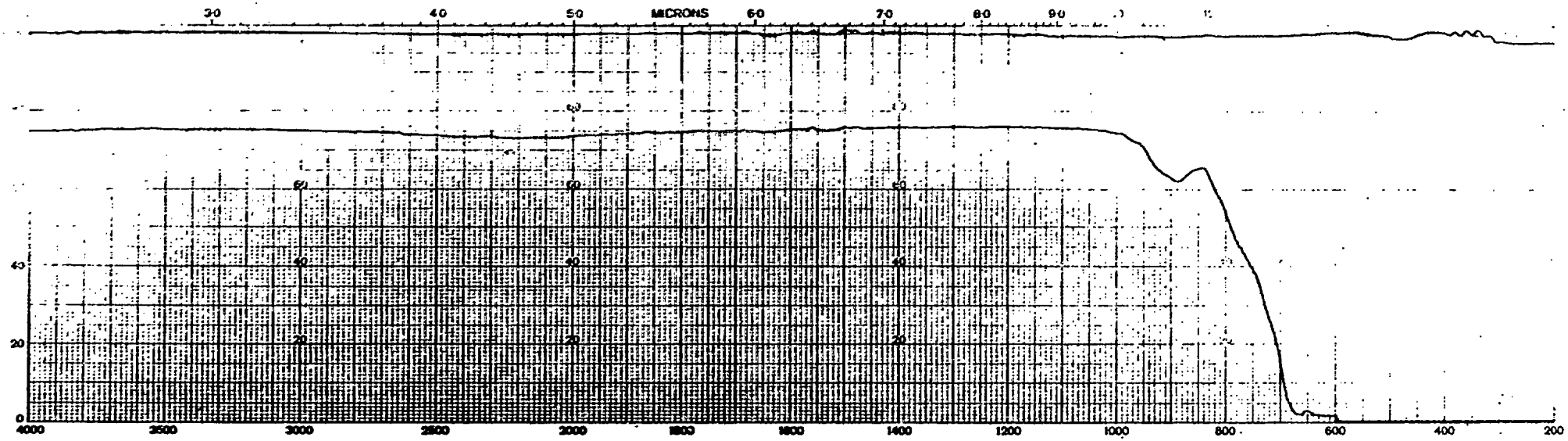

Fig. 3-6. Infrared Transmittance of Water-Clear AF-4 ZnS, Before Cd Diffusion Experiment.

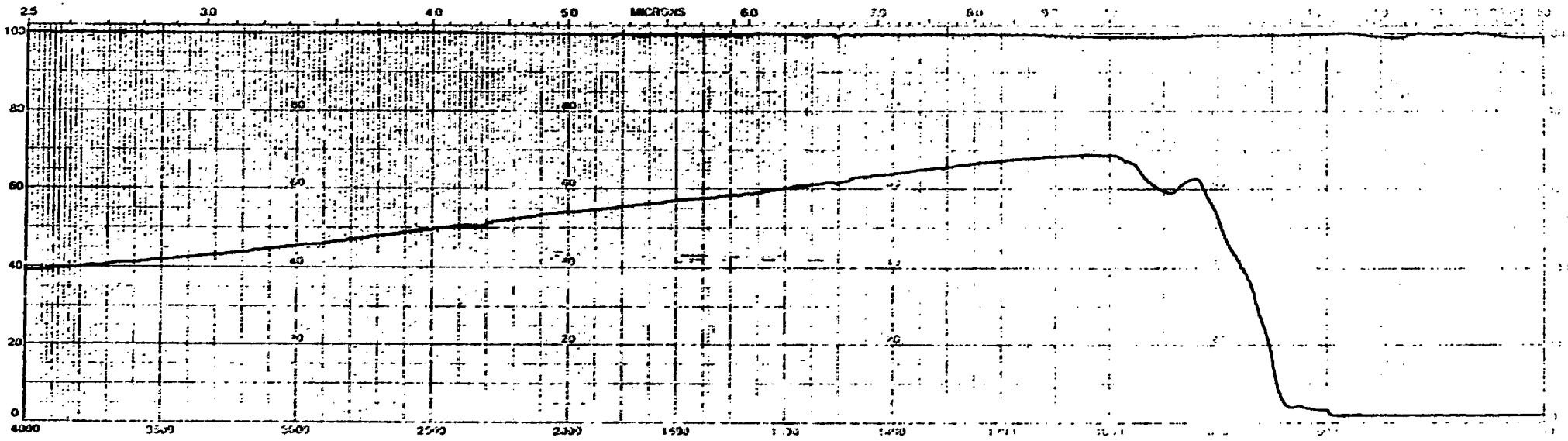

Fig. 3-7. Infrared Transmittance of Water-Clear AF-4 ZnS, After Cd Coating and HIP Processing at 750 C, 15 ksi for 12 h.

TABLE 3-9

CdS Coating Diffusion Experiment

50g Vickers (HV_{50}) and Knoop (HK_{50}) Hardness

Sample	Unpolished HV_{50} After CdS Coating HIP 830 C 15ksi 12.5 h, Graphite			Polished	
	As Deposited (HK_{50})	200 Å CdS	1000 Å Cds	200 Å CdS (HV_{50})	1000 Å (HK_{50})
AF1-110	222±7	232±23	250±29	-----	-----
AF1-111	234±9	232±37	255±23	-----	-----
AF4-110	210±8	200±10	192±16	184±9	182±11
AF4-111	208±11	194±14	200±14	163±7	207±21
AF6-110	232±7	212±49	211±26	-----	165±8
AF6-111	237±6	191±19	214±17	-----	-----

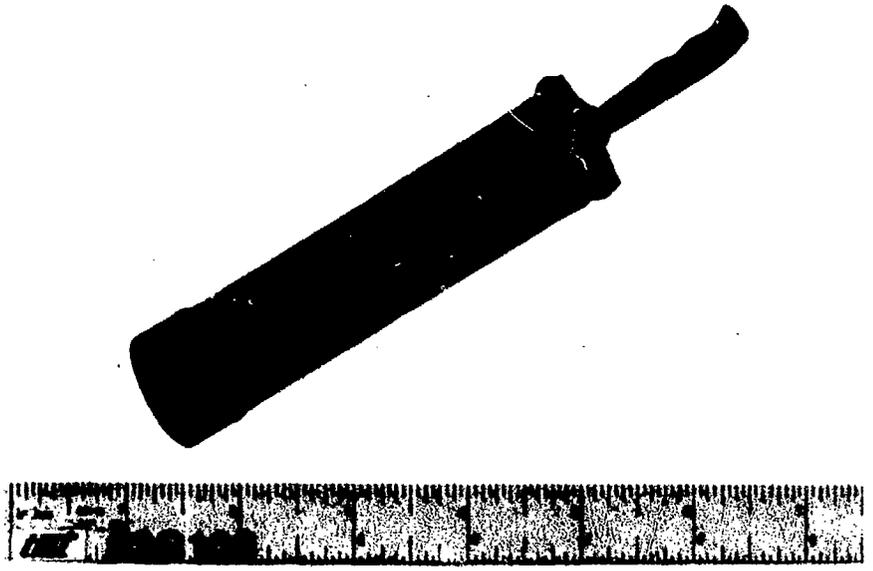

Figure 3-8. Photograph of Titanium Can Which Encloses ZnS and CdS Diameters

Figure 3-9. Photograph of Polished Surface of ZnS/CdS Diffusion Billet.

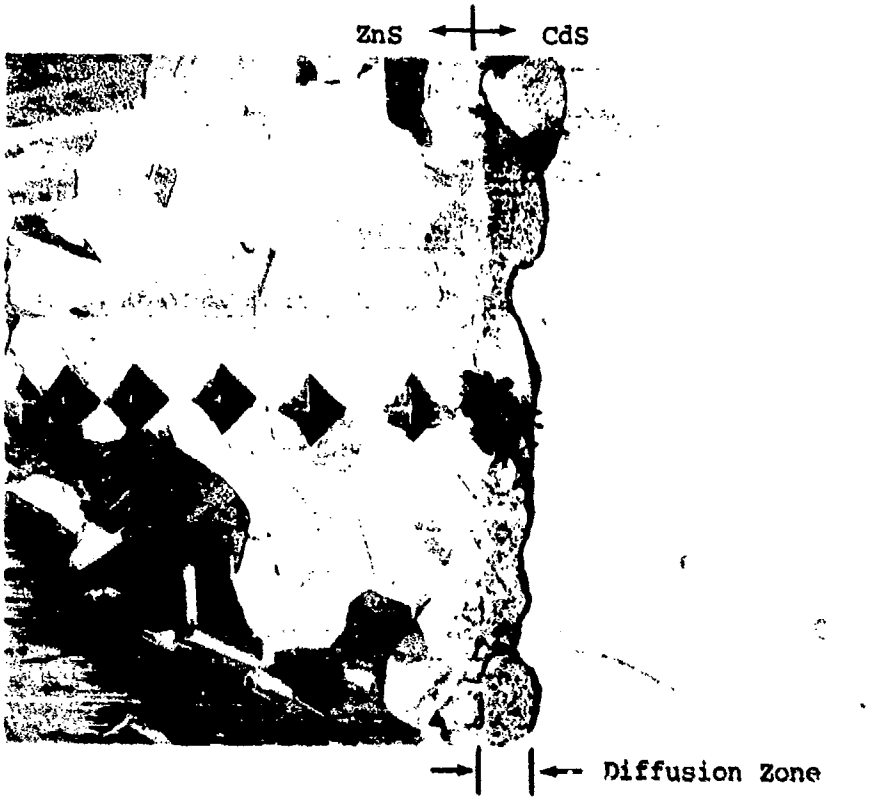

Figure 3-10. Photomicrograph of ZnS/CdS Surface Showing Vickers Indentation. 400x

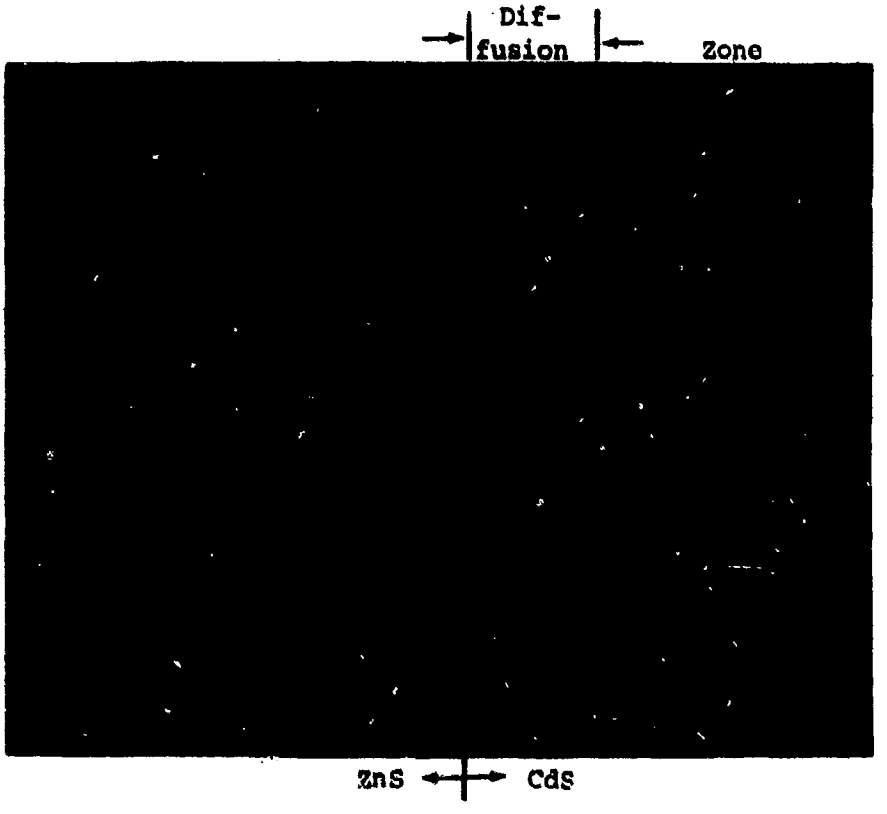

Figure 3-11. Photomicrograph of Etched ZnS/CdS Interface Showing Diffusion Zone. 1000x

TABLE 3-10

Vickers Hardness (HV_{50}) of Water-Clear ZnS from ZnS/CdS Diffusion Couple

Distance from CdS/ZnS Interface (μm)	HIP 845 C 30 ksi, 25 h				
	ZnS1	ZnS2	ZnS3	ZnS4	ZnS5
10	237	---	220	210	208
25	---	232	---	---	---
37	231	---	---	---	---
50	---	---	199	195	193
75	193	210	---	---	---
100	195	---	175	177	204
125	210	201	---	---	---
150	145	---	192	165	210
175	---	187	---	---	---
200	175	---	185	192	201
225	---	178	---	---	---
250	145	---	187	192	204
275	---	182	---	---	---
300	---	---	211	198	196
325	---	199	---	---	---
350	---	---	201	197	191
375	---	201	---	---	---
400	---	---	183	201	183
425	---	225	---	---	---
450	---	---	192	197	187
475	---	243	---	---	---
525	---	268	---	---	---
575	---	232	---	---	---
625	---	202	---	---	---
675	---	210	---	---	---
Average	191 ± 35	212 ± 25	194 ± 14	192 ± 13	198 ± 9
Overall Average	199 ± 22				

Figure 3-11 shows the surface morphology of the ZnS/CdS interface and the diffusion zone into the CdS at 1000X. It appears that the Zn has diffused into the CdS. This result is not surprising as Zn atoms are smaller than Cd atoms which would lead one to expect a higher atomic mobility of Zn. Although a reasonable increase in hardness was realized with this diffusion experiment, there was also substantial cracking due to the intimate contact of the material in the titanium can while being HIP processed. In addition, the ZnS and CdS fused together, requiring mechanical grinding to isolate the ZnS. As a result, this technique would need major technical revisions before being seriously considered as a practical method to increase the hardness of water-clear ZnS.

Although these Cd diffusion experiments did not provide a practical method for increasing the hardness of water-clear ZnS, they do demonstrate that the diffusion of Cd atoms into the ZnS lattice does provide strain and increase hardness, albeit in a thin diffusion layer. It strongly suggests that other experimental approaches might be tried, e.g., the incorporation of Cd into the ZnS during the deposition process. Due to limited resources, this was not tired during this program.

3.5 Coatings

An attempt was made to apply two thin film, hard coatings to water-clear ZnS and assess their effect on improved rain erosion (9-12). The first coating applied was a 1000 Å thick SiO_2 film. This was deposited by standard vacuum evaporation techniques. SiO_2 is hard compared to ZnS and has excellent short wavelength properties. As can be seen from Table 3-11, there was no apparent increase in hardness. The visible optical properties of the sample were not degraded, but a SiO_2 absorption band was observed in the 9.5 μm region (Fig. 3-12 and 3-13).

Cubic BN was another coating material evaluated on clear ZnS. Cubic BN is a very hard material that is visibly transparent in thin films. Figure 3-14 shows an infrared transmittance curve of BN. This material was deposited via a room temperature, plasma deposition process. A film approximately 1000 Å thick was applied to a sample of water-clear ZnS, although the ultimate goal was a thickness of 2-4 μm. As is evident from the results in Table 3-12,

TABLE 3-11

Knoop Hardness (HK_{50}) SiO_2 Coated Water-Clear ZnS

Sample	HK_{50} Initial	HK_{50} 1000Å SiO_2
AF4-20A	159 ± 4	154 ± 8

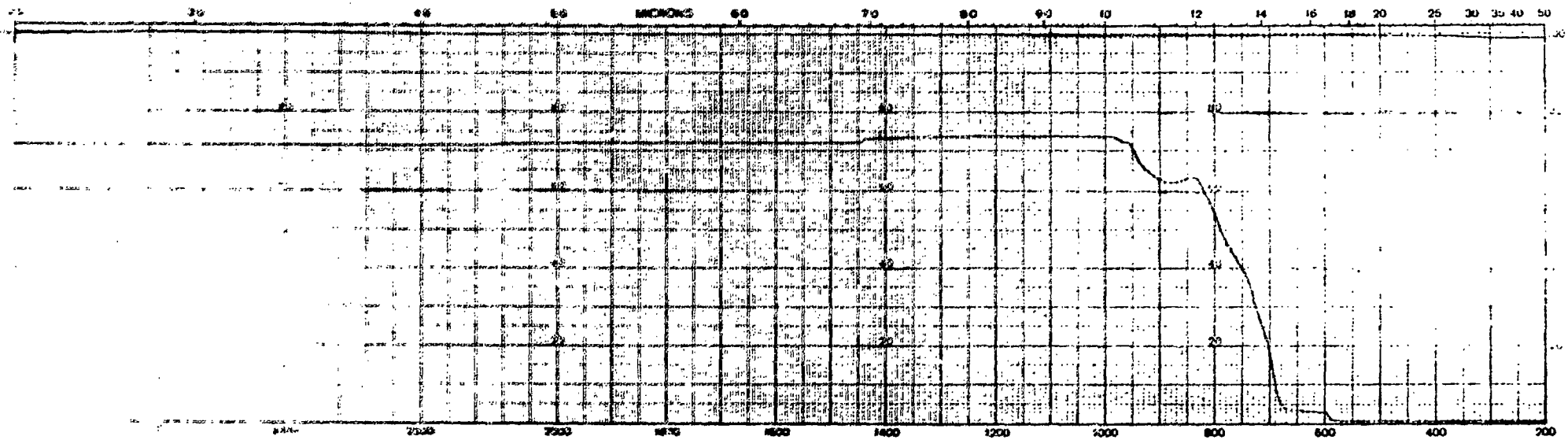

Fig. 3-12. Infrared Transmittance of AF-4 Water-Clear ZnS Before SiO_2 Coating.

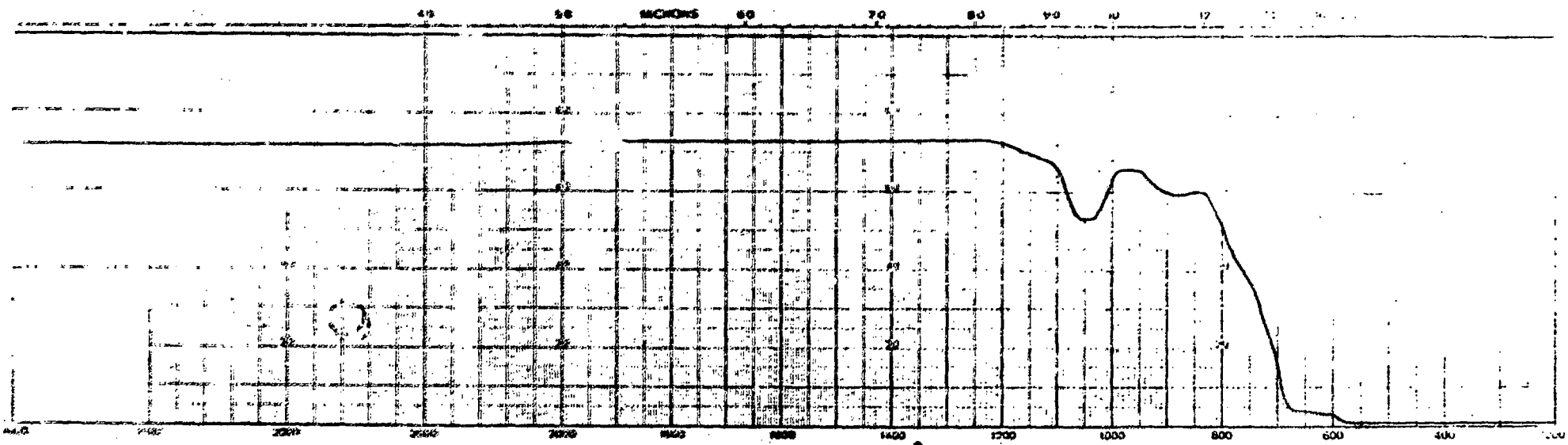

Fig. 3-13. Infrared Transmittance of AF-4 Water-Clear ZnS with 1000 Å SiO_2 Coating.

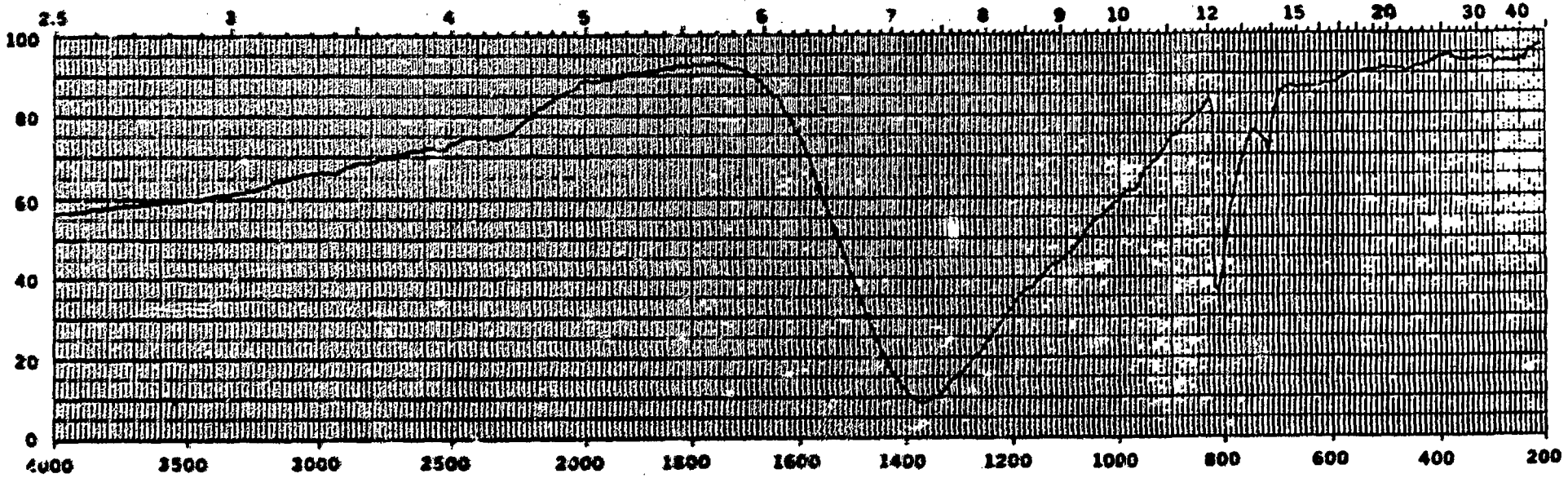

Fig. 3-14. Infrared Transmittance of BN, from Sadtler Grating Infrared Spectra.

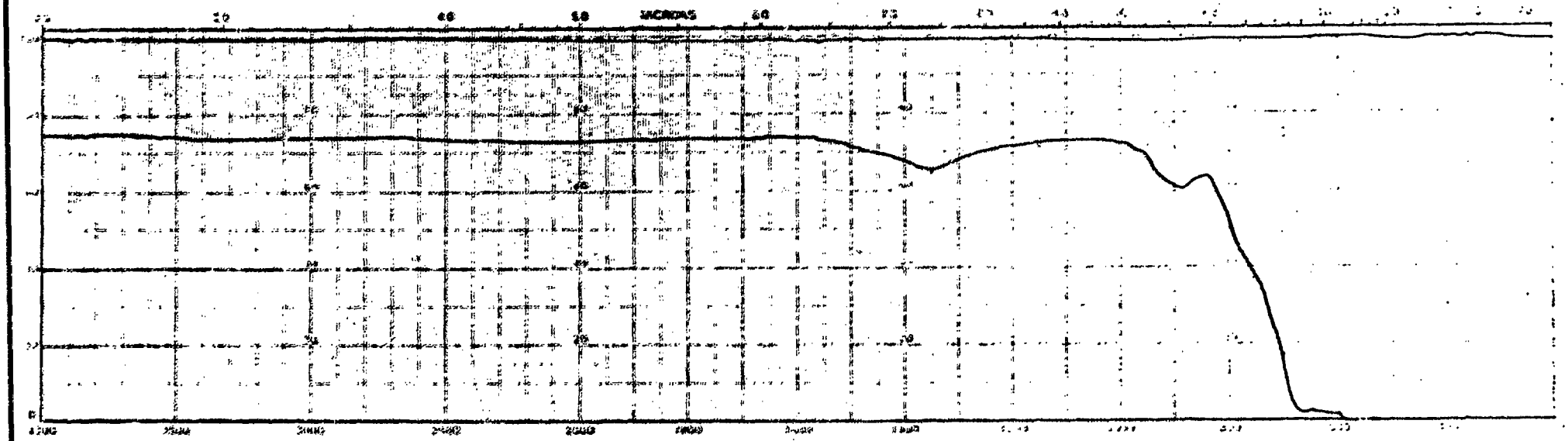

Fig. 3-15. Infrared Transmittance of AF-4 Water-Clear ZnS Coated with Approximately 1000 Å Cubic BN.

TABLE 3-12

Knoop Hardness (HK_{50}) Cubic BN Coated Water-Clear ZnS

Sample	HK_{50} Initial	HK_{50} 1000 Å C.BN
AF4-C	148 ± 10	152 ± 12

there was no increase in Knoop hardness. The infrared optical transmittance was only slightly degraded (Fig. 3-15) with an added absorption feature at approximately 7.4 μm which matches the expected absorption of BN.

Further depositions of cubic BN were attempted by this technique to increase the film thickness. Another deposition yielded samples with a 5000 Å coating of BN, but again, there was no increase in Knoop hardness although the absorption feature at ~ 7.4 μm was observed. Visual inspection showed no apparent visible optical degradation.

A final attempt was made to deposit a 1-2 μm uniform coating of cubic BN onto water-clear ZnS. Six samples were coated, two of which already had a 5000 Å thick coating of cubic BN from the previous deposit. The remaining four samples were untreated, water-clear ZnS. As can be seen from the photograph of the six samples on the mounting fixture (Fig. 3-16), there was a non-uniform, white, powdery deposit on all the samples. The infrared transmittance of the coated pieces show significant absorption at 7.4 μm (Fig. 3-17) which is characteristic of BN. However, this powdery film was easily wiped away with a cotton swab, and after removal, the samples displayed infrared transmittance typical of pure, uncoated water-clear ZnS. The samples that were previously coated with 5000 Å of cubic BN also exhibited similar behavior. It appears that the cubic BN film was completely removed by the cotton swab. A slight increase in hardness was observed before the removal (Table 3-13); however, the low adhesion of this film precludes it from any practical usage. From these and previous results, no further cubic BN coatings by room temperature, plasma deposition were attempted, since it was clear that a serious adhesion problem existed.

3.6 Pulsed Electron Beam Annealing*

Pulsed Electron Beam Annealing (PEBA) is another technique that was tried to refine the grain size of water-clear ZnS in order to increase the hardness of the material. In PEBA, the electron beam thermally (adiabatically) processes the material surface in a single submicrosecond pulse of electron beam energy. A schematic of the process is shown in Fig. 3-18. The pulse of high energy electrons first melts the substrate surface, then, depending on the sample configuration and thermal properties, the surface resolidifies

*Work performed at Spire Corp., Patriots Park, Bedford, MA 01730.

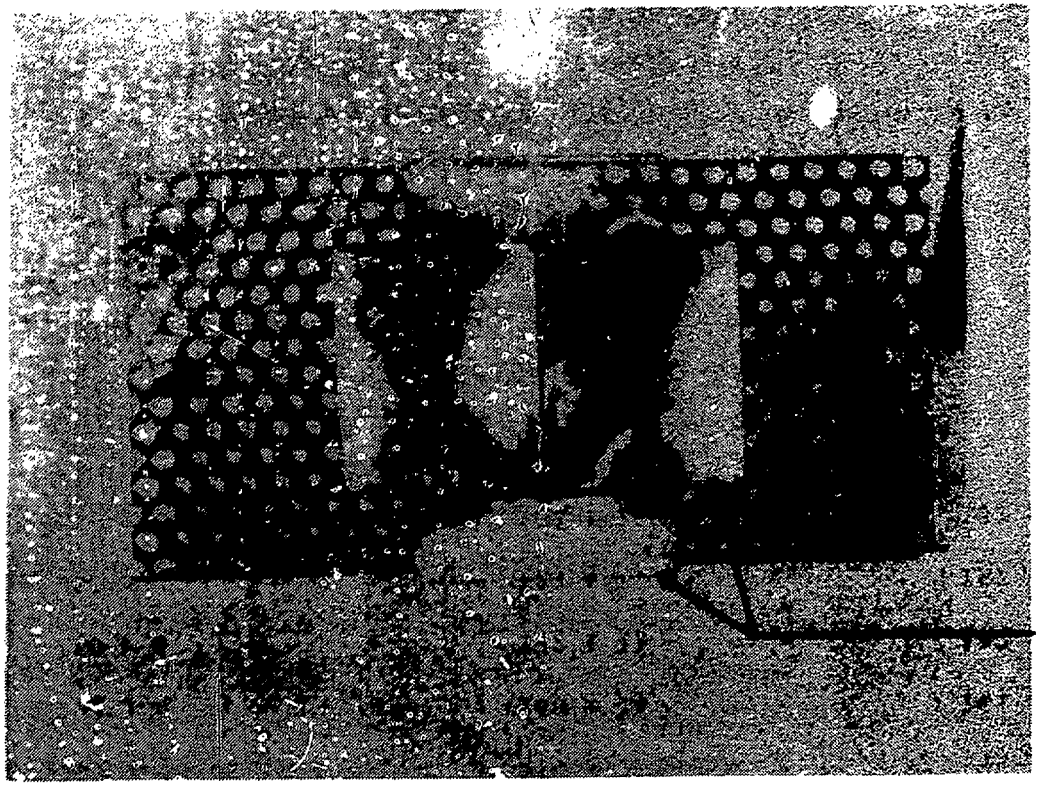

Fig. 3-16. Photograph of Water-Clear ZnS with ~ 1 μm Coating of Cubic BN, Showing the Powdery Film.

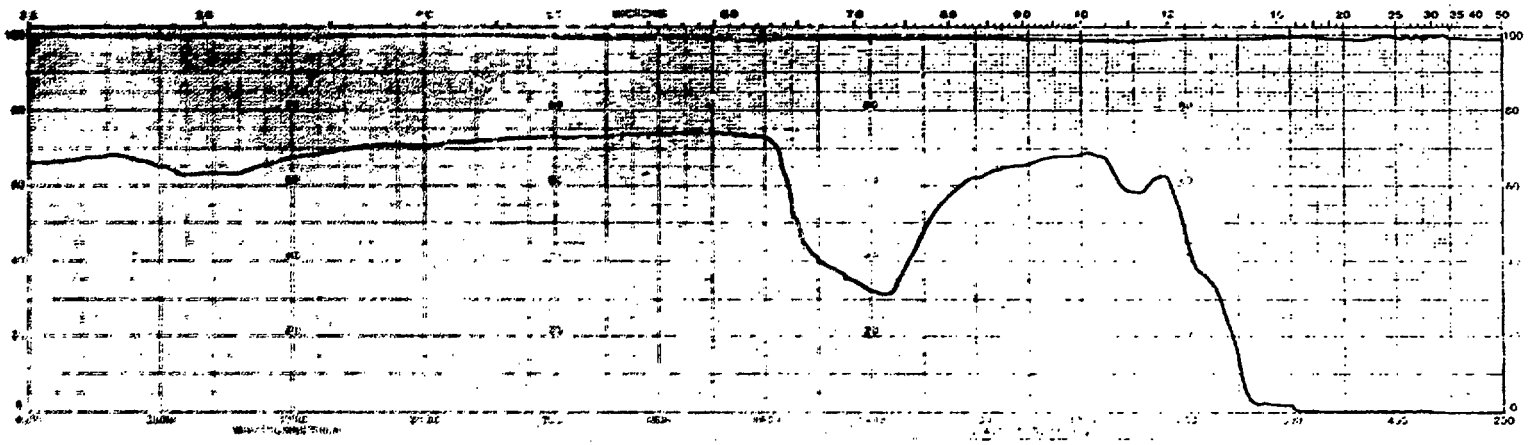

Fig. 3-17. Infrared Transmittance of Water-Clear ZnS Coated With ~ 1 μm Cubic BN. Film is White and Powdery.

TABLE 3-13

Knoop Hardness (HK_{50}) Cubic BN Coated Water-Clear ZnS

Sample	Initial Hardness	After Cubic BN Coating	After Wiping with Cotton Swab
AF-BN1	163 ± 8	170 ± 12	142 ± 7
AF-BN2	160 ± 5	174 ± 11	--------
AF-BN3	157 ± 3	168 ± 14	161 ± 7
AF-BN4	159 ± 6	172 ± 11	157 ± 7
*AF-R3	160 ± 7	173 ± 11	157 ± 11
*AF-R4	158 ± 6	162 ± 16	152 ± 9

* Initial Coating of 5000 Å Cubic BN

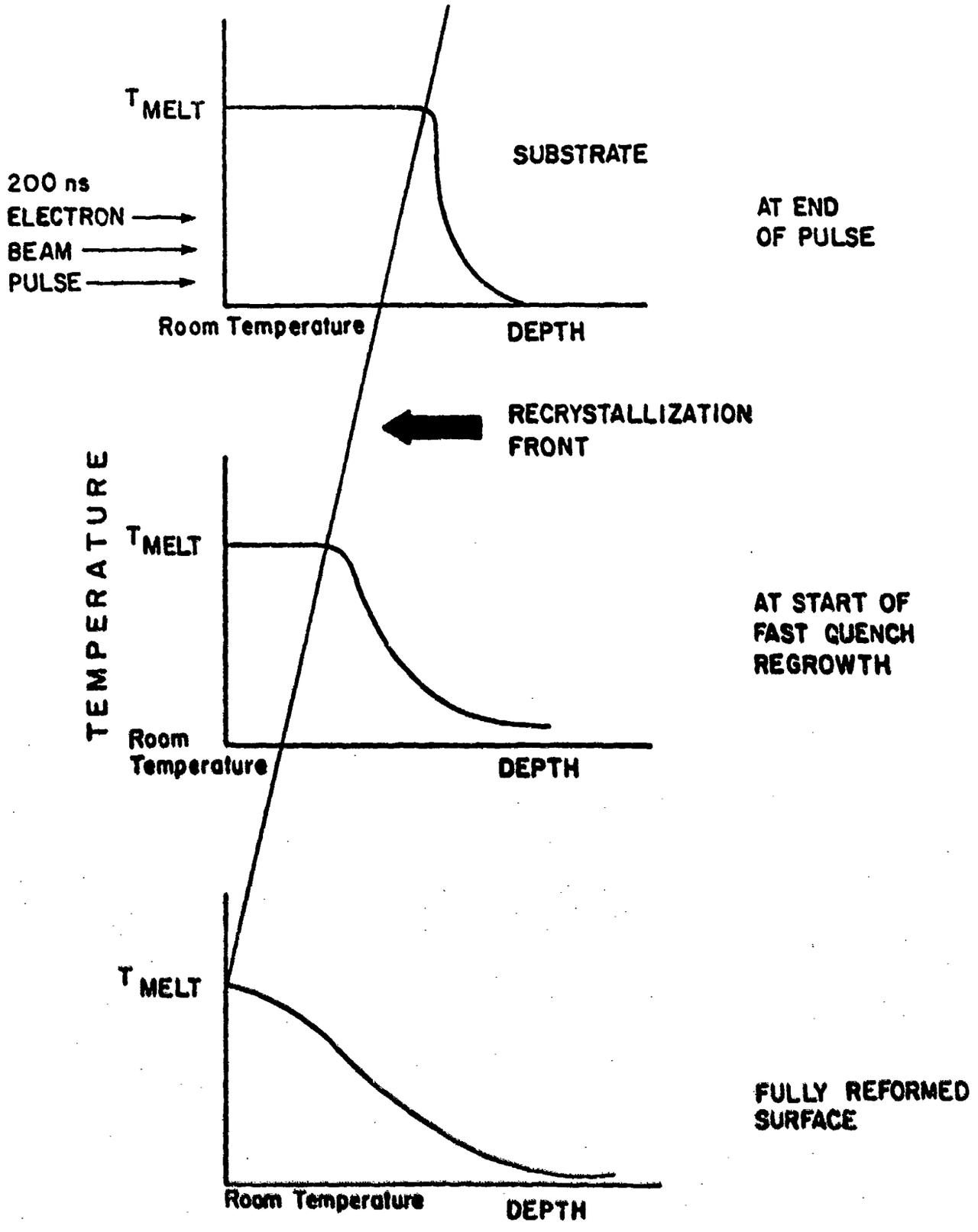

Fig. 3-18 Schematic of Pulsed Electron Beam Annealing Process Showing Recrystallization Front (Courtesy of Spire Corp.)

with a quench rate as high as 10^9 K/s. The resulting alteration of material properties due to this melt and ultra-fast quench varies considerably from meterial to material.

In contrast to conventional thermal furnace annealing or other quench annealing processes, PEBA is a "room temperature" process which eliminates sample distortion and subsurface stress. This is so because the deposition of the electron energy is so rapid that only the near surface layer of the sample is heated. However, the deposition of tens of kiloamperes of electrons at an energy up to hundreds of kilovolts per electron in less than a microsecond can easily melt the near surface region (a few micrometers) of the highest melting point materials.

The PEBA technique was used in an attempt to obtain rapid recrystallization from the melted layer, leaving the top layer of ZnS with a small grained (therefore hardened) surface. At the two beam energies employed, 0.09 and 0.20 cal/cm^2, theoretically there was sufficient energy to melt a 1-2 μm layer of material. However, experimentally there was no change in grain size or surface morphology of samples processed at both energies. The infrared transmittance and hardness were also unaffected. Due to the high cost and scheduling problems, this technique was discontinued as a means of increasing the hardness of ZnS through fine grain recrystallization. Further work was done with PEBA as a means to pulse diffuse various dopants as will be discussed under ion implantation in the next section.

3.7 Ion Implantation*

Ion implantation was another technique employed to increase the hardness of water-clear ZnS. Ion implantation has been found to have beneficial results on such surface sensitive properties as wear, erosion, fatigue and catalytic activity. This is in part due to the fact that ion implantation is a non-equilibrium process and can create surface morphologies and alloys unobtainable with other techniques.

In ion implanation, a high energy beam of ions is accelerated into the substrate under high vacuum. An analyzing magnet separates the ions of interest, and the resultant, pure ion beam can penetrate the substrate to a depth up to a few micrometers (Fig. 3-19). Standard alloys can be formed

*Work performed at Spire Corp., Bedford, MA 01730

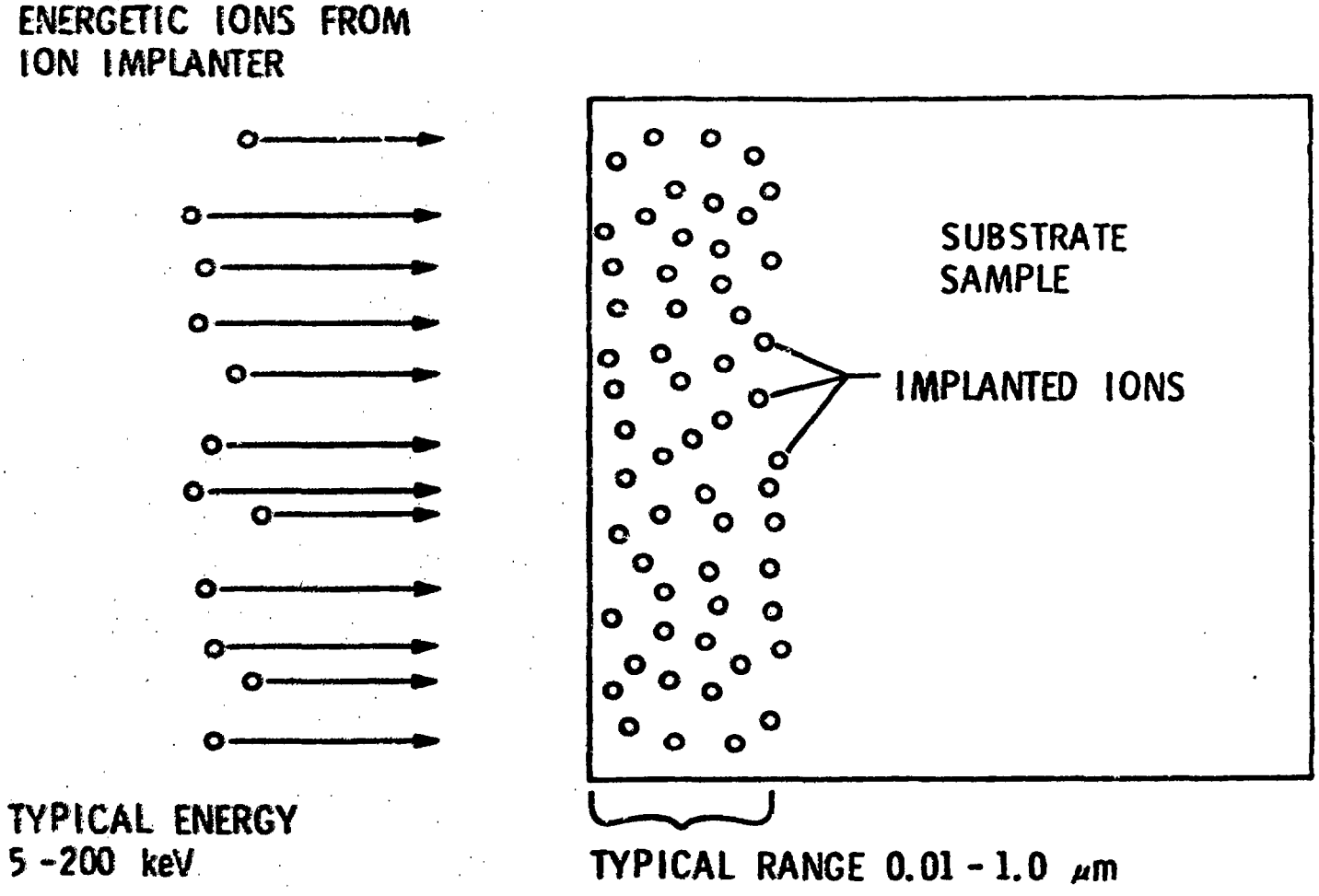

Fig. 3-19 Schematic of Ion Implantation Process (Courtesy of Spire Corp.)

in the substrate surface without affecting the bulk material. Novel alloys, metastable phases and non-equilibrium phases are also possible because the ions can be implanted well past the solid solubility limits. Amorphous surfaces and compressive or tensile stresses can also be formed by ion implantation.

Since there was no previous history of ZnS ion implanted to increase hardness, [S^{2-}] anions were initially chosen for a baseline data point. The sulphur anions were implanted with a flux of 2×10^{17} ions/cm^2 at 85 keV. It was expected that an ion penetration of approximately 800 Å would occur. As Table 3-14 shows, these samples show no increase in hardness. However, no deterioration of infrared optical transmittance was observed (Figs. 3-20 and 3-21).

The next batch of implants which were completed included Al^{3+} and I^- ions. It was calculated that the introduction of I^- anions into the ZnS lattice would yield a compressive stress in the implanted surface. The I^- ions were implanted at fluxes of 5×10^{14} and 2×10^{17} ions/cm^2 at 85 keV. The iodine ions implanted at the lower flux displayed a slight decrease in the short wavelength infrared transmittance (Fig. 3-22) and no increase in hardness (Table 3-15). The higher flux iodine implants displayed slightly greater infrared transmittance degradation (Fig. 3-23). The surface of the implanted side appeared to be etched, i.e., the grain structure of the material became visible. This made Knoop hardness measurements difficult, and may account for the observed variation in hardness. As can be seen, there was no substantial change in Knoop hardness.

Aluminum cations [Al^{3+}] were implanted at a flux of 2×10^{17} ions/cm^2 at 85 keV. A penetration of approximately 800 Å was expected. Table 3-16 shows there was no apparent increase in Knoop hardness. In addition, there is an interference band pattern on the implanted side, yet no decrease in infrared optical transmission was observed (Figs. 3-24 and 3-25).

The next impurity species selected for implantation was cadmium cations [Cd^{2+}]. It was hoped that the Cd cation would add a compressive strain to the crystal lattice, therefore, increasing the rain erosion

TABLE 3-14

Knoop Hardness (HK_{50}) of Sulfur Ion Implantation into Water-Clear ZnS

[S^{2-}] 85 keV, 2 x 10^{17} ions/cm^2

Sample	HK_{50} Initial Hardness	HK_{50} After [S^{2-}] Implant
AF1-18	160 ± 8	162 ± 13
AF6-B	162 ± 6	154 ± 7

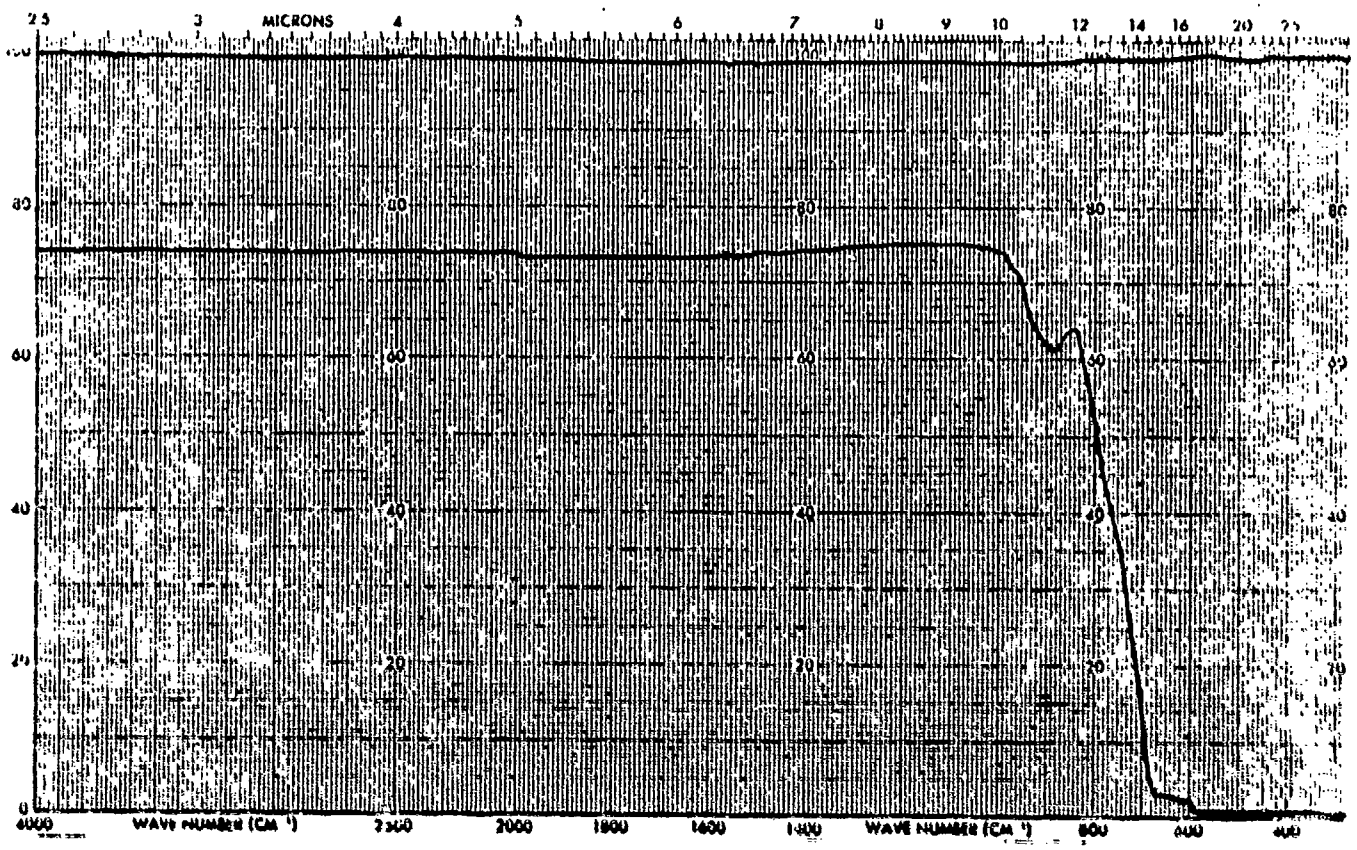

Fig. 3-20. Infrared Transmittance of Water-Clear ZnS Before [S^{2-}] Ion Implantation.

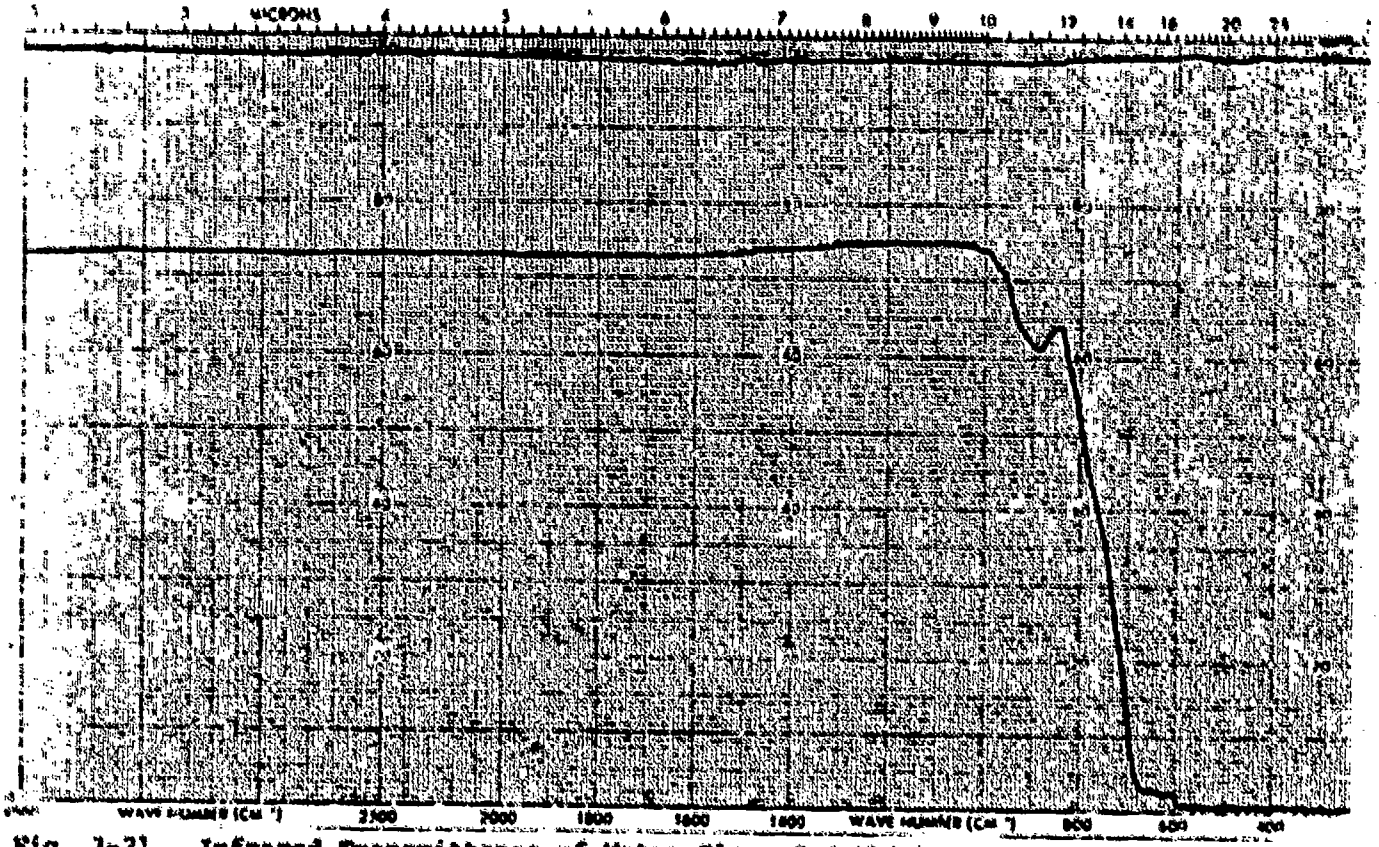

Fig. 3-21. Infrared Transmittance of Water-Clear ZnS Which Has Been Implanted with [S^{2-}] Ions at 85 keV and 2 x 10^{17} ions/cm^2.

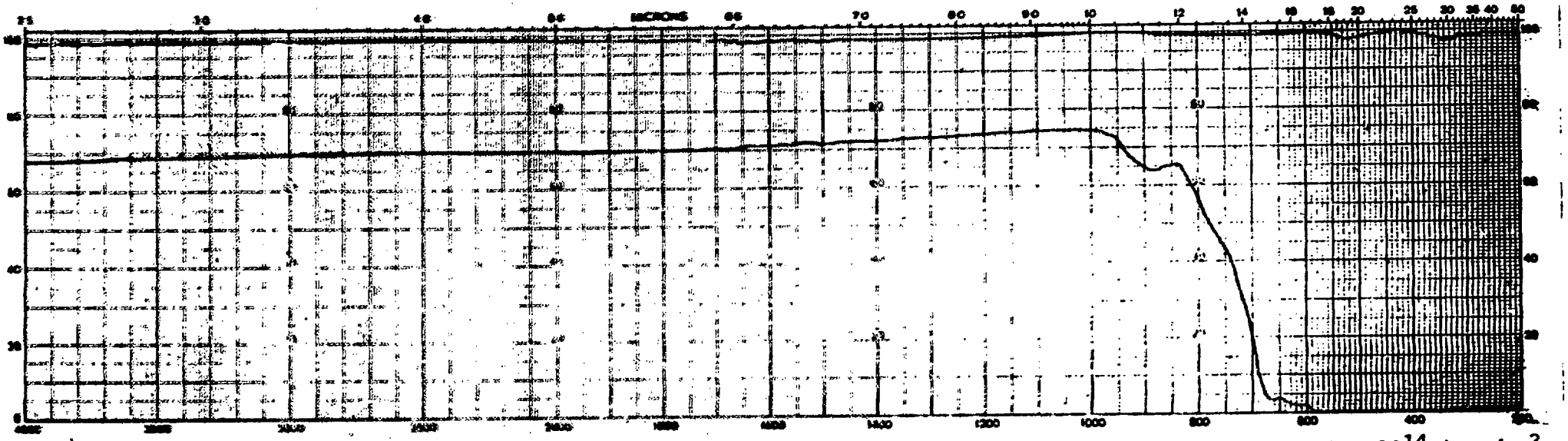

Fig. 3-22. Infrared Transmittance of AF-4 Water-Clear ZnS Subjected to [I⁻] Ion Implantation, 85 keV, 5 x 10^{14} ions/cm^2.

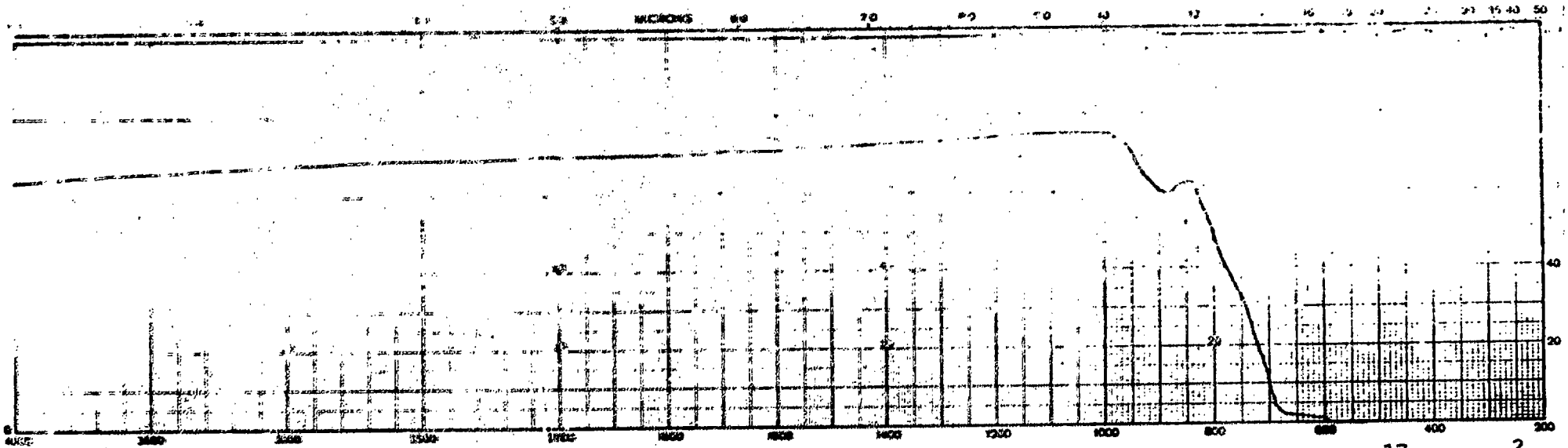

Fig. 3-23. Infrared Transmittance of AF-4 Water-Clear ZnS Subjected to I Ion Implantation, 85 keV, 2 x 10^{17} ions/cm^2.

TABLE 3-15

Knoop Hardness (HK_{50}) of Iodine Ion Implantation into Water-Clear ZnS

[I^-], 85 keV, 5×10^{14} and 2×10^{17} ions/cm^2

Sample	Initial Hardness HK_{50}	[I^-] Flux (ions/cm^2)	Final Hardness HK_{50}
AF-4A	150 ± 4	5×10^{14}	154 ± 5
AF-6B	153 ± 5		155 ± 6
AF4-13	143 ± 7	2×10^{17}	166 ± 12
AF6-A	152 ± 4		137 ± 7

TABLE 3-16

Knoop Hardness (HK_{50}) of Aluminum Ion Implantation into Water-Clear ZnO

[Al^{3+}], 85 KeV 2 x 10^{17} ions/cm^2

Sample	HK_{50} Initial Hardness	HK_{50} After Implant
AF4-10	152 ± 2	154 ± 14
AF4-16	154 ± 7	148 ± 3

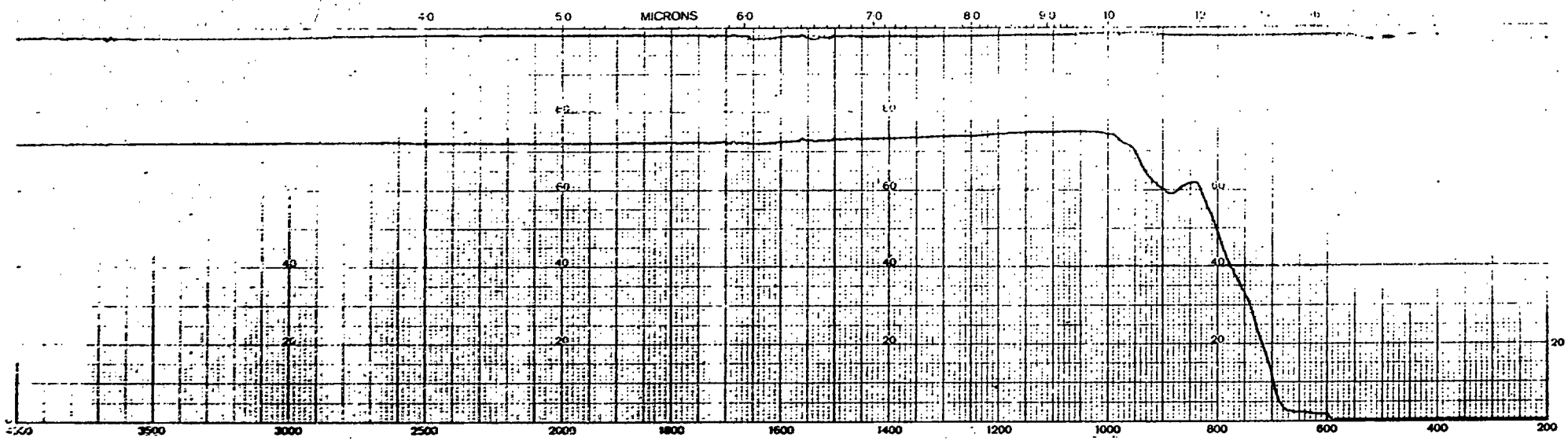

Fig. 3-24. Infrared Transmittance of AF-4 Water-Clear ZnS Before [Al^{3+}] Ion Implantation.

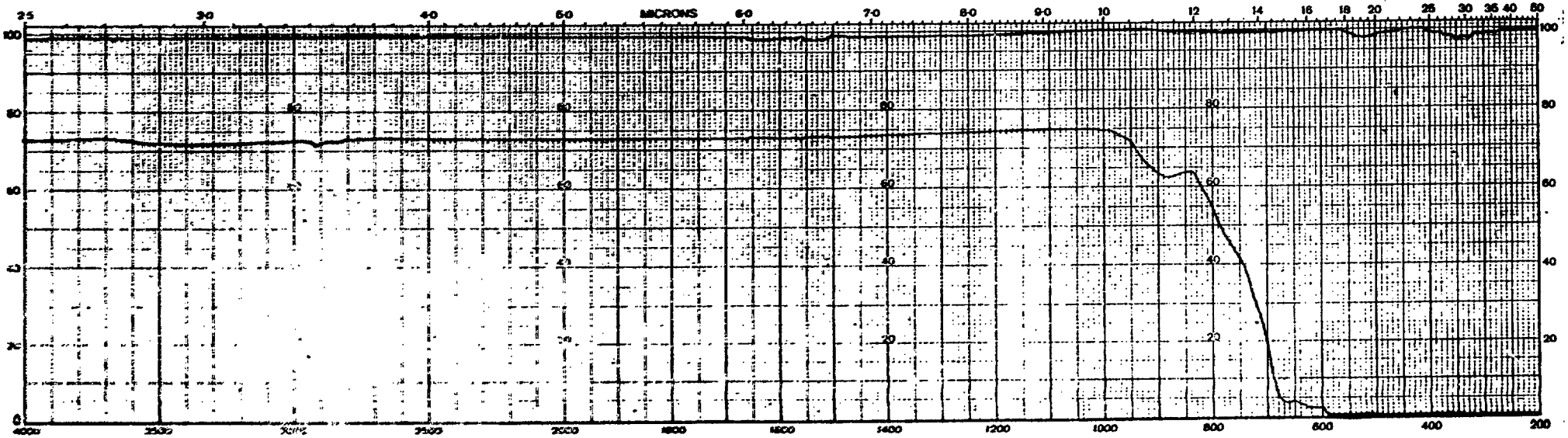

Fig. 3-25. Infrared Transmittance of AF-4 Water-Clear ZnS After [Al^{3+}] Ion Implanted at 85 keV, 2 x 10^{14} ions/cm^2.

resistance of water-clear ZnS. It was shown earlier that significant increases in hardness were obtained by thermal diffusion of Cd into the water-clear ZnS. However, as seen in Table 3-17, the implantation of Cd does not provide a measurable increase in hardness. This result is difficult to understand but may indicate that Cd cations are either not being implanted in sufficient concentration or that their depth of penetration is too shallow. There was also some surface damage to the implanted side, which decreased the short wavelength infrared transmittance of Cd implanted water-clear ZnS (Figs. 3-26 and 3-27).

Lithium cations [Li^+] were another ion implanted in water-clear ZnS. The Li ion, being considerably smaller than the previously implanted ions, should penetrate deeper into the bulk material. For example, Cd ion implantation was expected to penetrate about 800-1000 Å at the ion energies employed. At approximately equal implant conditions (75 keV, 2×10^{17} ions/cm^2), Li ions would be expected to penetrate approximately five times deeper. The Li implanted samples show a slight amber color, and a slight decrease in short wavelength transmittance (Figs. 3-28 and 3-29). Infrared transmittance remains unaffected (Figs. 3-30 and 3-31). As is evident from Table 3-18, some modest but consistent improvements in Knoop hardness were observed.

Of the five dopant species (I, Cd, Al, S and Li) chosen to study the effects of ion implantation, only one was expected to penetrate to an appreciable depth (Li ~ 5000 Å). Not surprisingly, this was also the only implantation that displayed, albeit small, consistent increases in hardness. As a result, two post-implantation treatments, HIP and PEBA, were tried to increase the depth of penetration of these implants. It was thought that these high temperature processes would provide for additional penetration through thermal diffusion.

Table 3-19 shows the values of Knoop hardness as measured before and after implantation and after subsequent HIP and PEBA treatment for three of the five ions implanted (Al and S ions were not selected for this testing). Samples of both as deposited and water-clear ZnS were implanted and thermally treated. Within the scatter of the data, there does not appear to be any noticeable increase in hardness. The deposited CVD ZnS sample implanted with I and Li both show an apparent small increase in hardness which disappears

TABLE 3-17

Knoop Hardness (HK_{50}) of Cadmium Ion Implantation into CVD (As Deposited and Water-Clear) ZnS

$[Cd^{2+}]$, 85 keV 2 x 10^{17} ions/cm^2

Sample	Initial State	HK_{50} Initial Hardness	HK_{50} After Implantation
AF 4-Z2	As Deposited	214 ± 3	224 ± 13
AF 4-Z2	As Deposited	203 ± 17	209 ± 11
AF4-Z3	As Deposited	210 ± 5	215 ± 19
AF4-Z4	As Deposited	207 ± 6	207 ± 12
AF 4-H2	Water-Clear ZnS	160 ± 9	159 ± 6
AF 4-H4	Water-Clear ZnS	166 ± 7	160 ± 9
AF 4-H5	Water-Clear ZnS	156 ± 4	150 ± 10
AF 4-H6	Water-Clear ZnS	159 ± 5	153 ± 13
AF 4-H8	Water-Clear ZnS	162 ± 7	157 ± 9

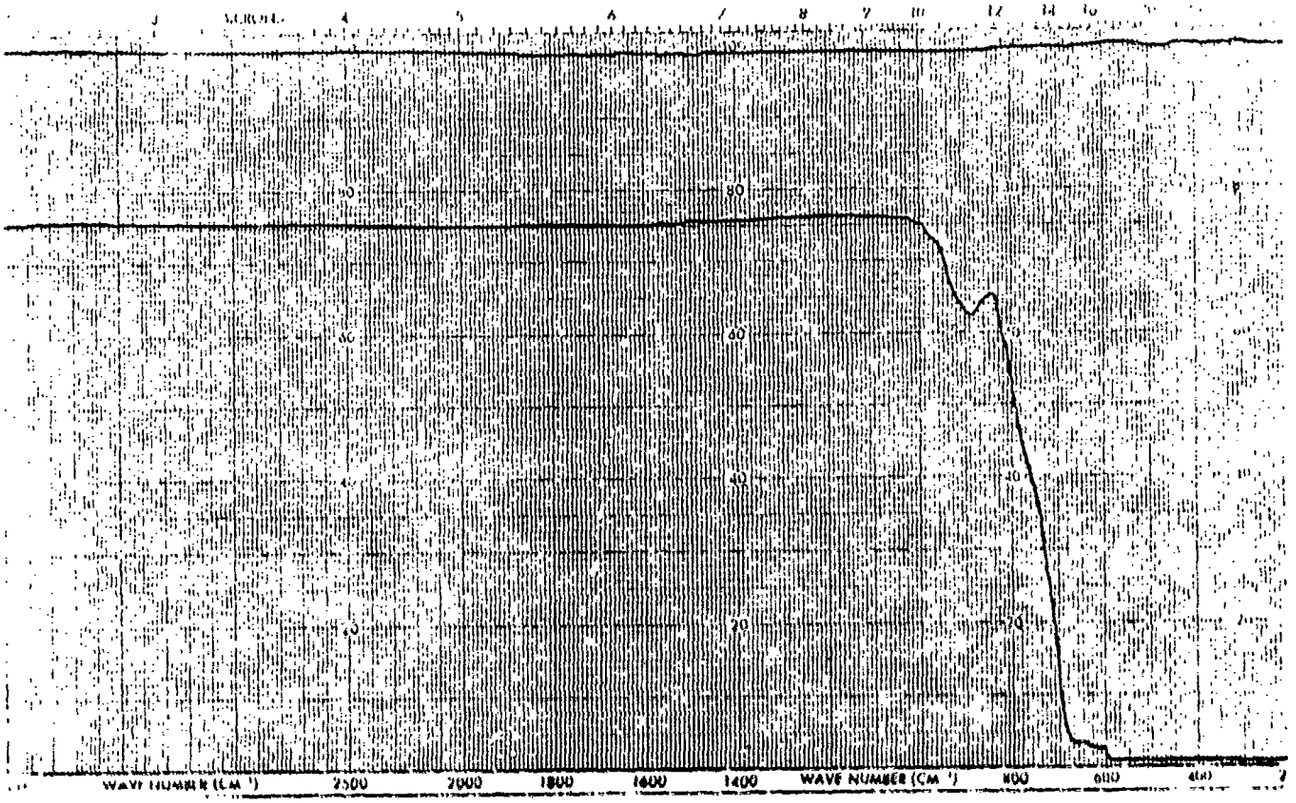

Fig. 3-26. Infrared Transmittance of AF-4 Water-Clear ZnS Before Cd Ion Implantation.

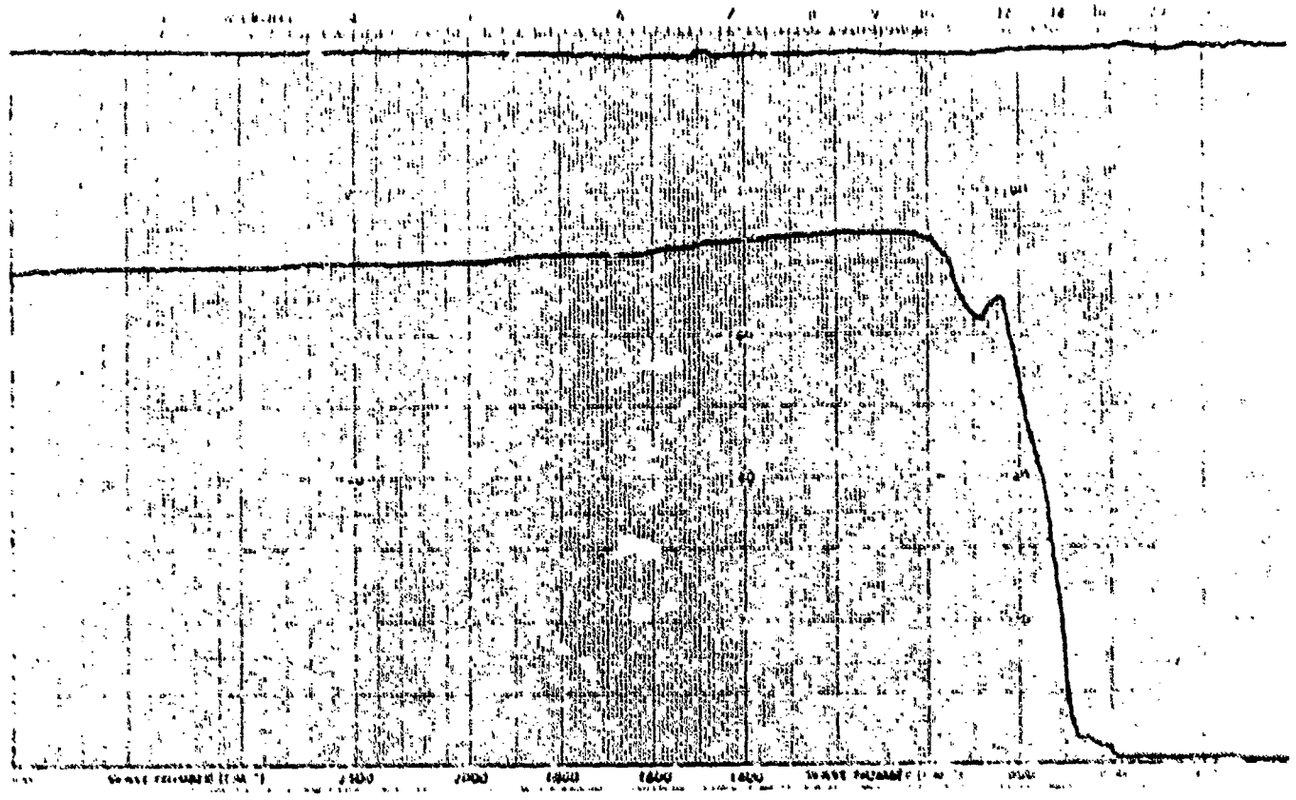

Fig. 3-27. Infrared Transmittance of AF-4 Water-Clear ZnS After $[Cd^{2+}]$ Ion Implanted, 85 keV, 2×10^{17} ions/cm^2.

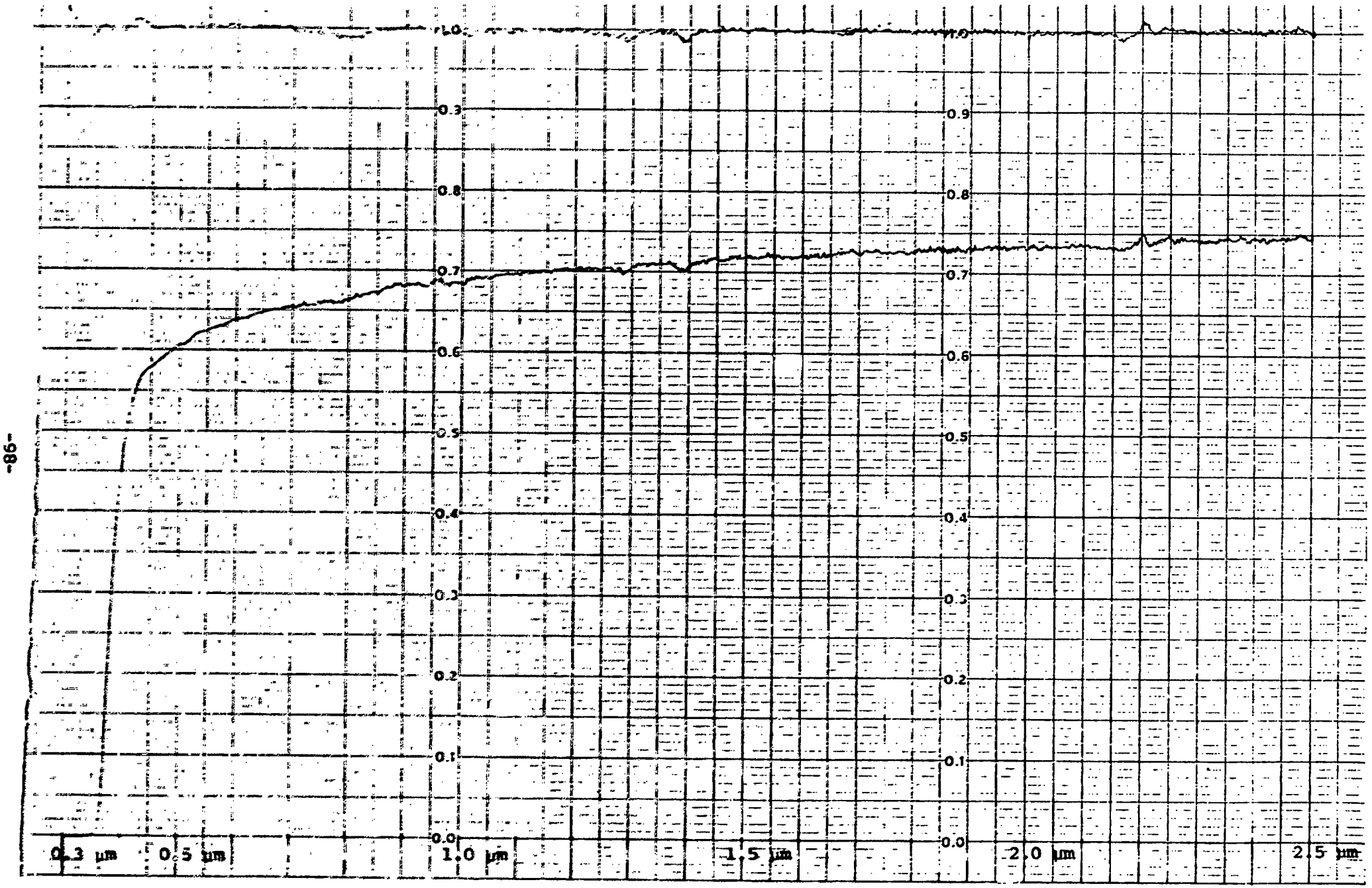

Fig. 3-28. Visible - Near Infrared Transmittance of Water-Clear ZnS Before [Li^+] Ion Implantation.

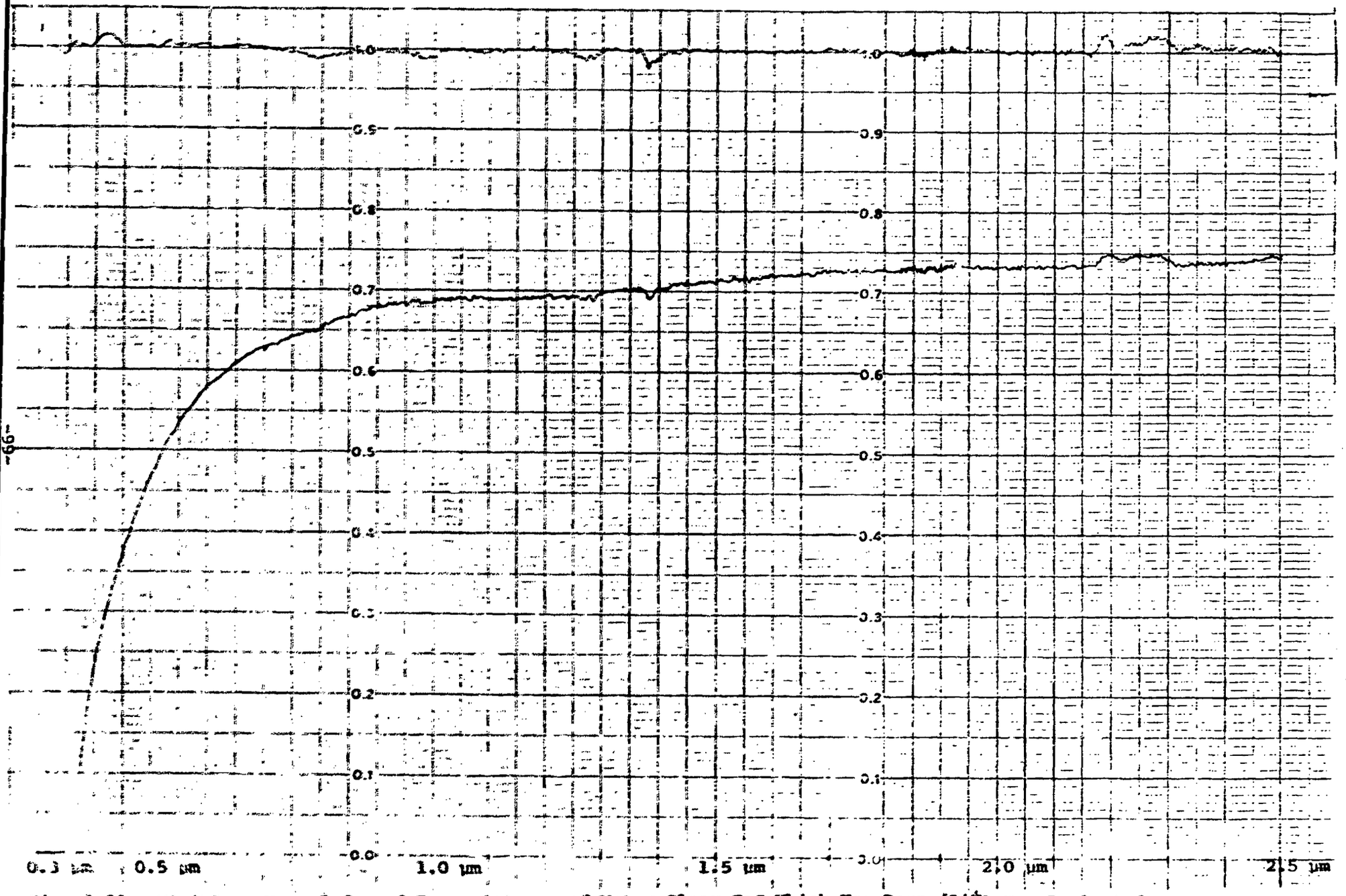

Fig. 3-29. Visible - Near Infrared Transmittance of Water-Clear ZnS Which Has Been [Li^+] Ion Implanted at 75 keV, 2 x 10^{17} ions/cm^2.

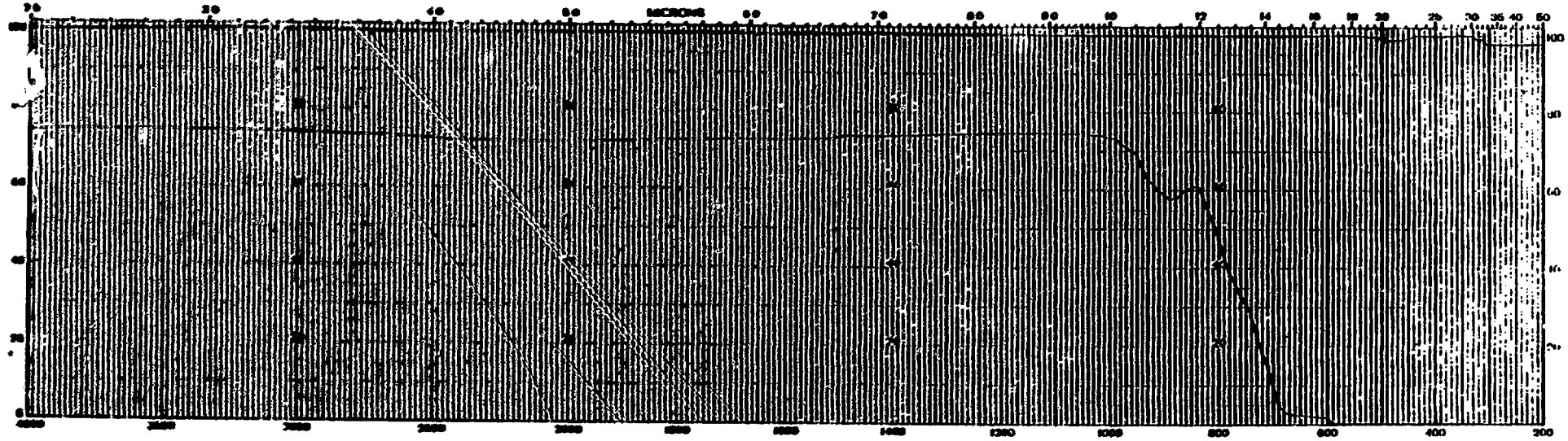

Fig. 3-30. Infrared Transmittance of Water-Clear ZnS Which Has Been Ion Implanted with [Li^+] Ions at 75 keV, 2 x 10^{17} ions/cm^2 Before PEBA Processing.

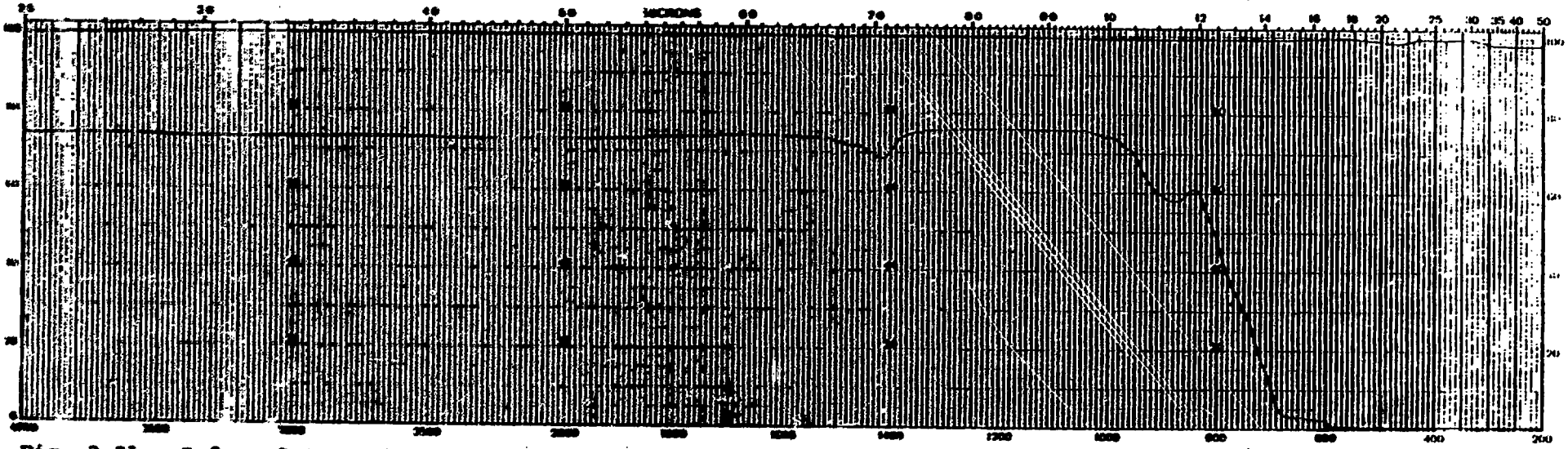

Fig. 3-31. Infrared Transmittance of Water-Clear ZnS Which Has Been Ion Implanted with [Li^+] Ions at 75 keV, 2 x 10^{17} After PEBA Processing at 0.20 cal/cm^2.

TABLE 3-18

Knoop Hardness (HK_{50}) of Lithium Ion Implantation into CVD (As Deposited and Water-Clear) ZnS

$[Li^+]$ 75 keV 2 x 10^{17} ions/cm^2

Sample	Initial State of ZnS	HK_{50} Initial Hardness	HK_{50} After Implantation
AF 4-2S	As Deposited	206 ± 13	222 ± 13
AF 4-2G		210 ± 9	225 ± 11
AF 4-2T		214 ± 9	230 ± 9
AF 4-2B		219 ± 12	235 ± 2
AF 4-1A	Water - Clear	153 ± 7	169 ± 9
AF 4-1B		152 ± 4	162 ± 9
AF 4-1C		147 ± 3	161 ± 9
AF 4-1D		149 ± 2	162 ± 7

TABLE 3-19

Knoop Hardness (HK_{50}) of Ion Implantation/Diffusion by PEBA and HIP

	As Deposited CVD ZnS			Water-Clear ZnS		
Ion	Initial	Implanted	HIP	Initial	Implanted	PEBA
I	210 ± 10	229 ± 15	165 ± 5	155 ± 5	171 ± 10	161 ± 10
Cd	210 ± 10	213 ± 15	165 ± 5	160 ± 5	158 ± 10	160 ± 15
S	---	---	---	160 ± 5	160 ± 5	---
Li	211 ± 10	228 ± 10	172 ± 10	151 ± 5	163 ± 10	157 ± 5

after HIP processing. For the water-clear samples, again only the I and Li implants showed any increase in hardness which was reduced after PEBA treatment.

As stated previously, the Li ion implanted water-clear ZnS samples displayed a slight amber coloration, but the infrared transmittance was not affected. After PEBA treatment a small absorption band is evident at about 7 μm (Fig. 3-31), the source of which is unknown at present. The remainder of the samples displayed comparable infrared transmittance results before and after PEBA.

As a result of the modest improvement of hardness of the Li implanted clear ZnS, further experiments were performed in which the Li ion flux and energy were increased over initial implantation conditions. The Li was implanted with an energy of 150 keV and beam doses of 2×10^{17} and 4×10^{17} ions/cm^2. As can be seen from Table 3-20, there is a modest increase in hardness, with the higher dose samples showing the larger increase. In addition to having an increased hardness, these implanted samples showed the characteristic amber coloration. However, unlike the lower energy Li implants, these samples exhibited an increase in surface damage, with some regions showing heavy surface etching. This damage was more frequent in the high dose samples. This surface damage also caused scatter in the Knoop hardness measurements. The lower dose samples displayed a slight absorption band at ~ 9.0 μm (Fig. 3-32), but, surprisingly the higher dose samples do not. These latter samples exhibited a broad, shallow doublet at about 6.8 and 7.0 μm (Fig. 3-33) which is similar to that of the PEBA processed low energy (Li^+) implant (Fig. 3-31). As yet, we do not have an explanation for these phenomena.

In order to understand the ion implanted material more quantitatively, Scanning Auger Microscopy (SAM) with depth profiling was done on a sample of untreated AF-4 water-clear ZnS. SAM uses a finely focused beam of electrons for sample excitation. The signal studied consists of Auger electrons which have energies that identify the elements they come from. Elements heavier than helium are detectable with this technique. SAM is a surface measurement; so in order to get depth profiling, ion beam sputtering was employed. Ar^+ ions bombard the surface, sputtering away surface atoms and exposing material below the contaminated surface layer. For many materials, sputter rates are

TABLE 3-20

Knoop Hardness (HK_{50}) of Lithium Ion Implantation into Water-Clear ZnS

$[Li^+]$ 150 KeV, 2×10^{17} and 4×10^{17} ions/cm^2

Sample	Initial Hardness HK_{50}	Ion Flux (ions/cm^2)	After Implant HK_{50}
AF4-R5	159 ± 8	2×10^{17}	163 ± 8
AF4-R6	161 ± 3	2×10^{17}	166 ± 10
AF4-R7	157 ± 6	2×10^{17}	168 ± 7
AF4-R8	159 ± 4	2×10^{17}	160 ± 13
*AF4-R9	161 ± 3	4×10^{17}	--------
AF4-R10	160 ± 6	4×10^{17}	186 ± 10
AF4-R11	159 ± 7	4×10^{17}	172 ± 28
AF4-R12	163 ± 5	4×10^{17}	169 ± 18

*Sample was destroyed due to improper mounting.

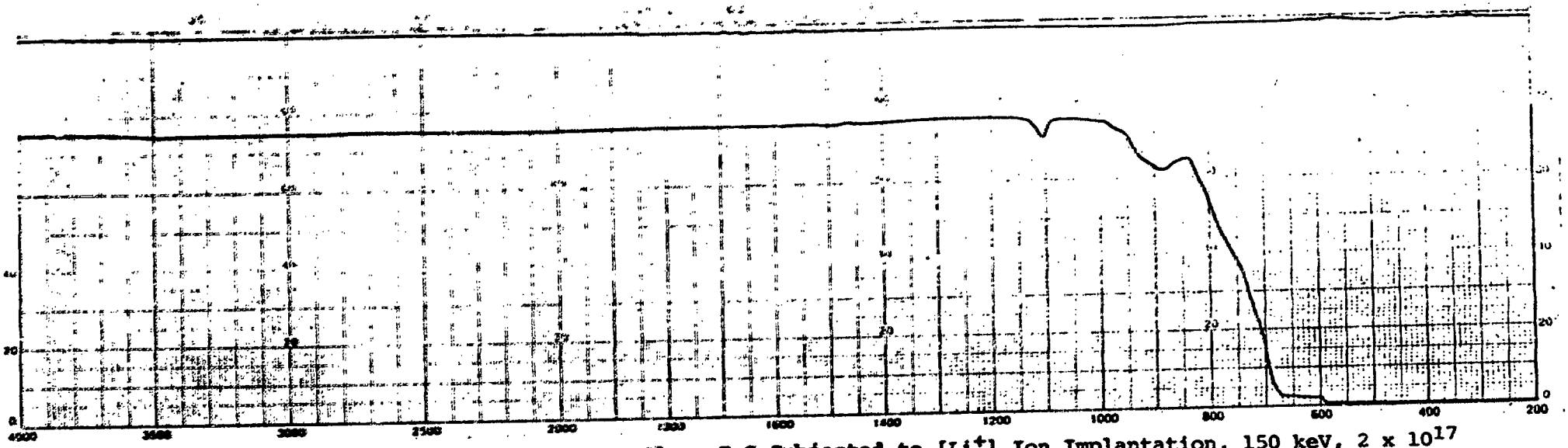

Fig. 3-32. Infrared Transmittance of AF-4 Water-Clear ZnS Subjected to [Li^+] Ion Implantation, 150 keV, 2 x 10^{17} ions/cm^2.

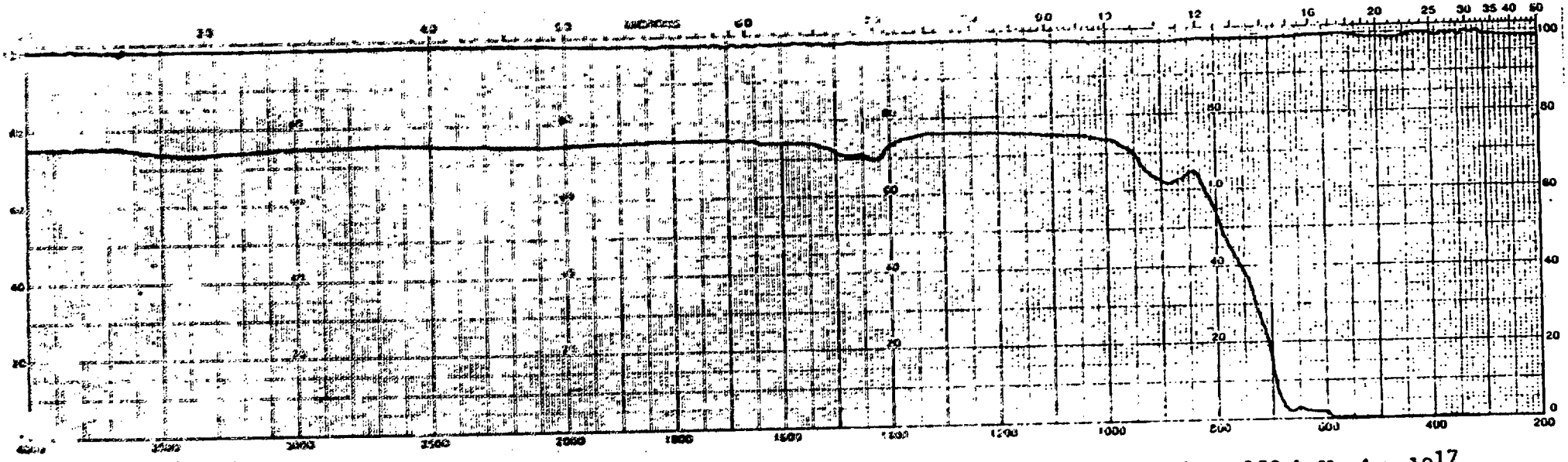

Fig. 3-33. Infrared Transmittance of AF-4 Water-Clear ZnS Subjected to [Li^+] Ion Implantation, 150 keV, 4 x 10^{17} ions/cm^2.

known which allow one to establish accurate composition-depth relationships. Unfortunately, sputtering rates are not known for CVD ZnS. In Table 3-21 we list sputtering times and the amount (in atomic percent) of various elements which were detected. As expected, the results show a high surface carbon content that rapidly decreases with increasing sputter times. After four minutes of sputtering, Zn and S represented 89.7% of material analyzed, with the remaining 10.3% composed of decreasing amounts of C and O. Because of the lack of quantitative depth measurement and the high compositional uncertainty (± 15 atomic %), Scanning Auger Microscopy was discontinued.

3.8 CVD Overcoat

A final, "thick-film", hard coating technique was tried on water-clear ZnS. Previous work has shown favorable improvements in rain erosion resistance of CVD ZnSe by depositing a layer of CVD ZnS onto the ZnSe (5, 12, 13). In a similar manner, CVD water-clear ZnS was used as the base material. A standard CVD ZnS deposition was made onto eight samples of water-clear ZnS. The samples were prepared with varying degrees of surface finish to determine which approach would yield the best optical and mechanical properties with adequate adhesion of the ZnS film. Table 3-22 lists the preparation parameters. The two polished samples gave poor adhesion of the subsequent deposit; the ZnS film had delaminated upon removal from the CVD furnace. Four of the remaining six samples have marginal thickness deposits on them; they are presently waiting final preparation. The two remaining samples had adequate thickness profiles and displayed excellent adhesion.

As is evident from Table 3-23, these ZnS coated pieces show a substantial increase in hardness. It is interesting that the thinner ZnS coated sample (.035" vs .085") displays the higher hardness (245 to 226). Visible-near infrared transmittance (Figs. 3-34 and 3-35) shows a substantial decrease which is also seen throughout the infrared region (Figs. 3-36 and 3-37). There are several reasons for this. (1) This was the first time a ZnS deposit was performed in this particular furnace; material quality was low. (2) The water-clear samples had rough grind finishes to help in the adherence of the film. As a result, there is substantial scattering along the as deposited/water-clear interface. This experiment was performed quickly to show feasibility and, clearly, there is room for improvement in both material quality (ZnS) and sample surface preparation.

TABLE 3-21

Scanning Auger Microscopy of AF-4 Water-Clear ZnS

Total Sputter Time (s)	Atomic %				
	Zn	S	C	O	N
0	22.7	6.9	64.3	4.5	1.6
10	31.5	23.7	39.0	5.8	--
70	34.9	40.3	18.9	4.4	1.5
130	50.5	36.0	10.2	3.3	--
240	45.5	44.2	7.4	2.9	--

TABLE 3-22

Predeposition Surface Preparation

CVD ZnS/Water-Clear ZnS Composite

Sample	Surface Preparation
CL-1P	60/40 Scratch/Dig
CL-2P	
CL-1R	30 μm Al_2O_3 Grind
CL-2R	
CL-1A	Acid Etch
CL-2A	
CL-1E	Edge Roughened
CL-2E	

TABLE 3-23

Knoop Hardness (HK_{50}) of CVD ZnS/Water-Clear ZnS Composite

Sample	Initial Hardness HK_{50}	ZnS Coating Thickness (inch)	Final Hardness HK_{50}
CL-1A	160 ± 4	.085	226 ± 16
CL-1R	164 ± 6	.035	245 ± 14

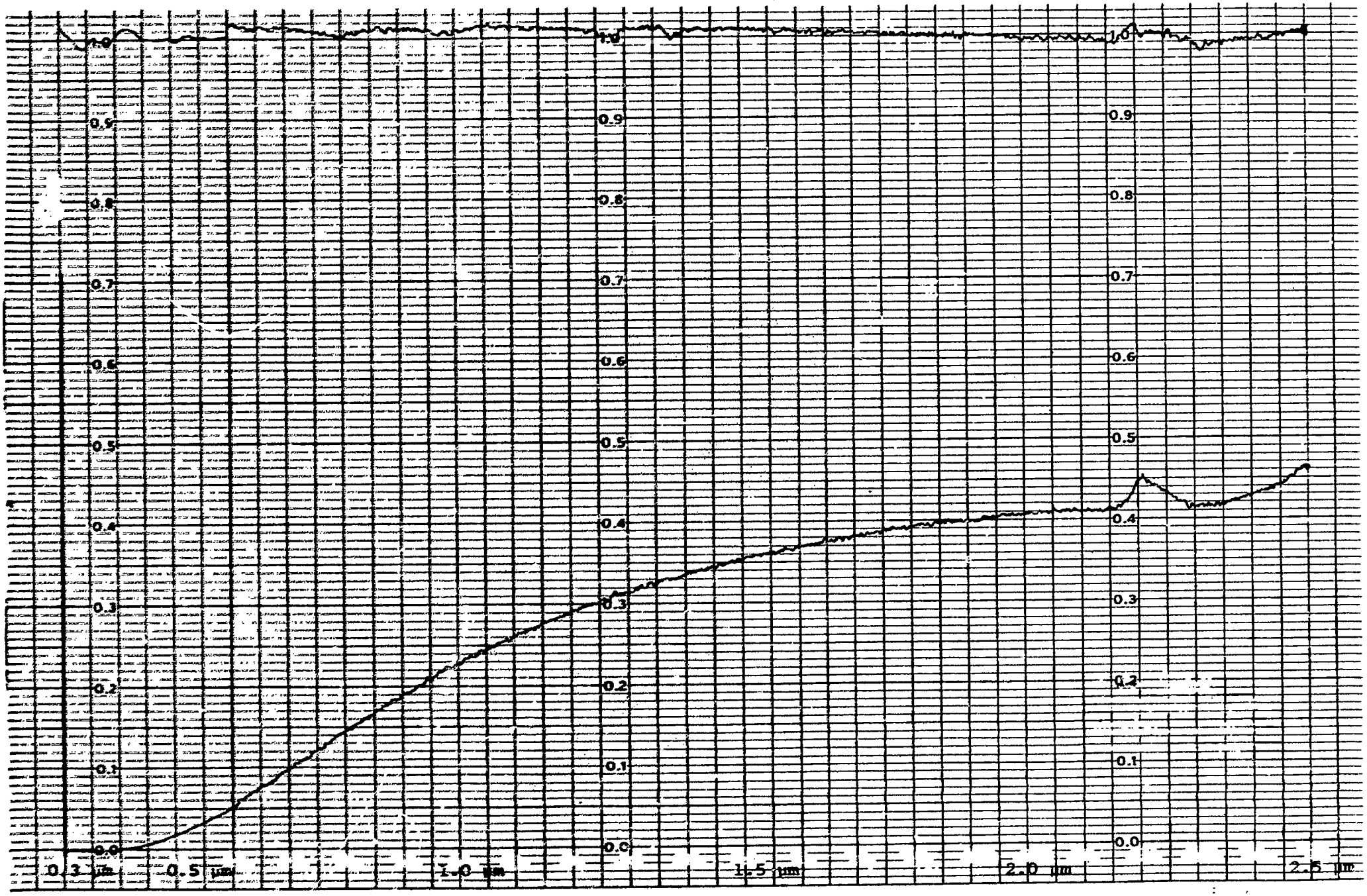

Fig. 3-34. Visible-Near Infrared Transmittance of CVD ZnS/Water-Clear ZnS Sandwich Composite. CVD ZnS Layer =.085 in, Total Thickness = .275 in.

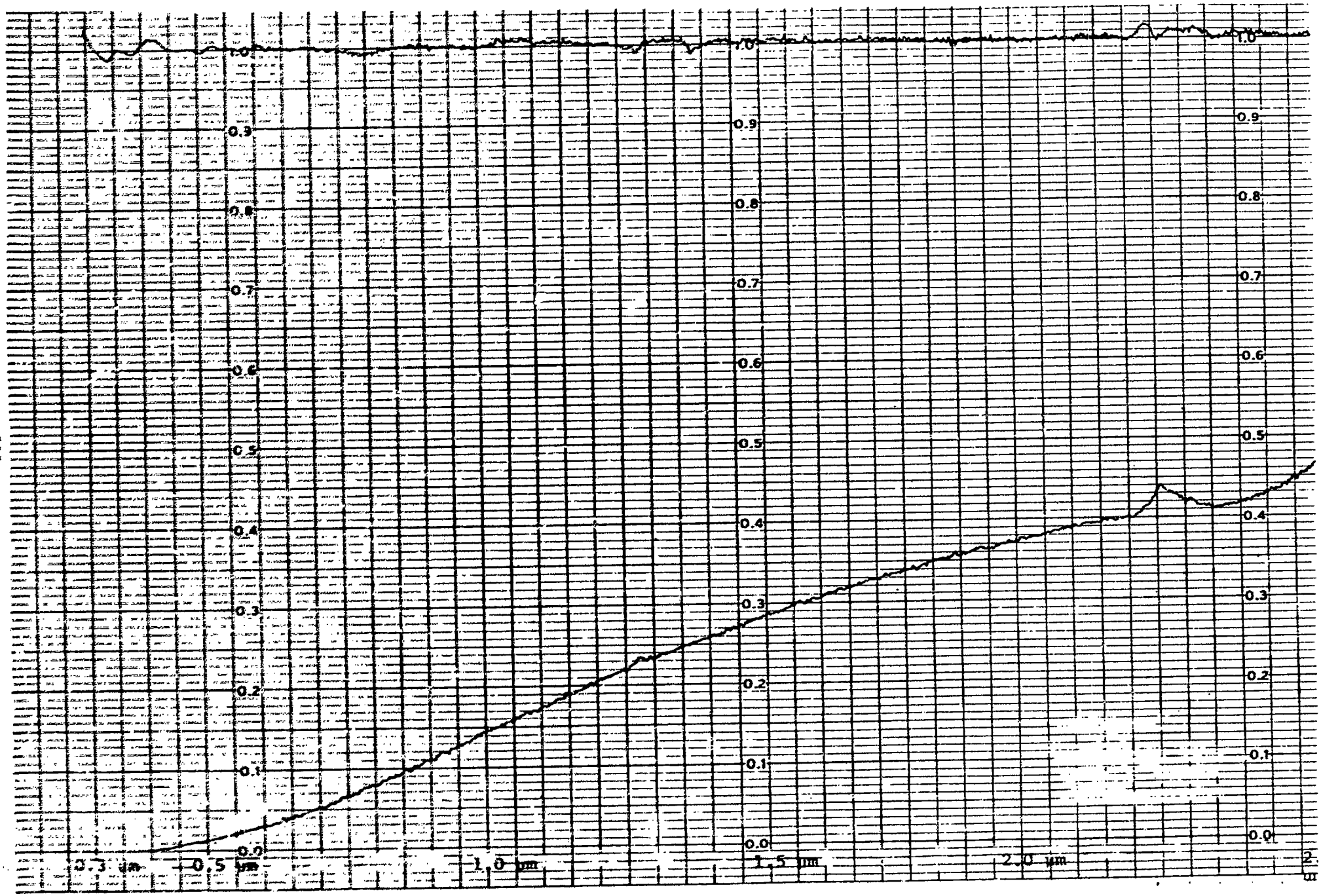

Fig. 3-35. Visible-Near Infrared Transmittance of CVD ZnS/Water-Clear ZnS Sandwich Composite. CVD ZnS Layer=.035 in, Total Thickness = .240 in.

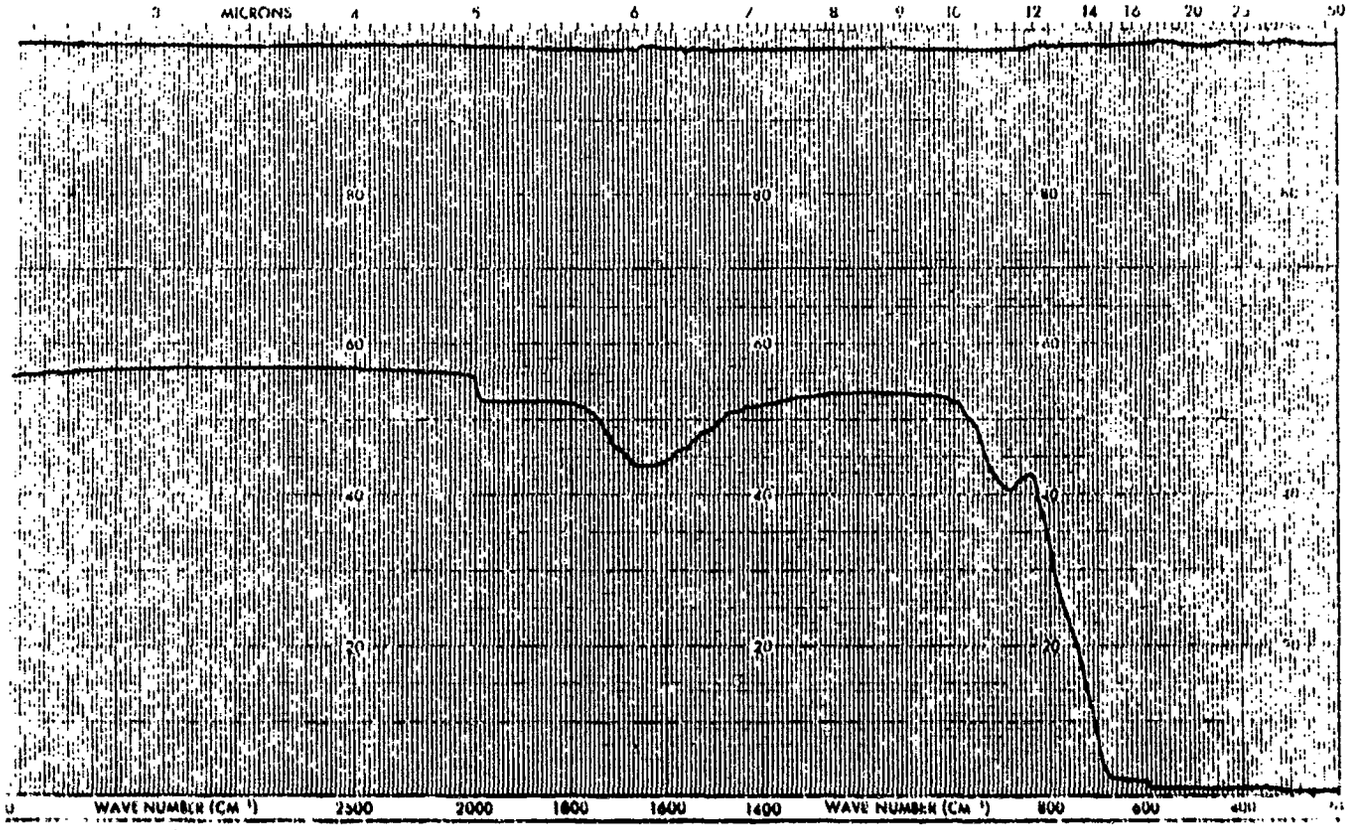

Fig. 3-36. Infrared Transmittance of CVD ZnS/Water-Clear ZnS Sandwich Composite. ZnS Layer=.085 in, Total Thickness=0.275 in.

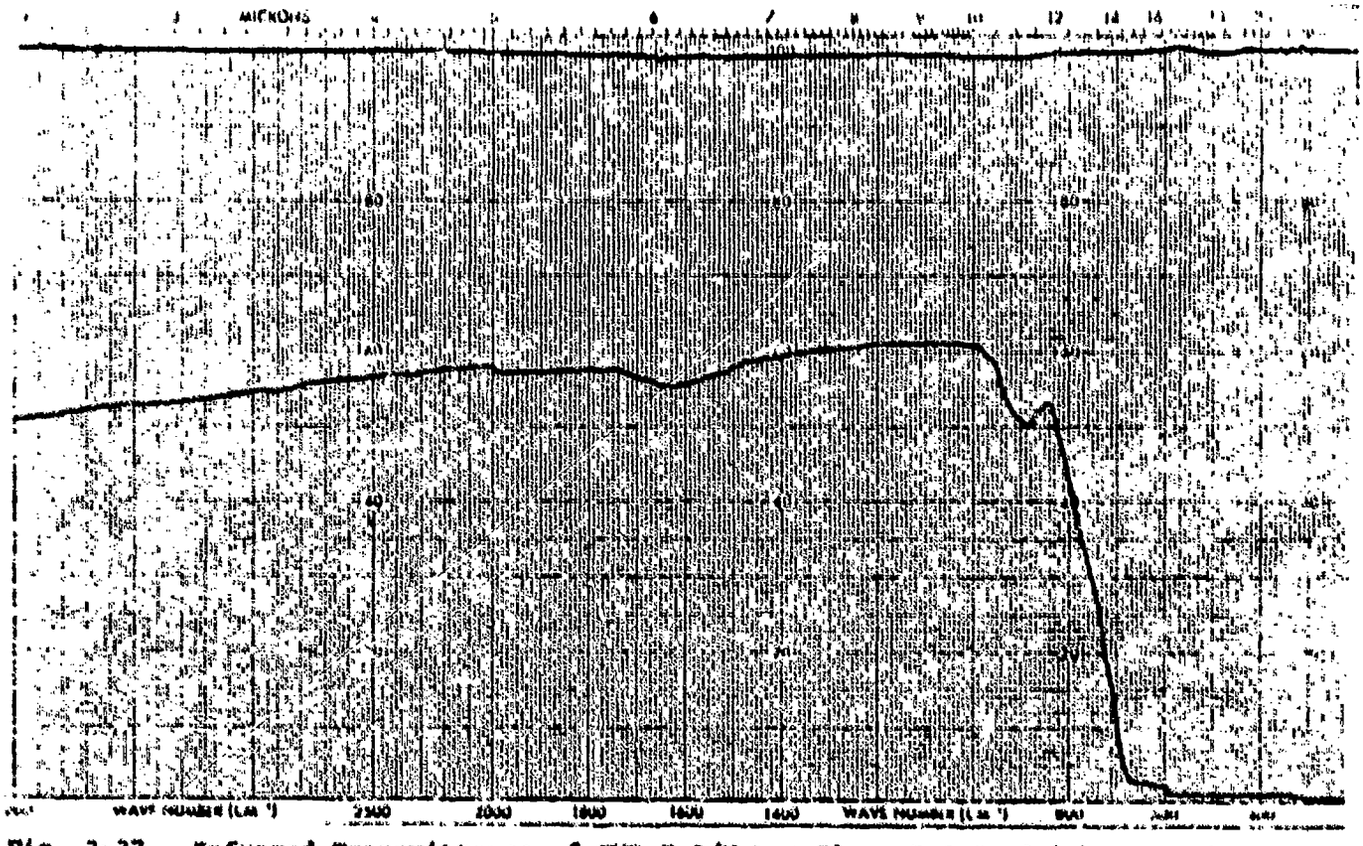

Fig. 3-37. Infrared Transmittance of CVD ZnS/Water Clear ZnS Sandwich Composite. ZnS Layer=.035 in, Total Thickness=0.240 in.

3.9 Summary and Conclusions - Task II

Various surface and/or bulk treatments were investigated to provide a harder water-clear material. Although a direct correlation between hardness, particularly surface hardness, and rain erosion resistance is not established, it was felt that if any treatment could produce a water-clear ZnS with hardness comparable to that of the initial CVD ZnS, then improved rain erosion would be likely. In any event, hardness measurements were used as an indicator of the effectiveness of all the treatments investigated.

Two approaches appeared to offer some promise of improved hardness. The first involves the diffusion of Cd atoms into the ZnS lattice to produce strain and a hardened surface layer. Data shown in Section 3.4 demonstrated that substantial increase in hardness could be obtained in a thin surface layer. However, it is also obvious that the thermal diffusion of Cd into the bulk water-clear ZnS is not a controlled nor practical technique for the production of optical material. Substantial optical degradation of the surface layer occurred during the diffusional process, and subsequent optical polishing to remove this degradation also removed all or most of the hard surface layer produced by the Cd diffusion. However, these data suggest an alternate approach in which the Cd would be codeposited during the production of the CVD ZnS. In this manner the concentration and uniformity of the Cd could be closely controlled. The idea would be to produce a harder CVD ZnS (with a small amount of Cd) than the standard CVD ZnS. Subsequent HIP treatment to produce water-clear material would presumably yield a softer material but not as soft as current water-clear ZnS. Since the Cd would be introduced throughout the lattice, removal of material during fabrication would not be relevant.

The second promising approach involves the deposition of a thin layer of CVD ZnS over the water-clear material. This concept follows directly from the ZnS/ZnSe sandwich construct, in which the ZnS layer is applied via CVD over a ZnSe substrate to produce improved rain erosion and environmental protection. In the present application both the layer and substrate are ZnS, and no difference in thermal expansion coefficients exists. Therefore, this approach should be applicable to curved surfaces, such as domes. Conversely, the surface strain produced by the mismatch in thermal expansion between ZnS

and ZnSe which produces an added hardness in the ZnS layer, will not occur for the water-clear sandwich. Although the limited experimentation on this approach performed in this program is insufficient to demonstrate its effectiveness, it is concluded that this approach warrants additional investigation.

Other treatments attempted under this task were unsuccessful or showed limited usefulness. Grain size refinement was unsuccessful, presumably because insufficient hexagonal phase was formed in the HIP treatment to act as nucleation sites for fine-grained, cubic recrystallization. Ion implantation of various anions and cations did not produce any significant increase in hardness. In view of the results with Cd atom diffusion, it would appear that similar improvements in hardness might be achieved by implantation of Cd ions and other similar species. However, ion implantation does not appear to be a practical technique to produce substantial concentration of impurity species at depths sufficient for subsequent optical fabrication. A similar comment can be made for pulsed electron beam annealing (PEBA). This technique does not appear to be capable of producing recrystallization of a sufficient layer of material without also producing optical degradation. Finally, attempts to apply hard coatings to water-clear ZnS were not successful. It is generally known that CVD ZnS and ZnSe are difficult to successfully coat with most materials. Research is currently underway in several organizations and countries to apply hard coatings to these CVD infrared optical materials. This work should be followed, as it may eventually produce an alternate means of improved environmental protection for water-clear ZnS.

4.0 TASK III - VALIDATING MEASUREMENTS AND TESTS

4.1 Introduction

As with any new material, there is a lack of data on mechanical and optical properties of water-clear ZnS. It was the purpose of this task to provide a well documented base line set of physical constants. The measurements were all performed on samples produced by the optimized conditions as described in Section 2.0, unless otherwise noted. A list of the measurements and tests performed is given in Table 4-1.

4.2 Test Results

Figures 4-1 to 4-3 represent spectral transmittance measurements of water-clear ZnS from 0.3 to 25 μm at room temperature (23 C) and at 200 C. At the higher temperature there is evidence of a more rapid decrease in transmission at the multiphonon edge in the infrared as expected theoretically. However, the transmission in the visible/ultraviolet region is unchanged. The infrared scan (2.5 - 25 μm) was performed on a Perkin Elmer 580 spectrophotometer, while the shorter wavelength measurement was made on a Cary 17D spectrophotometer.

The optical absorption coefficients of water-clear ZnS were measured using laser rate calorimetry. The lasers employed consisted of a Nd: YAG laser operating at 1.06 and 1.32 μm, HF and DF lasers operating at 2.7 and 3.8 μm respectively, and CO_2 laser operating at 9.27 and 10.6 μm. Results are shown in Table 4-2 for water-clear ZnS produced from three CVD depositions, and with the exception of values at 10.6 μm, the absorption is considerably lower throughout for AF-4 material. It should be noted that these absorption data are not 'bulk' coefficients because surface losses are included. The overall system sensitivity is approximately 10^{-5} cm^{-1}.

Figure 4-4 shows the amount of light scattered out of a 4 degree half angle cone in the 0.2 - 2.5 μm spectral region for water-clear ZnS produced from three CVD depositions. Once again, we see that AF-4 water-clear ZnS displays superior optical performance.

Figure 4-5 shows three interferograms of a sample of AF-4 water-clear ZnS. Figure 4-5 (top and middle) are Twyman-Green interferograms and

TABLE 4-1

Material Validating Measurements and Tests

Test	Organization
Spectral Transmission 23°C and 200°C; 0.3-14 μm	CVD Inc. Perkin-Elmer Corp.
Optical Absorption 1.06, 1.32, 2.7, 3.8, 9.27, and 10.6 μm	Univ. of Dayton Research Institute (UDRI)
% Forward Scatter 0.3-2.5 μm	UDRI
Refractive Index Inhomogeneity 0.6329 μm	UDRI
Modulation Transfer Function 8-12 μm	Diversified Optics
Effects of UV Exposure on Optical Properties	CVD Inc.
Thermo-Optic Coefficient (dn/dT) 0.6328, 1.15, and 3.39 μm	UDRI
Microstructure	CVD Inc.
Knoop Hardness	CVD Inc.
Flexural Strength	CVD Inc.
Thermal Conductivity	UDRI
Thermal Diffusivity	UDRI
Thermal Expansion	UDRI
Specific Heat	UDRI
Electrical Resistivity	UDRI
Rain Erosion Testing	UDRI

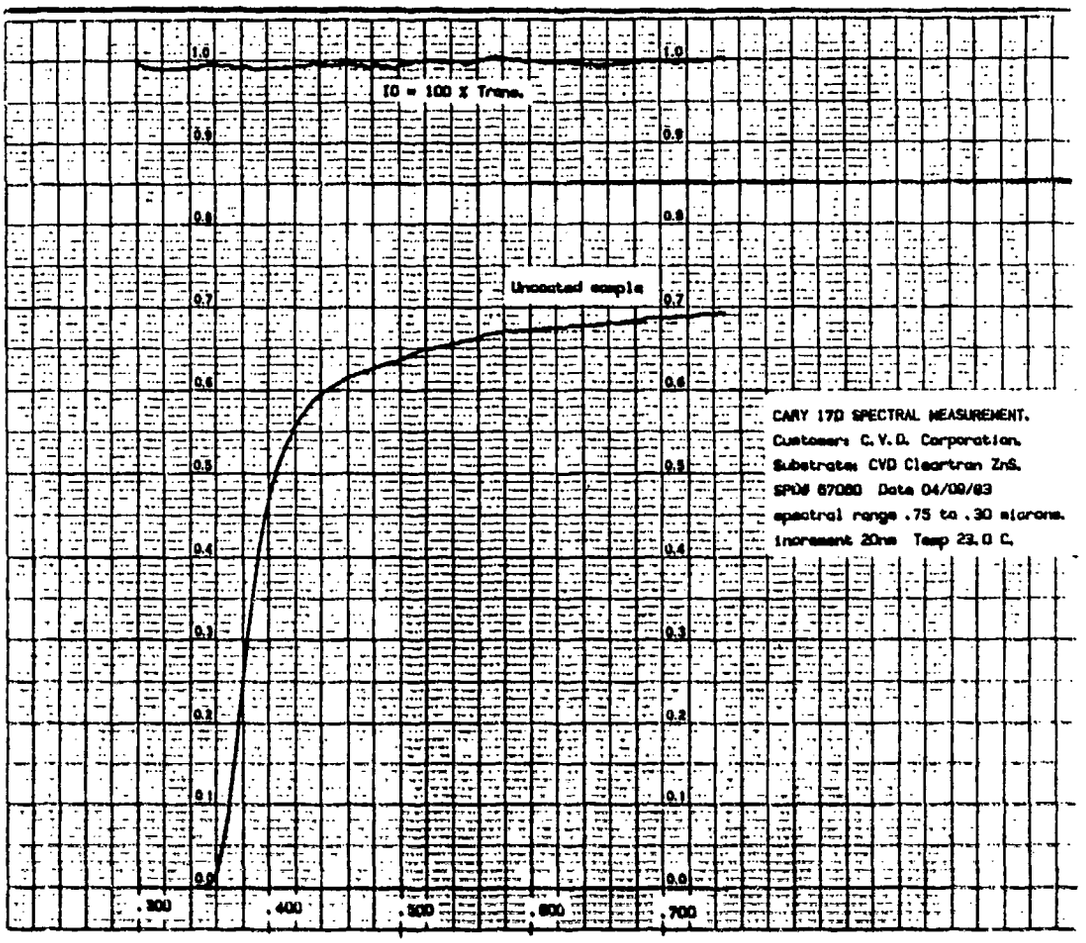

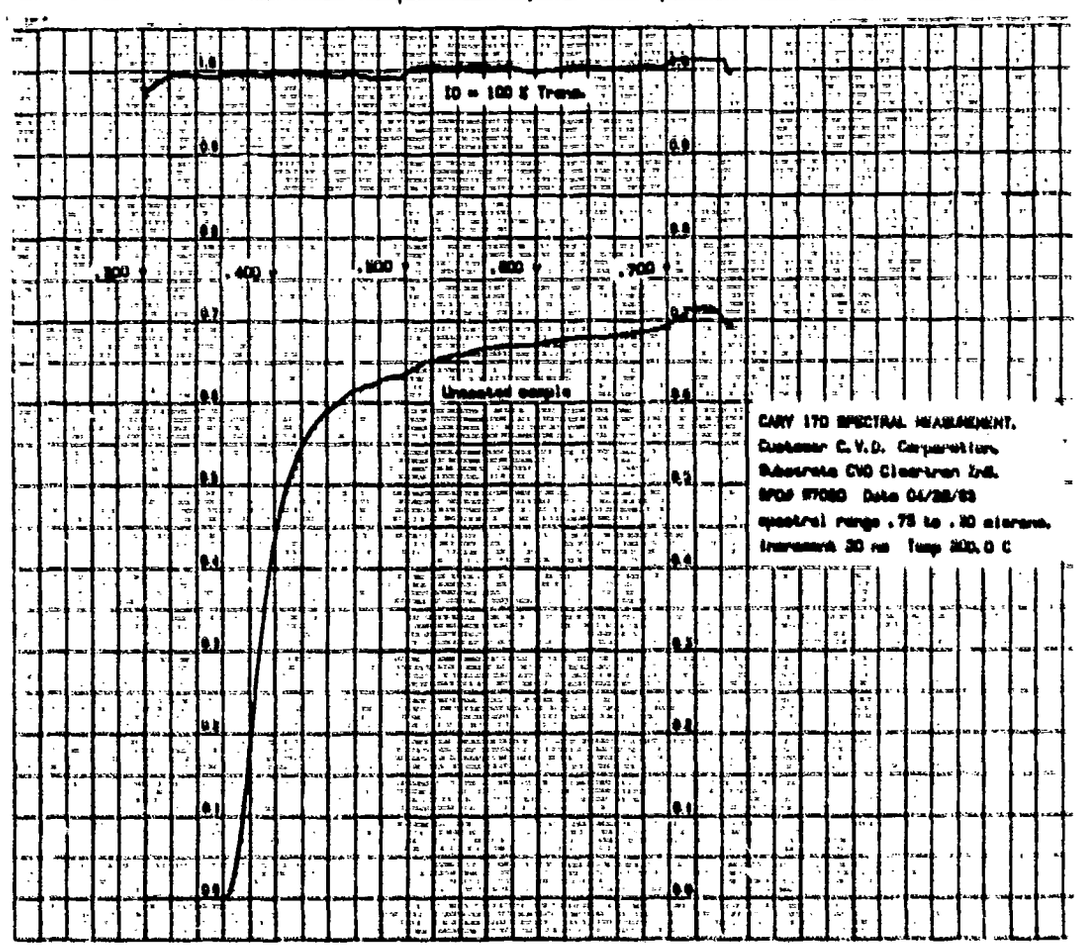

Figure 4-1. Visible Transmittance of Water-Clear ZnS at 23°C (top) and 200°C (bottom).

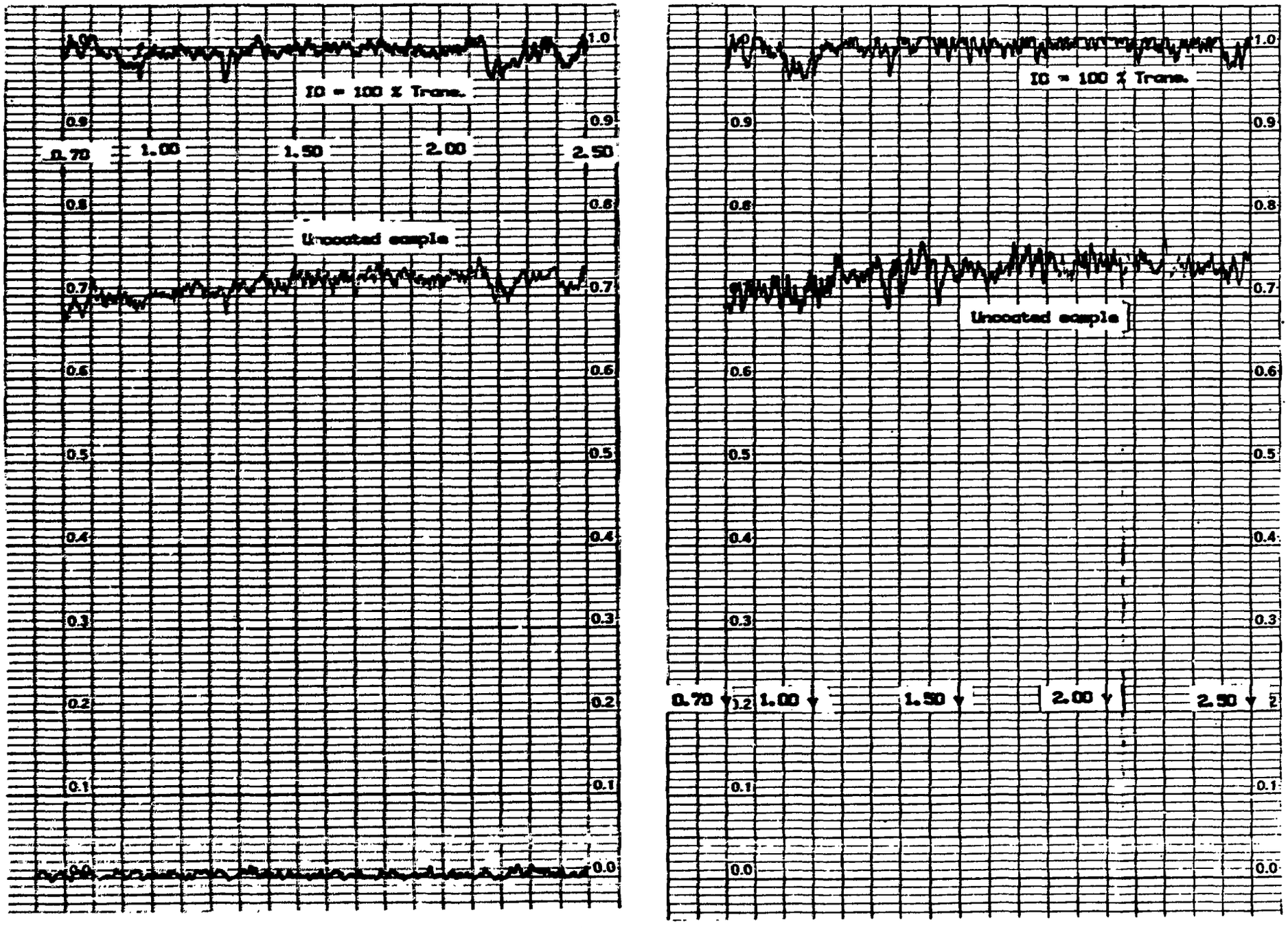

Fig. 4-2. Near-Infrared (0.7-2.5 μm) Transmittance Curve of Water-Clear ZnS at 23°C (left) and 200°C (right).

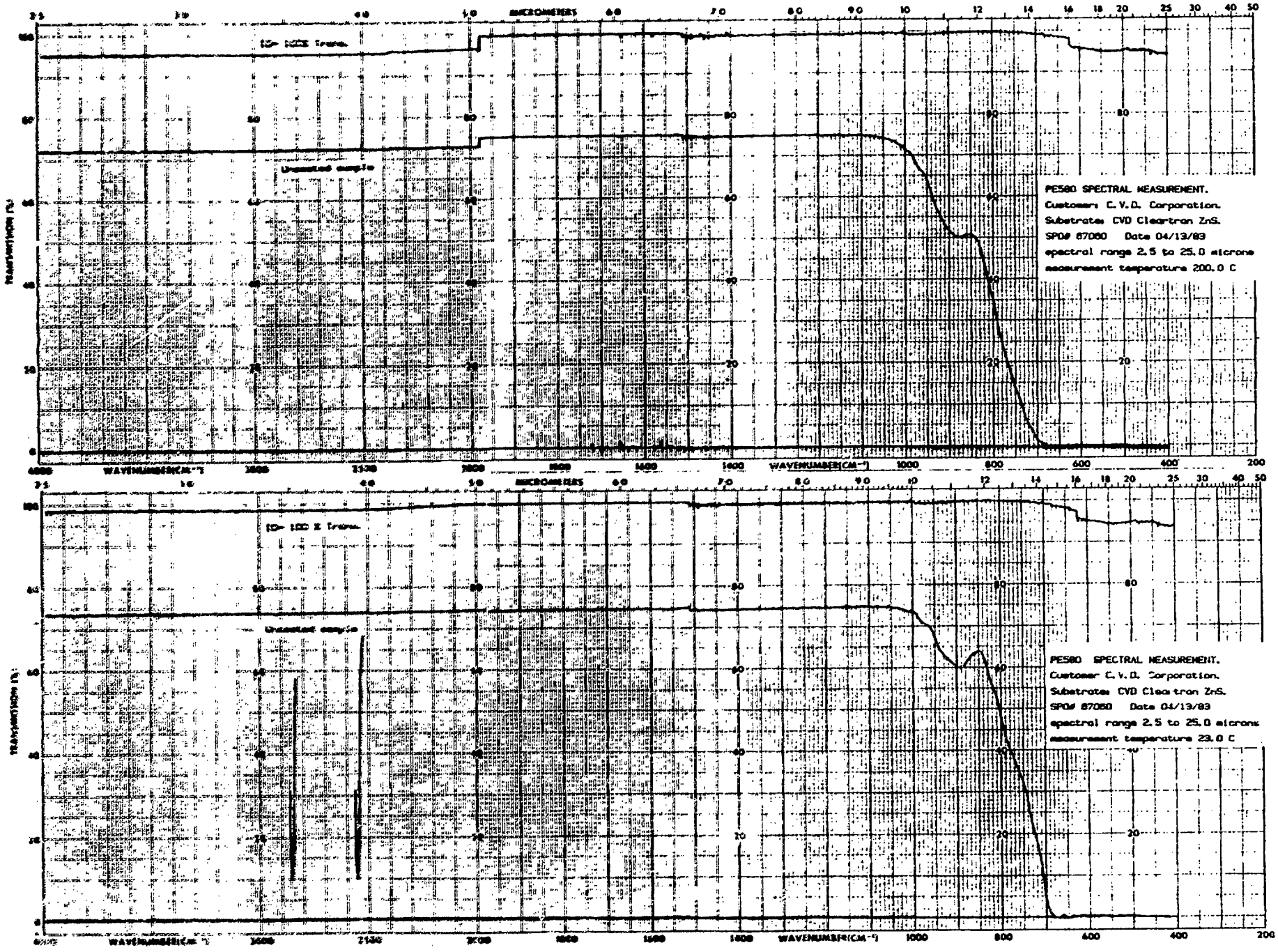

Fig. 4-3. Infrared Transmittance Curve of Water-Clear ZnS at 23°C (bottom) and 200°C (top).

TABLE 4-2

Effective Absorption Coefficients* x 10^{-3} of Water-Clear ZnS

Sample	1.06 μm	1.32 μm	2.7 μm	3.8 μm	9.27 μm	10.6 μm
AF1-4093	15.7	13.6	17.1	16.4	19.0	259.0
AF1-4099	23.4	16.2	21.3	20.7	22.0	245.5
AVG.	19.6 ± 5.4	14.9 ± 1.8	19.2 ± 3.0	13.6 ± 3.0	20.5 ± 2.1	252.3 ± 9.5
AF4-4100	4.25	3.15	5.16	2.91	9.90	244.5
AF4-4101	3.44	2.98	5.33	2.29	10.0	224.0
AF4-4112	--	--	2.95	2.11	4.40	268.0
AF4-4113	--	--	3.07	2.52	4.47	246.0
AF4-4114	--	--	3.40	3.29	4.53	260.0
AF4-4115	--	--	3.52	2.68	4.45	237.0
AVG.	3.85 ± 0.57	3.07 ± 0.12	3.91 ± 1.06	2.63 ± 0.43	6.29 ± 2.83	246.6 ± 15.8
AF6-4102	5.53	5.88	15.7	7.63	13.3	228.5
AF6-4103	10.3	10.0	21.6	9.23	13.5	237.5
AVG.	7.92 ± 3.37	7.94 ± 2.91	18.7 ± 4.2	8.43 ± 1.13	13.4 ± 0.14	233.0 ± 6.4

* Includes surface losses.

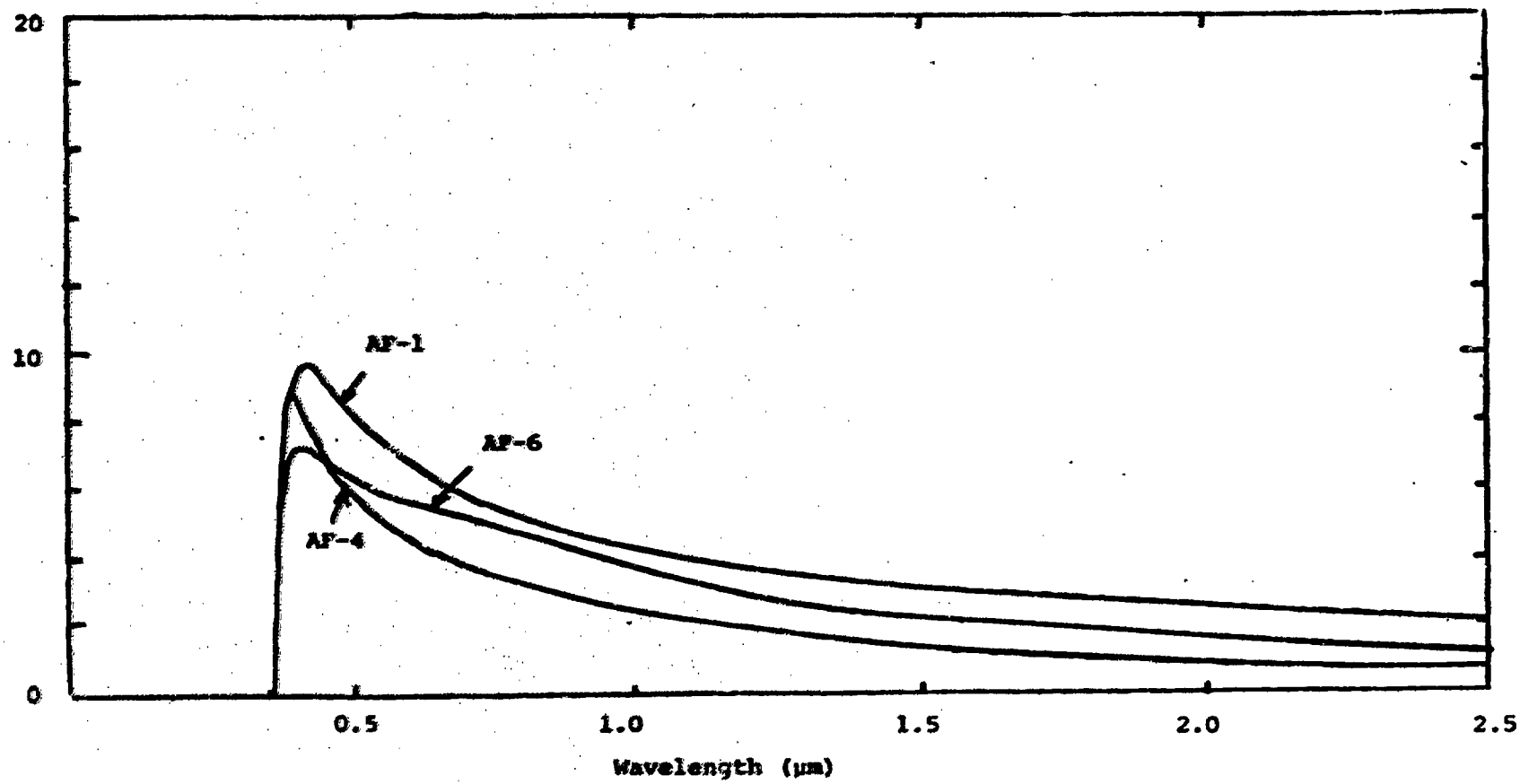

Figure 4-4. Percent of Light Scattered Out of a 4-degree Half Angle Cone by Water-Clear ZnS, Runs AF-1, 4 and 6.

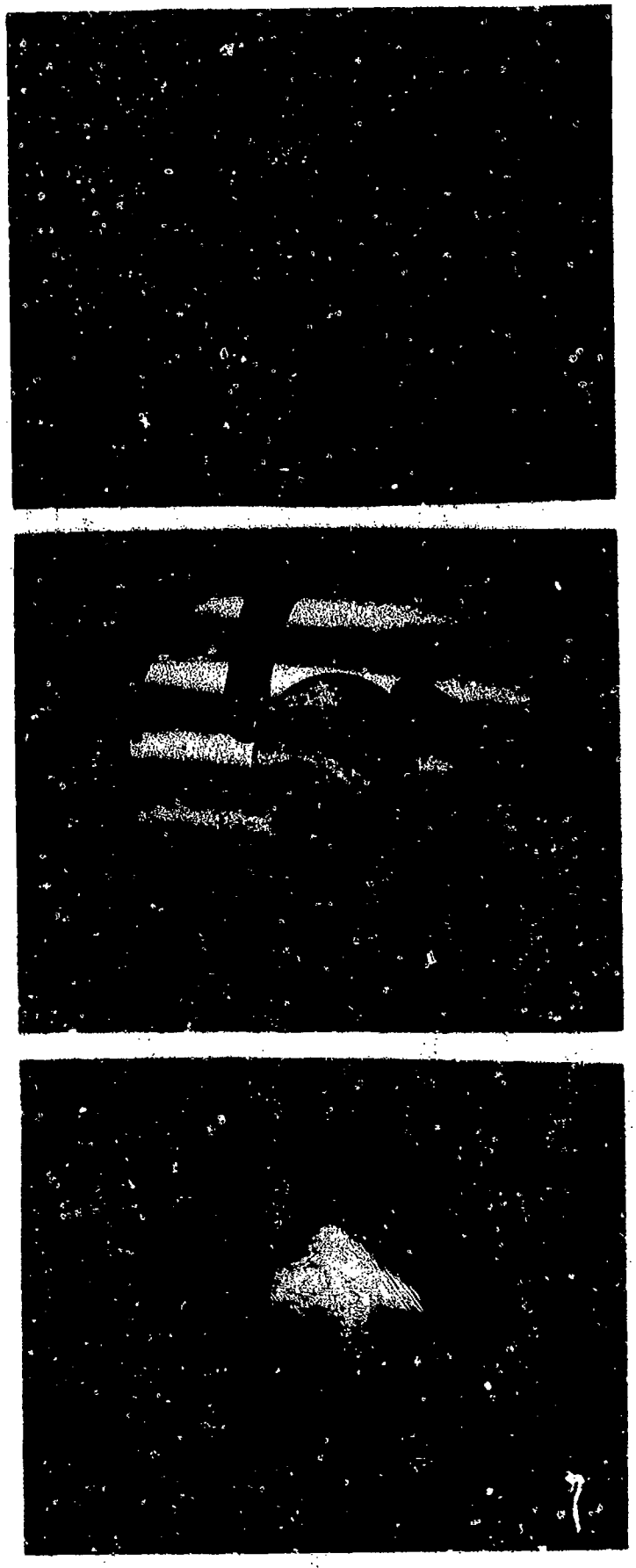

Fig. 4-5 Twyman-Green (top and middle) and Fizeau (bottom) Interferograms of AF-4 Water-Clear ZnS

the bottom figure is a Fizeau interferogram. The fringe displacement in these interferograms is likely due to figure errors, not refractive index inhomogeneities. The small spot at the bottom of the interferograms is a surface defect. The overall light ring structure is from the interferometer, not the sample. Close inspection shows the granularity typical of vapor deposited materials. This high spatial frequency optical path inhomogeneity is considerably less than one fringe, or half wave at 6328 μm. This translates to an index inhomogeneity of $\Delta n << 5 \times 10^{-4}$.

Modulation Transfer Function (MTF) measurements in the 8-12 μm wavelength range are shown in Figs. 4-6 to 4-8 and Table 4-3. The MTF reference scans were made on a 50 mm f/0.7 lens assembly over the frequency range of 2-20 cycles/μm. The collimator has an effective focal length of 60 in., and a 300 μm pinhole was used at the source. The sample of water-clear ZnS tested was 1.5 in. diameter by 0.251 in. thick. Once the reference lens MTF measurements were completed, the water-clear ZnS blank was inserted and the process repeated.

As can be seen in Figs. 4-6 to 4-8, the ZnS follows the reference lens within 10%. However, at higher frequencies the sample slightly surpasses the MTF of the reference lens. This is due to a slight power in the sample (2 fringes). From these data we conclude that the water-clear ZnS sample does not degrade the wavefront transmission more than $\lambda/4$ up to 20 LP/mm.

Table 4-4 shows the thermo-optic coefficients (dn/dT) for water-clear ZnS at three wavelengths. Measurements were made using laser interferometric techniques at 0.6328, 1.15 and 3.39 μm with a HeNe laser. This technique has a system sensitivity of 1×10^{-6}/°C.

Spectral transmittance curves were generated for water-clear ZnS before and after exposure to UV radiation. Samples were placed in a solar simulator* for 1, 2, and 3 weeks of continuous cycling. One week in this solarization chamber is approximately equal to one year of natural sunlight exposure. As can be seen from Figures 4-9 to 4-12, there is no apparent loss of transmittance in either the visible or infrared spectral regions. The samples showed no visible discolorations.

---

* Sunlighter Model 50, Test-Lab Apparatus Co.

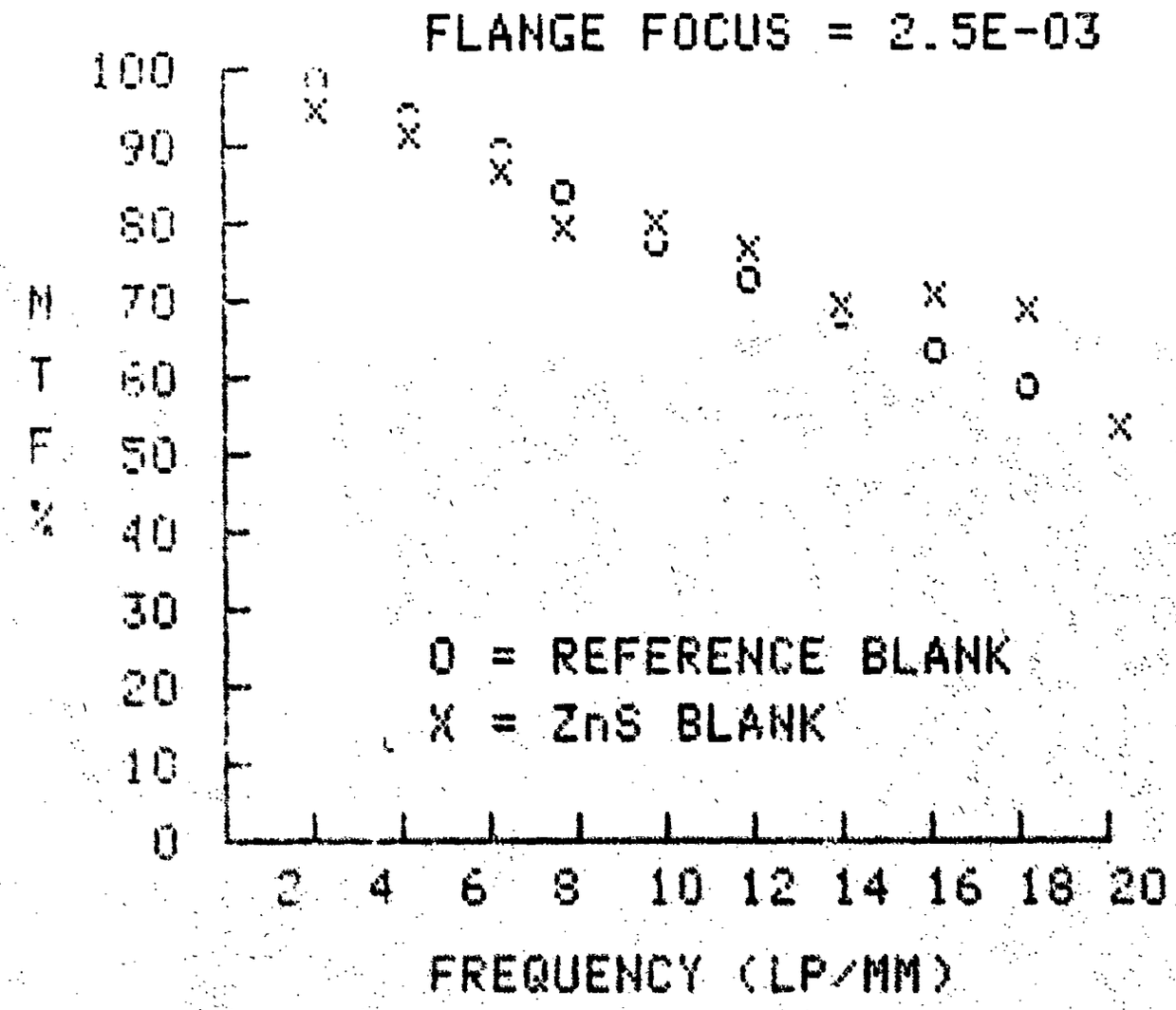

Fig. 4-6. NTF Curve of Water-Clear ZnS, 8-12 μm.

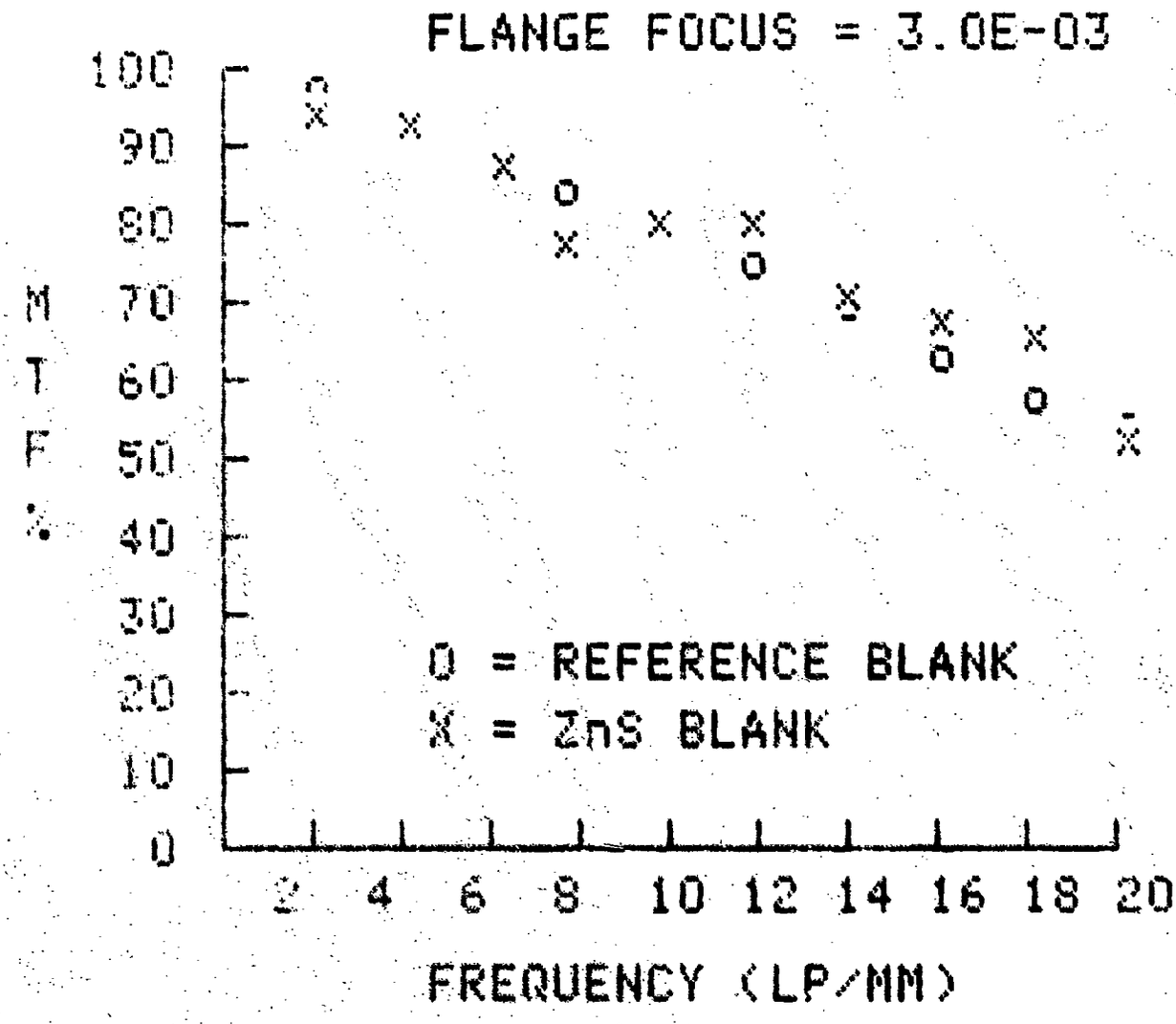

Fig. 4-7. MTF Curve of Water-Clear ZnS, 8-12 μm.

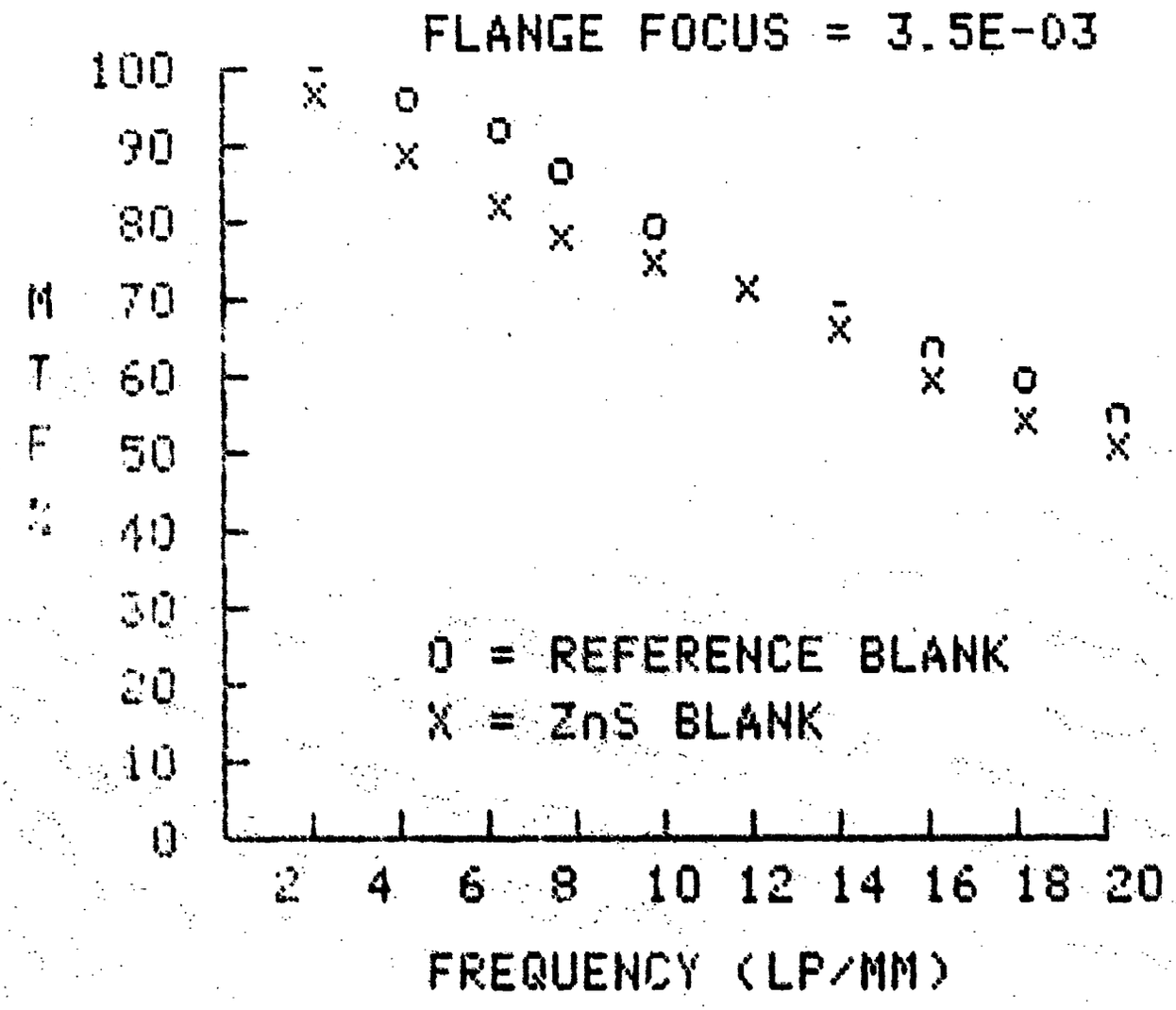

Fig. 4-8. MTF Curve of Water-Clear ZnS, 8-12 μm.

TABLE 4-3

MTF of Water-Clear ZnS 8-12 μm

	REFERENCE LENS			WATER-CLEAR ZnS AND REFERENCE LENS		
ON AXIS FLANGE FOCUS	2.5E-Ø3	3.0E-Ø3	3.5E-Ø3	2.5E-Ø3	3.0E-Ø3	3.5E-Ø3
FREQUENCY (LP/MM)	MTF	MTF	MTF	MTF	MTF	MTF
2	.987	.98	.99	.949	.945	.969
4	.946	.935	.961	.918	.927	.891
6	.900	.885	.926	.867	.874	.823
8	.842	.841	.868	.796	.779	.785
10	.775	.796	.794	.803	.804	.753
12	.727	.753	.732	.772	.800	.716
14	.683	.697	.685	.697	.711	.665
16	.636	.631	.636	.708	.677	.595
18	.592	.578	.595	.690	.658	.544
20	.545	.540	.549	.539	.524	.507

TABLE 4-4

Thermo-optic Coefficients of Water-Clear ZnS

$dn/dT \times 10^{-5}\ C^{-1}$

.6328 μm	1.15 μm	3.39 μm
5.43	4.21	3.87

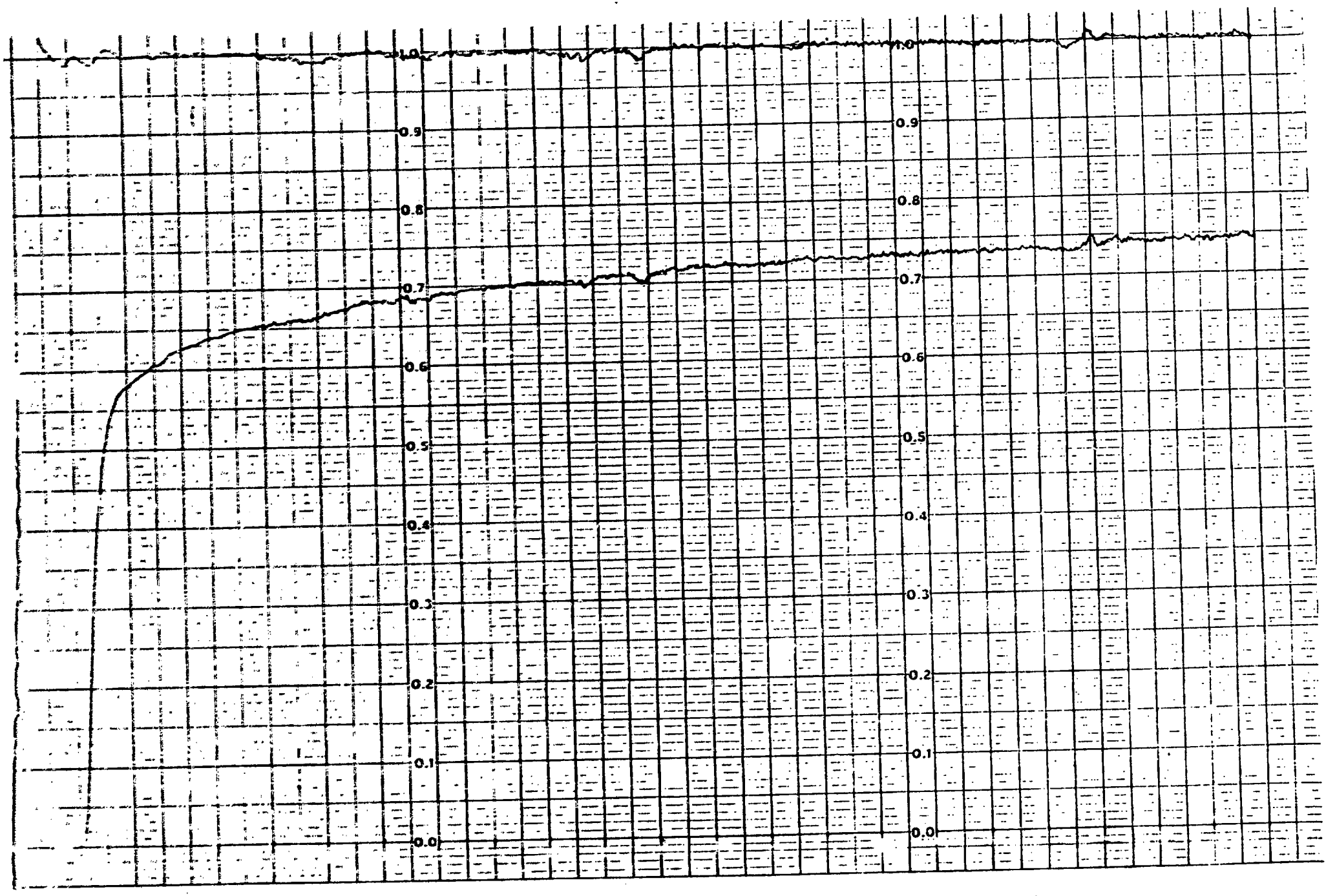

Fig. 4-9. Visible - Near Infrared Transmittance of Water-Clear ZnS Before Exposure to UV Radiation.

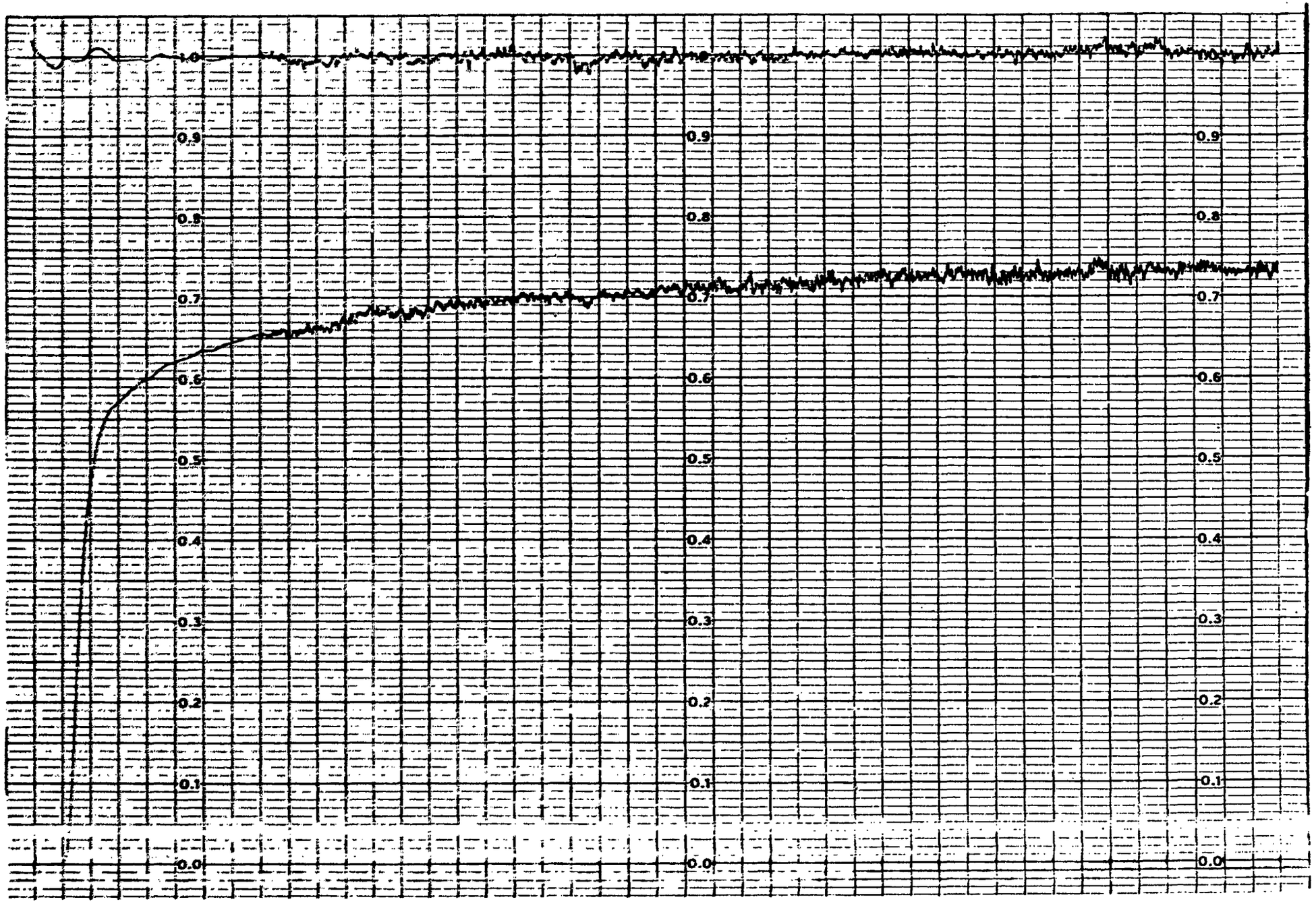

Fig. 4-10 Visible-Near Infrared Transmittance of Water-Clear ZnS After Exposure to UV Radiation.

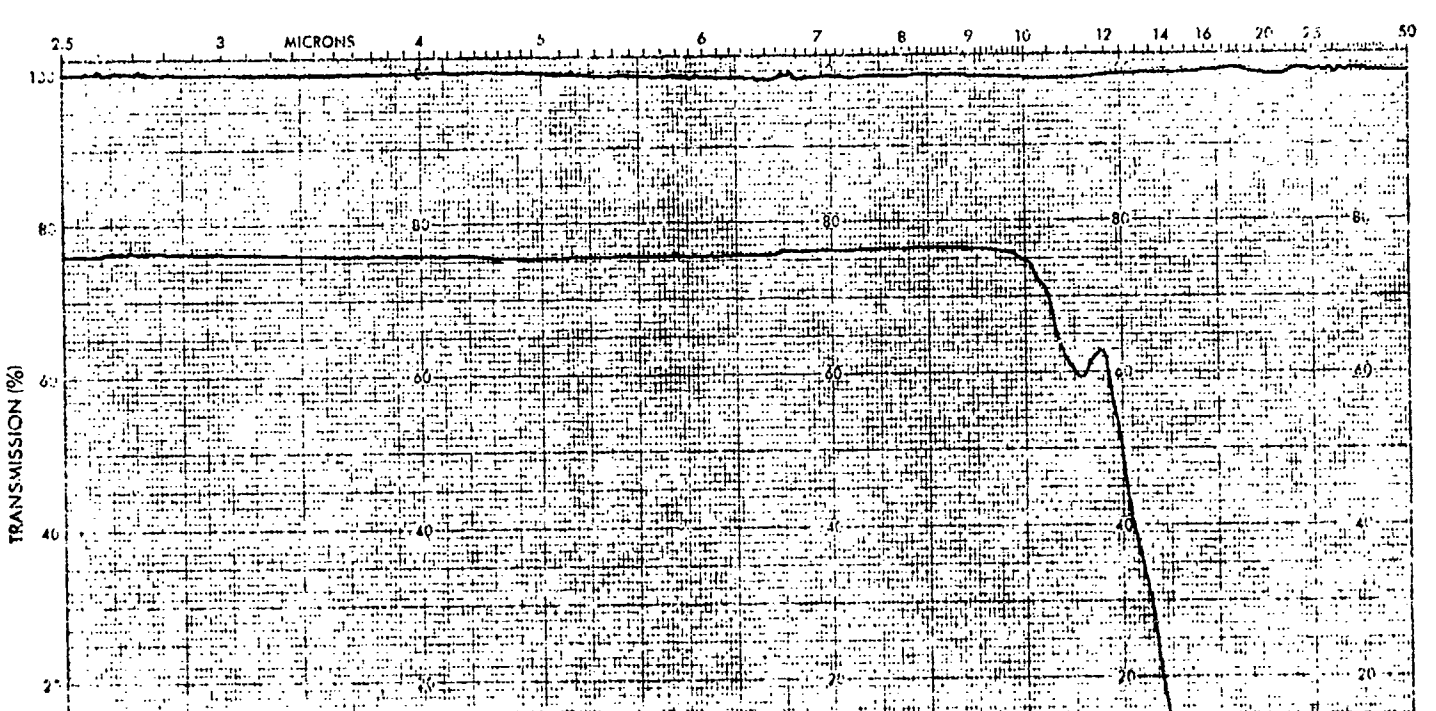

Fig. 4-11. Infrared Transmittance of Water-Clear ZnS Before Exposure to UV Radiation.

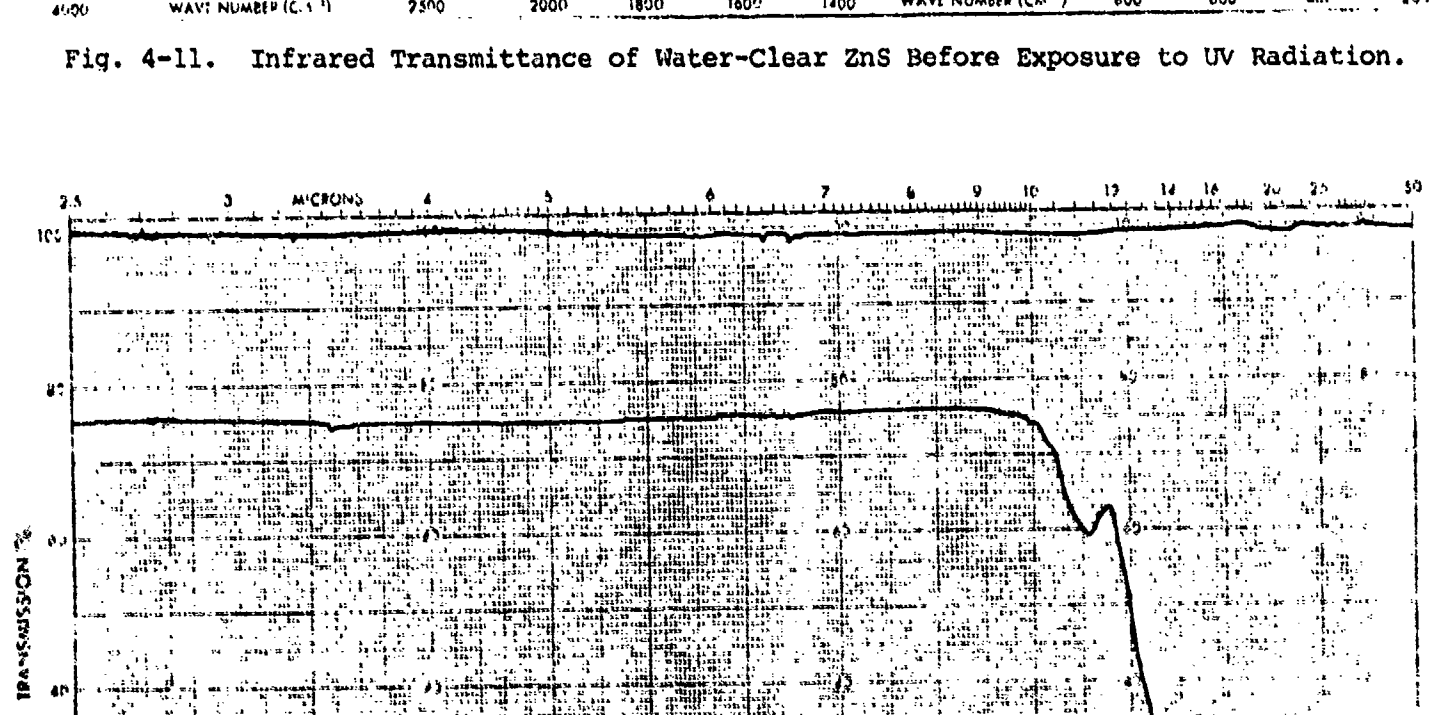

Fig. 4-12. Infrared Transmittance of Water-Clear ZnS After Exposure to UV Radiat

The microstructure of water-clear ZnS is shown in the photomicrographs of Figure 4-13. These samples were highly polished, then etched in a fuming, dilute HCl solution. The grains show random orientation with a fairly consistent grain size of approximately 20-35 μm in diameter.

Numerous Knoop hardness measurements have been performed on this water-clear ZnS. Table 4-5 shows an average value of AF-4 material. All measurements were made with a 50 g load.

Four-point flexural strength tests were made on 0.3 x 0.3 x 3.0 in. beams of polished water-clear ZnS. Samples produced from AF-1, 4 and 6 were tested. As is evident from the data in Table 4-5, there was no significant difference between material produced from the various CVD deposits.

Various thermal and electrical measurements were also made on the water-clear ZnS. Results are summarized in Table 4-5. The thermal expansion coefficient was measured from -65 to 300 C using a quartz dilatometer. The thermal diffusivity was measured using a Xenon flash technique. Specific heat was determined at 0, 50 and 100 C using differential scanning calorimetry. The electrical resistivity was measured using a 6-point Hall probe. Due to the limitations of the Hall probe apparatus, an exact value could not be determined; therefore, a lower limit value is reported in Table 4-5.

Various samples of CVD as deposited and water-clear (coated and uncoated) ZnS were subjected to rain erosion testing at 475 miles/hour in a 1 inch/hour simulated rainfall.

The variable speed (up to Mach 1.2) rotating arm facility consists of an eight foot double arm propeller blade mounted horizontally and powered by a 400 hp motor. A pipe ring with hypodermic needles is positioned to spray controlled water droplets on the speciments which are inserted in the blade tips. A stroboscopic unit and close circuit TV camera enable observation of the specimen while running. Sample dimensions are 1 1/2 x 1/2 x 1/8 inch thick with a 60/40 scratch/dig surface finish.

Test results are given in Table 4-6. The two grades of CVD ZnS displayed similar erosion characteristics, with the damage (fractures and surface pitting) occurring sooner and more severely in the clear materials. Figures 4-14 to 4-16 are infrared transmittance curves of as deposited,

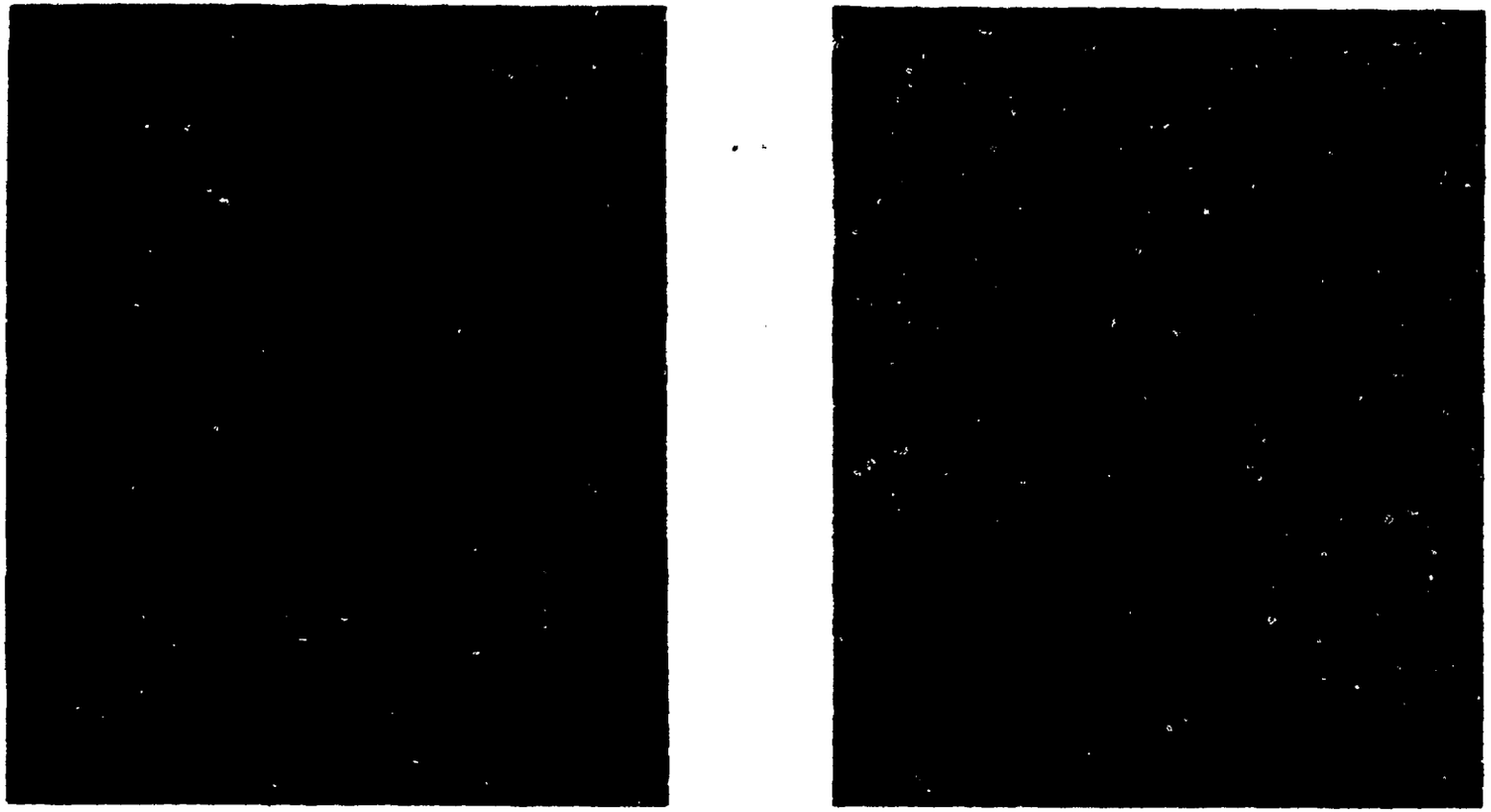

Figure 4-13. Photomicrographs of Etched Surface of Two Samples of CVD Water-Clear ZnS, 500 x.

TABLE 4-5

Mechanical, Thermal and Electrical Properties of Water-Clear ZnS

Test		Value
Knoop Hardness		160 ± 11
Flexural Strength (lb_f/in^2)	AF-1	8310 ± 1560
	AF-4	8670 ± 720
	AF-6	8320 ± 1040
Thermal Conductivity (W/cm C)		0.27
Thermal Diffusivity (cm^2/s)		0.13
Thermal Expansion Coefficient (C^{-1})		6.5×10^{-6}
Specific Heat (cal/g C)	0 C	0.123
	50 C	0.126
	100 C	0.126
Electrical Resistivity (ohm-cm)	20 C	$> 5 \times 10^{13}$

TABLE 4-6

CVD ZnS Rain Erosion Data

475 miles/hour, 90° impact angle, 1 inch/hour simulated rainfall (1.8 mm drops)

Sample	Sample Condition	Time of Exposure (min)	Comments
AF1-1	As Deposited	30.0	Subsurface ring fractures at 15.0 min
AF1-2	As Deposited	30.0	Subsurface ring fractures at 15.0 min, extending to surface at 30 min
AF1-3	As Deposited	30.0	Subsurface ring fractures at 15.0 min, extending to surface at 30 min
AF2-4	As Deposited	30.0	Subsurface ring fractures at 15.0 min, extending to surface at 30 min, pitting, cracking
AF2-5	As Deposited	30.0	Subsurface ring fractures at 15.0 min, extending to surface at 30 min, pitting, cracking
AF2-6	As Deposited	30.0	Subsurface ring fractures at 15.0 min, extending to surface at 30 min, pitting
AF3-7	As Deposited	30.0	Subsurface ring fractures at 15.0 min, extending to surface at 30 min, pitting

TABLE 4-6 (cont.)

CVD ZnS Rain Erosion Data

475 miles/hour, 90° impact angle, 1 inch/hour simulated rainfall (1.8 mm drops)

Sample	Sample Condition	Time of Exposure (min)	Comments
AP3-8	As Deposited	30.0	Subsurface ring fractures at 15.0 min, extending to surface at 30 min, pitting
AP3-9	As Deposited	30.0	Subsurface ring fractures at 15.0 min, extending to surface at 30 min, pitting
AP4-10	As Deposited	30.0	Subsurface ring fractures at 15.0 min, extending to surface at 30.0 min, pitting
AP4-11	As Deposited	15.0	Subsurface ring fractures, cracked at 11.0 min, severe pitting
AP4-12	As Deposited	15.0	Subsurface ring fractures, surface pitting
AP5-13	As Deposited	30.0	Subsurface ring fracture at 15.0 min, extending to surface at 30 min, pitting
AP5-14	As Deposited	30.0	Subsurface ring fracture at 15.0 min, extending to surface at 30 min, pitting
AP5-15	As Deposited	30.0	Subsurface ring fracture at 15.0 min, extending to surface at 30 min, pitting

TABLE 4-6 (cont.)

CVD ZnS Rain Erosion Data

475 miles/hour, 90° impact angle, 1 inch/hour simulated rainfall (1.8 mm drops)

Sample	Sample Condition	Time of Exposure (min)	Comments
AF6-16	As Deposited	30.0	Subsurface ring fracture at 15.0 min, extending to surface at 30 min, pitting
AF6-17	As Deposited	30.0	Subsurface ring fracture at 15.0 min, extending to surface at 30 min, pitting
AF6-18	As Deposited	30.0	Subsurface ring fracture at 15.0 min, extending to surface at 30 min, pitting, specimen cracked
AF4-1	Water-Clear	20.0	Subsurface ring fractures extending to surface at 15.0 min, surface pitting, specimen fractured
AF4-2	Water-Clear	20.0	Subsurface ring fractures extending to surface at 15.0 min, surface pitting
AF4-3	Water-Clear	15.0	Subsurface ring fractures extending to surface at 15.0 min, surface pitting
AF4-4	Water-Clear	15.0	Subsurface ring fractures extending to surface at 15.0 min, surface pitting
AF4-5	Water-Clear	30.0	Subsurface ring fractures extending to surface at 15.0 min, severe surface pitting

TABLE 4-6 (cont.)

CVD ZnS Rain Erosion Data

475 miles/hour, 90° impact angle, 1 inch/hour simulated rainfall (1.8 mm drops)

Sample	Sample Condition	Time of Exposure (min)	Comments
AF4-6	Water-Clear	30.0	Subsurface ring fractures extending to surface at 15.0 min, severe surface pitting
AF4-7	1000 Å Cubic BN on Water-Clear	30.0	Subsurface ring fractures extending to surface at 15.0 min, severe surface pitting
AF4-8	1000 Å Cubic BN on Water-Clear	30.0	Subsurface ring fractures extending to surface at 15.0 min, severe surface pitting

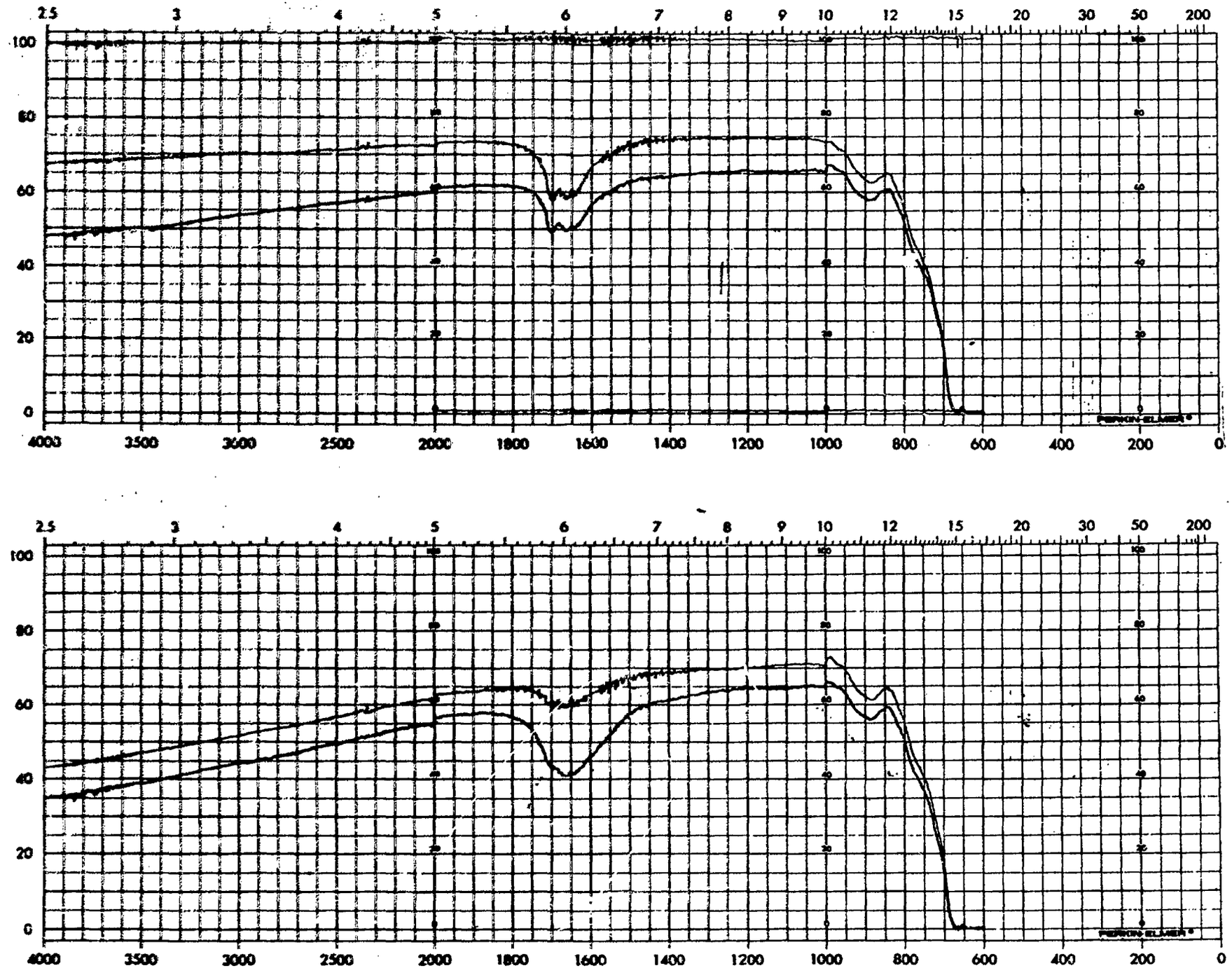

Fig. 4-14. Infrared Transmittance of As Deposited AF-1 (top) and AF-4 (bottom) ZnS Before and After Rain Erosion Testing at 475 miles/hour, 90° Impact Angle, 1 inch/hour Simulated Rainfall for 30.0 min.

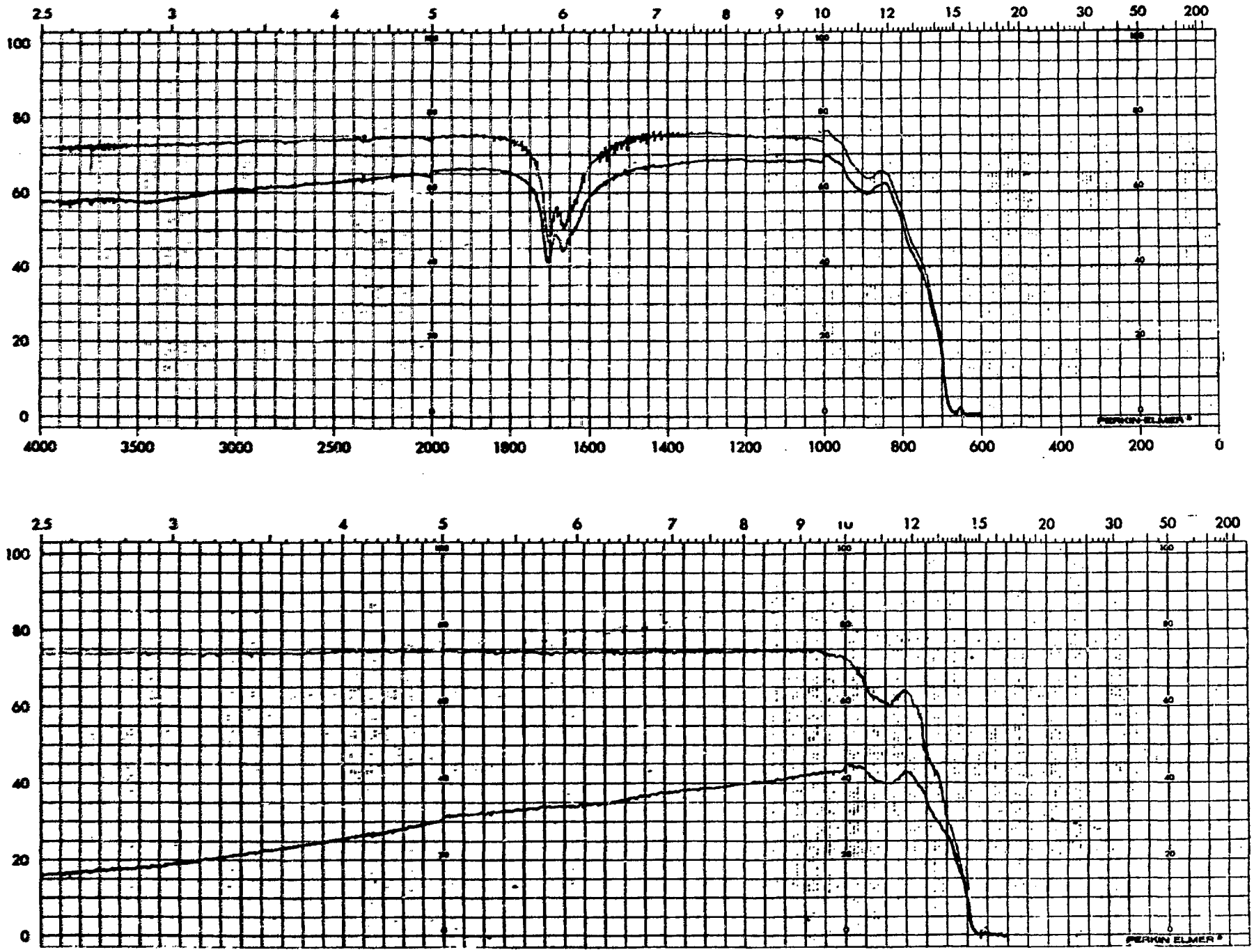

Fig. 4-15. Infrared Transmittance of As Deposited AF-6 (top) and AF-4 Water-Clear (bottom) ZnS Before and After Rain Erosion Testing at 475 miles/hour, 90° Impact Angle, 1 inch/hour Simulated Rainfall for 30 min.

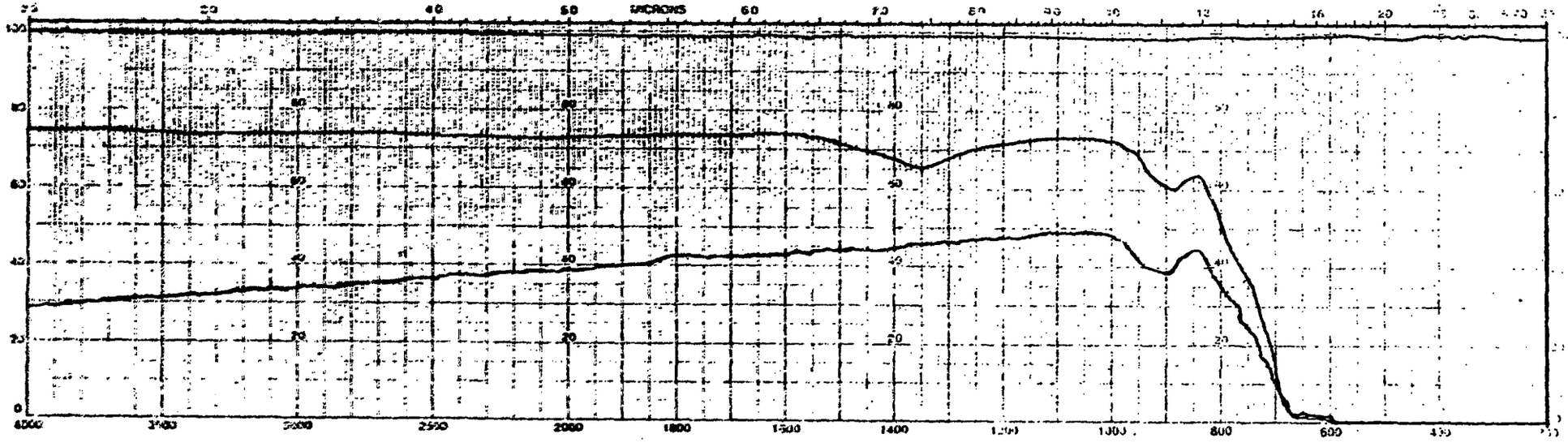

Fig. 4-16. Infrared Transmittance of AF-4 Water-Clear ZnS Coated with 1000 Å Cubic BN Before and After Rain Erosion Testing at 475 miles/hour, 90° Impact Angle, 1 inch/hour Simulated Rainfall for 30.0 min.

water-clear and cubic BN coated water-clear ZnS, before and after rain erosion testing. As was expected, the as deposited ZnS transmittance does not decrease after the rain erosion testing as much as the water-clear ZnS. The cubic BN coated water-clear ZnS displayed slightly improved transmittance after rain erosion testing as compared to the uncoated clear material. It should be noted that the second BN coated sample fragmented into three pieces. It is evident that more than two BN coated samples must be tested before a confident conclusion can be made regarding its effect on the rain erosion resistance of water-clear ZnS. Also, it should be remembered that the adhesion of the BN coating was poor (see Section 3.8).

Best Available Copy

REFERENCES

1. K. L. Lewis, Royal Signals and Radar Establishment, Malvern, U.K. Private Communication, to be published.

2. T. Bansagi et al, "Kinetics of Hexagonal-Cubic Phase Transformation of ZnS in Valuo, in Zinc Vapor, and in Sulfur Vapor". Can. J. Chem 46, 18, September 15, 1968.

3. M. B. Geilikman, "Mechanisms of Polytype Stabilization During the Wurtzite-Sphalerite Transition", Phys. Chem. Min. 8, 2, 1982.

4. S. D. Scott, H. C. Barnes "Sphalerite-Wurtzite Equilibria and Stoichiometry", Geochimica et Cosmochemicha et Acta, 36.

5. J. V. Hackworth, L. H. Kocher, "Rain Erosion Resistance of Infrared Transparent Materials", Bell Aerospace Textron Final Report AFML-TR-79-4218, Jan. 1980.

6. R. Flinn, P. Trojan, Engineering Materials and Their Applications. Houghton Mifflin Co., pp 305-306, 1975.

7. W. D. Kingery, H. K. Bowen, D. R. Uhlmann, Introduction to Ceramics, 2nd ed., John Wiley and Sons Inc., pp 816, 1976.

8. C. Barret, P. B. Massalski, Structure of Metal, 3rd rev. ed., Pergamon Press, pp. 248, 1980.

9. J. E. Field, D. Townshend, "Rain Erosion Resistance of Coated ZnS at Angle", Univ. of Cambridge, Dept. of Physics, U.K., 1983.

10. W. Hasan, D. Mathur, A. Ledger, "Rain Erosion Resistant AR Coatings for ZnS windows", Perkin Elmer Corp. Final Report AFWL-TR-80-4059, May 1980.

11. W. W. Doerfler, H. Y. B. Mas, T. Board, J. Brown, "Erosion Resistant AR Coatings for IR Windows", Honeywell Inc. Final Report AFML-TR-77-8, February 1977.

12. R. W. Tustison, "Erosion Resistant FLIR Window Materials", Raytheon Co. Final Report AFWAL-TR-4199, March 1981.

13. R. N. Donadio, A. W. Swanson, J. Pappis, "Hardened CVD Zinc Selenide for FLIR Windows", Raytheon Co., Final Report AFML-TR-75-142, September 1975.

Best Available Copy

* U.S.Government Printing Office: 1984 — 759-062/1049